



**International Symposium
on
Ligaments and Tendons-XII**

**Hilton San Francisco Financial District
San Francisco, CA
February 3, 2012**

By:

**Savio L-Y. Woo, PhD, DSc, DEng – Chair (Honorary)
Kai-Ming Chan, MD, PhD - Chair
Pauline Po-Yee Lui, PhD
Chih-Hwa Chen, MD, PhD
Diann DeCenzo, MS
Kwang Kim, BS
Po-Yee Tong, BSSc**

ISL&T-XII Sponsors

We gratefully acknowledge our kind sponsors. They contribute to the greatness of the meeting.



Department of Orthopaedics
and Traumatology,
The Chinese University of
Hong Kong



Musculoskeletal
Research Center



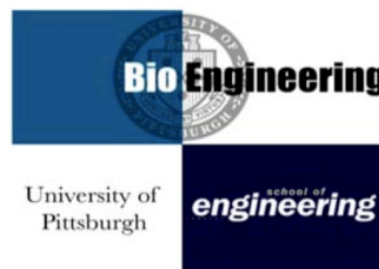
Asian American Institute
for Research & Education



Flexcell International
Corporation



Orthopaedic
Research Society



University of Pittsburgh
Department of
Bioengineering



Let People Move
Research Institute



Nicola's Foundation



Steadman Philippon
Research Institute



The Hong Kong Jockey Club Sports
Medicine and Health Sciences Centre,
Faculty of Medicine,
The Chinese University of Hong Kong



Chang Gung Memorial
Hospital, Taiwan

Volume 12

Table of Contents

	<u>Page</u>
Welcome by Prof. Savio L-Y. Woo	2
Welcoming Note by Prof. Kai-Ming Chan	3
ISL&T-XII Committees	4
ISL&T-XII Awards	5-7
Instructions to Presenters	8
Program	
● Podium Sessions	9-13
● Poster Sessions	14-15
Savio Woo Young Researcher Award winner's abstract	16-18
ISL&T-XII Abstracts	
● Session 1: ACL	19-31
● Session 2: Tendon and Ligament Tissue Engineering	32-41
● Session 3: Rotator Cuff	42-45
● Session 4: Tendinopathy	46-51
● Session 5: Biology and Biomechanics of Tendons and Ligaments	52-66
● Poster Session 1	67-81
● Poster Session 2	82-96

Welcome by Professor Savio L-Y. Woo

It is my distinct pleasure and honor to welcome you to the Twelfth International Symposium on Ligaments and Tendons (ISL&T-XII).

For twelve years now, we have brought together ligament and tendon enthusiasts from all walks to present and to discuss new developments and important topics related to a subject dear to us. Our mission has been to gather together graduate students as well as junior and senior level biologists, engineers, clinicians and surgeons for a day so that we can exchange ideas freely, learn from one another, and establish collaborations.



At ISL&T-XII, you all will enjoy the beautiful scientific program that was put together by our Program Co-Chairs, Dr. Pauline Lui and Professor Chih-Hwa Chen. Please participate by actively sharing your ideas and new data, as well as asking a lot of questions.

I also wish to congratulate all our younger colleagues who are finalists for this year's awards. A special acknowledgement must also be given to Dr. and Mrs. Al Banes of Flexcell International for their generous support of a number of ISL&T awards over the years!

To help us to move forward, we have formed the International Advisory Committee (IAC). This body of leading experts in ligaments and tendons has governed the ISL&T since 2009. It has also developed new strategies to move the field forward, including the formation of a society as well as creating an association to a high quality international journal.

The IAC has approved plans for future ISL&T meetings. Both Professors Kai-Ming Chan and Giuliano Cerulli will be presenting their exciting plans. Please mark your calendar and plan to join us.

Finally, I want to represent the organizing committee to thank our sponsors for their generous support. Also, I am particularly pleased to tell you that a number of laboratory directors have gone the extra distance – by giving financial support for the banquet and award ceremony this evening.

Please enjoy the day!

Savio L-Y. Woo, PhD, DSc (Hon.), DEng (Hon.)

Welcoming Note by Professor Kai-Ming Chan

Dear Friends and Colleagues,

Welcome to the ISL&T-XII in San Francisco, USA!

It is an honour to chair the organizing committee of the ISL&T-XII meeting with the advice of Prof. Savio Woo and the International Advisory Committee and the capable leadership of the co-chairs of the International Program Committee, Prof. Chih-Hwa Chen and Prof. Pauline PY Lui, as well as the efforts of its Committees.



We started a bit late in 2011, but we soon caught up with the momentum with the organization. This year we had a record-high number submission of abstracts from around the world leading to a very much enriched and balanced program with 6 invited lectures, 43 oral presentations and 30 posters. We are particularly delighted to see the enthusiastic responses from young investigators and their brilliant work. We shall maintain the well-cherished tradition of facilitating presentation of the highest standard of research with vigorous deliberation in a vibrant, friendly and scholarly atmosphere. You will enjoy this challenging and rewarding experience with old and new friends!!

ISL&T has now grown to such an international stature that we will need to consider building a structural framework to sustain the long-term development. One of the suggestions is to establish a professional and academic society, the *International Society of Ligament and Tendons*, using the same ISL&T logo that we have built over the past decade. We shall discuss among the International Advisory Committee and also solicit views from around the world.

ISL&T is also actively harnessing international rapport, with a dedicated meeting in Hong Kong in 2010. Plans are already in the pipeline to initiate a one-day meeting at the 2012 COA (Chinese Orthopaedic Association) Congress in Beijing on November 15, 2012. Certainly, we are all looking very much forward to attending the first ever ISL&T meeting in Europe with Prof. Giuliano Cerulli hosting in Italy in October 2013. There are also some requests to host satellite meetings of ISL&T in other cities around the world.

ISL&T will definitely go international!!

Our sincere gratitude goes to all the reviewers, organizing institutions and sponsors to make this 2012 meeting a great success.

K.M. Chan
Chair, Planning Committee, ISL&T-XII

ISL&T-XII Committees

PLANNING COMMITTEE

Savio L-Y. Woo, PhD, DSc, DEng (Chair, Honorary) Kai-Ming Chan, MD, PhD (Chair)
Pauline P.Y. Lui, PhD Chih-Hwa Chen, MD, PhD
Diann DeCenzo, MS Kwang Kim, BS
Po-Yee Tong, BSSc

INTERNATIONAL PROGRAM COMMITTEE

CO-CHAIRS

Chih-Hwa Chen, MD, PhD (Taiwan) Pauline P.Y. Lui, PhD (Hong Kong)

COMMITTEE

Paul Ackermann, MD, PhD (Europe) Nicola Maffulli, MD (Europe)
Cheng-Kung Cheng, PhD (Asia) Hong-Wei Ouyang, PhD (Asia)
Braden Fleming, PhD (North America) Graham Riley, PhD (Europe)
Wei-Hsiu Hsu, MD (Asia) Christer Rolf, MD, PhD (Europe)
Catherine Kuo, PhD (North America) Roger Smith, PhD (Europe)
Guoan Li, PhD (North America) Louis Soslowsky, PhD (North America)
Zong-Ming Li, PhD (North America) Stavros Thomopoulos, PhD (North America)
Helen Lu, PhD (North America)

INTERNATIONAL ADVISORY COMMITTEE

CHAIR

Savio L-Y. Woo, PhD, DSc, DEng (North America)

COMMITTEE

Tom Andriacchi, PhD (North America) Steven Arnoczky, DVM (North America)
Albert A. Banes, PhD (North America) David Butler, PhD (North America)
Giuliano Cerulli, MD (Europe) Kai-Ming Chan, MD (Asia)
Chih-Hwa Chen, MD, PhD (Asia) Mahmut Doral, MD (Europe)
Toru Fukubayashi, MD (Asia) James Goh, PhD (Asia)
Sinan Karaoglu, MD (Europe) Catherine Kuo, PhD (North America)
Guoan Li, PhD (North America) Thay Lee, PhD (North America)
Christos Papageorgiou, MD (Europe) Nicola Maffulli, MD (Europe)
Louis Soslowsky, PhD (North America) Per Renstrom, MD (Europe)
Ray Vanderby, PhD (North America) Richard Steadman, MD (North America)
Kazunori Yasuda, MD (Asia) Jennifer Wayne, PhD (North America)

ISL&T-XII Awards

We established awards to stimulate high quality scientific research by investigators in the study of ligaments and tendons. The awardees are selected by members of the program committee based on the quality of the abstract and presentation as well as the overall merit of the study.

1. Savio L-Y. Woo Young Researcher Award

Award: up to USD\$1000 and Certificate (up to 4)

Purpose: Professor Savio L-Y. Woo founded the International Symposium on Ligaments and Tendons (ISL&T) to promote awareness of the field, the exchange of information, and collaboration both nationally and internationally. The ISL&T has been a venue for lively discussion of current topics in connective tissue research and clinical applications. In addition to his leadership and significant scientific contributions to our field, Professor Woo has been an internationally recognized intellectual ambassador for training, mentoring, and for inspiring students in the field of biomedical engineering and orthopaedic surgery. We are honored to present the Savio L-Y. Woo Young Researcher Award to individuals who perform the best research in three major areas: biomechanical, biological and clinical, and have submitted their work to the ISL&T meeting.

The Award is intended to provide partial support (up to \$1000) towards the applicant's research or for travel expenses to attend the ISL&T-XII meeting. Up to four awards will be given.

Eligibility: Open to graduate students and post-doctoral fellows. Applicant must be the first and presenting author of the abstract and be present at the ISL&T meeting and banquet to accept the award. Advisor's verification of eligibility with a letter is required.

Award Committee

Albert Banes, PhD – Chair, Award Committee
Kai-Ming Chan, MD, PhD – Chair, ISL&T-XII
Jennifer S. Wayne, PhD – Reviewer
Per Renstrom, MD – Reviewer
Graham Riley, PhD – Reviewer

Acknowledgements: Sponsored by Flexcell International Corp. and the Asian♦American Institute for Research + Education (ASIAM).

Past Recipients of the Savio L-Y. Woo Young Researcher Award

ISL&T-X, Hong Kong, China (2010 Inaugural Year)



Biological Research – **Xiao Chen**, Advisor: H-W. Ouyang, School of Medicine, Zhejiang University, Zhejiang, China

Abstract Title: TENDON-LINEAGE DIFFERENTIATION OF HUMAN EMBRYONIC STEM CELLS INDUCED TENDON-LINEAGE DIFFERENTIATION BY OVER-EXPRESSION OF SCLERAXIS AND DYNAMIC MECHANICAL STRESS



Clinical Research – **Saira Chaudhry**, Advisor: D. Morrissey, School of Engineering and Material Science, Queen Mary University of London, London, UK

Abstract Title: ECCENTRIC & CONCENTRIC CALF MUSCLE LOADING: AN IN VIVO STUDY OF FORCE & EMG

ISL&T-XI, Irvine, CA



Biomechanical Research – **Joo H. Oh**, Advisor: T.Q. Lee, Orthopaedic Biomechanics Laboratory, VA Long Beach Healthcare System and University of California, Irvine, CA

Abstract Title: BIOMECHANICAL EFFECTS OF LATISSIMUS DORSI TENDON TRANSFER IN IRREPARABLE MASSIVE ROTATOR CUFF TEAR



Biological Research – **Jeffrey P. Brown**, Advisor: C.K. Kuo, Department of Biomedical Engineering, Tufts University, Medford, MA

Abstract Title: SPINAL LIGAMENT TISSUE DEVELOPMENT IN VIVO AND CELL RESPONSE TO GROWTH FACTORS IN VITRO

ISL&T-XII Award Recipient

Biological Research – **Jonathan P. Gumucio**, Advisor: C.L. Mendias, School of Kinesiology, University of Michigan, Ann Arbor, MI

Abstract Title: CHRONIC ROTATOR CUFF TEAR CHANGES THE EXPRESSION OF SEVERAL SMALL NON-CODING RNA MOLECULES THAT REGULATE MUSCLE ATROPHY, FIBROSIS AND AUTOPHAGY

2. Best Research Fellow Paper Award

Award: USD\$200 and Certificate

Eligibility: Open to clinical fellows or post-doctoral research fellows. Applicant must be the first author of the abstract and be present at the ISL&T meeting/banquet to accept the award.

Application: Upon submission of the abstract by the regular submission deadline, applicant must indicate his/her intention to be considered for this award.

Selection Criteria: Applicant's abstract submitted for the ISL&T-XII will be reviewed by the program committee through the regular evaluation process based on scientific merit and research quality.

Selection Process: The Program Committee will select the best paper during the international meeting. Award winner will be announced at the banquet and must be present at the announcement to receive the award.

Acknowledgement: Sponsored by Flexcell International Corporation.

3. Best Student Paper Award

Award: USD\$200 and Certificate

Eligibility: Open to current graduate students. Applicant must be the first author of the abstract and be present at the ISL&T meeting/banquet to accept the award. Advisor's verification of eligibility is required.

Application: Upon submission of the abstract by the regular submission deadline, applicant must indicate his/her intention to be considered for this award.

Selection Criteria: Applicant's abstract submitted for the ISL&T-XII will be reviewed by the program committee through the regular evaluation process based on scientific merit and research quality.

Selection Process: The Program Committee will select the best paper during the international meeting. Award winner will be announced at the banquet and must be present at the announcement to receive the award.

Acknowledgement: Sponsored by Flexcell International Corporation.

4. Best Poster Award

Award: USD\$200 and Certificate

Eligibility: Open to all participants of poster presentation. Applicant must be the first author of the abstract and be present at the ISL&T meeting/banquet to accept the award.

Application: Upon submission of the abstract by the regular submission deadline, applicant must indicate his/her intention to be considered for this award.

Selection Criteria: Applicant's abstract submitted for the ISL&T-XII will be reviewed by the program committee through the regular evaluation process based on scientific merit and research quality.

Selection Process: The Program Committee will select the best poster during the international meeting. Award winner will be announced at the banquet and must be present at the announcement to receive the award.

Acknowledgement: Sponsored by Flexcell International Corporation.

Instructions to Presenters

Podium Presenters

Each podium presentation is 5 minutes in length with discussion time (10-15 mins) allocated after several presentations. Please be seated in the 'speakers' seating area at least 5 minutes before your session begins.

To encourage discussion, the presentation time is limited. Your moderators have been asked to adhere to the allocated time for your presentation and number of slides.

In view of time and the large number of presentations, the presentation files have been uploaded in advance to the computer provided by the organizers. No personal computer may be used during the session.

Award winner will be announced at the banquet and must be present at the announcement to receive the award.

Poster Presenters

Poster should be limited to 4 feet by 4 feet.

Please hang your poster during breakfast time (7:00-7:45 am) / social time on the designated board (marked with your poster code) before the meeting begins. Pins are available on the board. Poster boards will be placed in the back of the lecture hall where the podium presentations will be held.

There are two poster sessions, please refer to the poster program to find out which session your poster belongs to. Please arrive at the poster viewing venue as soon as your session begins. Each poster presenter will be given 1 minute during his/her respective poster session to give a pitch to introduce the presented work to the audience.

Each board has a ribbon that is marked with your poster code. Please tie the ribbon onto your shirt / jacket for easy identification when you are doing the 1 minute presentation.

Please remove your poster promptly at the end of the meeting.

Award winner will be announced at the banquet and must be present at the announcement to receive the award.

PROGRAM

Podium Sessions

<u>Time</u>	<u>Code</u>	<u>Topics</u>	<u>Speakers</u>
7:00		Registration and Light Breakfast	
7:45		Welcome	Savio L-Y. Woo, PhD, DSc, DEng
7:55		Welcome	K.M. Chan, MD, PhD
8:10		Clinical Talk	Chair: Ranjan Gupta, MD
		<i>ACL Injury and Tunnel Length -Transtibial versus Far Anteromedial Portal Technique for Posterolateral Femoral Tunnel Drilling in Anatomic Double-Bundle Anterior Cruciate Ligament Reconstruction</i>	<i>Mitsuo Ochi, MD</i>
		Podium Session 1: ACL	Session Chairs: Mitsuo Ochi, MD, Guoan Li, PhD
8:25		Keynote Lecture: Biology of Healing and Biomechanics after ACL Reconstruction	<i>Cyril Frank, MD</i>
8:40	S1-1	Local Administration of Alendronate Reduced Peri-Tunnel Bone Loss and Promoted Graft-Bone Tunnel Healing in ACL Reconstruction	Yuk Wa Lee
8:46	S1-2	Effects of Altering Grade on Vertical Ground Reaction Forces and ACL Forces in the Sheep Model	Rebecca J. Nesbitt
8:52	S1-3	Effect of Combined ACL and Meniscus Injuries on Knee Joint Kinematics	Guoan Li
8:58	S1-4	Characterization of Inflammation Following ACL Injury	Carla Haslauer
9:04		<i>Discussion</i>	
9:19	S1-5	Biplanar X-ray Derived ACL Excursions during a Jump-Cut Maneuver Associated with ACL Injury	Daniel L. Miranda
9:25	S1-6	Effect of Graft Fixation Angles on Knee Kinematics, Graft Tension Curves and Load Sharing in Double-Bundle Anterior Cruciate Ligament Reconstruction	Hideyuki Koga
9:31	S1-7	Intra-operative Supplementation of Vitamin C Improved Knee Laxity Restoration in Anterior Cruciate Ligament Reconstruction	Wai Hang Cheng

9:37	S1-8	Knee Kinematics After ACL Reconstruction Using Transtibial and Anteromedial Portal Surgical Techniques	Hongsheng Wang
9:43		<i>Discussion</i>	
9:58	S1-9	Intra-operative Assessment of Joint Laxity in the ACL-deficient and Contralateral Healthy Knees	Claudio Belvedere
10:04	S1-10	Biomechanical Evaluation of Bioabsorbable Polymer Interference Screws for ACL Reconstruction at Time Zero and 12 Weeks of Healing in a Goat Model	Kwang Eun Kim
10:10	S1-11	Relationship Between Medial-to-Lateral Femoral Cartilage Thickness Ratio and Peak Knee Abduction Moment During Walking for ACL Reconstructed and Healthy Contralateral Knees	Michael Zabala
10:16		<i>Discussion</i>	
10:26		Break / Poster Session	Session Chairs: Louis Soslowsky, PhD, Stavros Thomopoulos, PhD
		Podium Session 2: Tendon and Ligament Tissue Engineering	Session Chairs: Helen Lu, PhD, Paul Ackermann, MD, PhD
10:56		<i>Keynote Lecture: Working across Model Systems at the Interface between Functional Tissue Engineering and Developmental Biology to Improve Adult Tendon Repair</i>	<i>David Butler, PhD</i>
11:11	S2-1	Type I Collagen Synthesis in Scaffold-free, Single Fibers for Engineered Tendon	Nathan R. Schiele
11:17	S2-2	Fabricating Scaffolds of Electrospun Nanofibres from Synthetic Biopolymers for Tendon Repair	Lucy Bosworth
11:23	S2-3	Fibrin Hydrogels Exhibit Improved Biological and Mechanical Properties Compared to Collagen Hydrogels in Tissue-Engineered Constructs In Vitro	Andrew P. Breidenbach
11:29	S2-4	Addition of Collagen Fibers to MPC-Collagen Gels to Promote Tissue Engineered Construct Stiffness and Matrix Production	Andrea Lalley
11:35	S2-5	Effect of Nanofiber Alignment and Mechanical Loading on hMSC Differentiation	Siddarth Subramony
11:41		<i>Discussion</i>	

11:56	S2-6	BMP-2 Eluting Biphasic Hybrid Silk Scaffold for Ligament and Bone Tunnel Regeneration	Thomas Kok Hiong Teh
12:02	S2-7	Localized, Controlled Release of Human PDGF from Highly Aligned Collagen-Nanoparticle Fiber for Tendon Repair	Xing Guo Cheng
12:08	S2-8	Low Oxygen Tension Promotes Proliferation and Enhances the Stemness of Human Tendon Stem Cells	James H-C. Wang
12:14	S2-9	Alginate Encapsulated Platelet-rich Plasma and Synovial Fluid Mesenchymal Stem Cells Provided Potential to Repair the Partial Ligament Tear	Ying-Chih Wang
12:20		<i>Discussion</i>	
12:35		Group Photo & Lunch	
		Podium Session 3: Rotator Cuff	Session Chairs: Zong-Ming Li, PhD, Chih-Hwa Chen, MD, PhD
13:35		<i>Keynote Lecture: Long Head of the Biceps Tendon is Damaged Following a Rotator Cuff Tear in A Rat Model: Initiation of Damage and Possible Mechanism of Injury</i>	<i>Louis J. Soslowsky, PhD</i>
13:50	S3-1	<i>Savio L-Y. Woo Young Researcher Award Winner:</i> Chronic Rotator Cuff Tear Changes the Expression of Several Small Non-Coding RNA Molecules that Regulate Muscle Atrophy, Fibrosis and Autophagy	Jonathan P. Gumucio
14:00		<i>Discussion</i>	
14:05	S3-2	Effect of the Adipose-derived Stem Cell for the Improvement of Fatty Degeneration of the Rotator Cuff Muscle in Rabbit Model	Seok Won Chung
14:11	S3-3	Biomechanical Factors Predisposing to Propagation of Rotator Cuff Tears: Tear Size, Shoulder Elevation and Rotation, and Rotator Cuff Muscle Strength	Teruhisa Mihata
14:17	S3-4	The Arthroscopic Bone Needle. A New, Safe and Cost-effective Technique for Rotator Cuff Repair	Jens Stehle
14:23		<i>Discussion</i>	

		Podium Session 4: Tendinopathy	Session Chairs: Braden Fleming, PhD, Nicola Maffulli, MD
14:33		<i>Keynote Lecture: Biochemical Causes of Tendinopathy?</i>	<i>Patrik Danielson, MD, PhD</i>
14:48	S4-1	Diclofenac and Trimcinolone Acetonide Impairs Medenchymal Stem Cell Growth and Their Differentiation to Tenocytes	Maritha Fredriksson
14:54	S4-2	Evidence that Aggrecan-Rich Deposits Cause Tendinopathies by Blocking Fibrogenesis	Vincent M. Wang
15:00	S4-3	Lipoxin A4 Receptor Mediated Inflamm-Aging in Flexor Tendinopathy: A Mechanism for Immunosenescence	Stephanie Georgina Dakin
15:06	S4-4	Visualization of Collagen Matrix Damage in a Tendon Fascicle Fatigue Model	Stephen J. Ros
15:12	S4-5	Effect of Degenerative Rotator Cuff Tears and Subacromial Bursa Steroid Injection on the Structural Properties of the Supraspinatus Tendon	Jennifer Tilley
15:18		<i>Discussion</i>	
15:33		Break / Poster Session	Session Chairs: Catherine K. Kuo, PhD, Wei-Hsiu Hsu, MD
		Podium Session 5: Biology and Biomechanics of Tendons and Ligaments	Session Chairs: PPY Lui, PhD, Christer Rolf, MD, PhD
16:03		<i>Keynote Lecture: Regulation of Tendon Elongation by Strain and Scleraxis Dependent Tenocytes Induction</i>	<i>Ronen Schweitzer, PhD</i>
16:18	S5-1	Differential Expression and Cellular Localization of Novel Isoforms of the Tendon Biomarker Tenomodulin	Jie Qi
16:24	S5-2	Effects of Stress Deprivation on Lubricin Synthesis and Gliding of Flexor Tendon	Chunfeng Zhao
16:30	S5-3	BMP12 and BMP14 Promote Tenogenesis in the Adipose-Derived Stem Cells	Hua Shen
16:36	S5-4	Cyclic and Static Stress-relaxation Properties of Bovine Tendon Fascicles – The Effect of Recovery Time	Hazel Screen

16:42	S5-5	Tendon Glycosaminoglycans - Interfibril Glue or Lube? AFM Observations of Collagen Ultrascale Mechanics	Jess G. Snedeker
		<i>Discussion</i>	
16:57	S5-6	Tracking of Mesenchymal Stem Cells in Tendon Injuries Following in vivo Administration	Jay Dudhia
17:03	S5-7	The Effect of Increasing Load on Tendon Biomechanics During Eccentric and Concentric Triceps Surae Exercises	Hazel Screen
17:09	S5-8	A High Calcium Diet Improves the Adaptive Response of Tendon to Exercise	Nelly Andarawis-Puri
17:15	S5-9	Mechanical and Molecular Effects of Aging on Normal Ligaments	Gail M. Thornton
		<i>Discussion</i>	
17:30	S5-10	Investigating Fiber Mechanics in Functionally Distinct Tendons	Chavaunne Thorpe
17:36	S5-11	Measuring Transverse Carpal Ligament Thickness by Ultrasound	Zhilei Liu Shen
17:42	S5-12	Does Locking Configuration Affect the Biomechanical Characteristics of Extensor Tendon Repair in Zone IV?	Kyung Chil Chung
17:48	S5-13	Effects of Collagen Crosslink Inhibition on Embryonic Tendon	Joseph E. Marturano
17:54	S5-14	Rapamycin Attenuates Age-associated Changes in Tibialis Anterior Tendon Viscoelastic Properties	Lauren Wood
18:00		<i>Discussion</i>	
18:15		2012 ISL&T - COA	K.M. Chan, MD, PhD
18:20		ISL&T - XIII, Perugia/Arezzo, Italy	Giuliano Cerulli, MD
18:25		Closing Remarks	Chih-Hwa Chen, MD, PhD
18:30		<i>Proceed to Dinner Venue</i>	
19:00		Reception / Dinner and Award Ceremony	Far East Café

PROGRAM

Poster Sessions

10:26-10:56

Poster Session I

**Chairs: Louis
Soslowsky, PhD,
Stavros Thomopoulos,
PhD**

<u>Code</u>	<u>Title</u>	<u>Speakers</u>
P1	BMP-2 Promoted Proteoglycan Deposition and Stimulated Non-Tenogenic Differentiation of Tendon-derived Stem Cells (TDSCS) in vitro – Potential Roles of Ectopic BMP-2 in the Pathogenesis of Tendinopathy	Pauline Po-Yee Lui
P2	Altered Fate Of Tendon-Derived Stem Cells (TDSCS) in Ossified Failed Tendon Healing	Pauline Po-Yee Lui
P3	Future Treatment of ACL Arthrosis: Complete Cartilage Replacement	Kevin R. Stone
P4	MRI Derived Morphology and Signal Intensity to Determine Structural Properties of an ACL Reconstruction Graft or ACL Primary Repair at One Year in a Porcine Model	Alison Biercevicz
P5	Biomechanical and Histological Analysis after Tenotomy of the Long Head of the Biceps in the Rabbit Shoulder Model	Sae Hoon Kim
P6	Expression of IGF-1 Receptor and Myosin Heavy Chain in Rabbit's Rotator Cuff after Rotator Cuff Repair and Injection of Adipose-derived Stem Cell	Sae Hoon Kim
P7	Efficiency of Ultrasound Therapy in Prevention of Adhesions after Zone-II Flexor Tendon Repair: A Randomized, Controlled, Clinical Trial	Muqing Liu
P8	Fiber-type Switching and Reduction in Specific Force Production Following Rotator Cuff Tear	Max E. Davis
P9	Induction in Scleraxis Expression and Neotendon Formation in the Plantaris Tendon Following Achilles Tendon Ablation	Christopher L. Mendias
P10	Changes in Cartilage Oligomeric Matrix Protein and C-Reactive Protein in Patients Undergoing Anterior Cruciate Ligament Reconstruction and Rehabilitation	Evan B. Lynch
P11	Intra-operative Vitamin-C Supplementation Promotes Tendon Healing in Rats	Sai Chuen Fu
P12	The Femoral Insertion of the Anterior Cruciate Ligament: Relationship between the Direct Insertion and the Depth of the Calcified Fibrocartilage and Bone Layer	Norihiro Sasaki
P13	Increased Metabolic Activity in Human Achilles Tendon Repair can be Enhanced by Intermittent Pneumatic Compression Treatment	Erica Arverud
P14	Relationship between Stiffness and Failure: Experiment and Meta-analysis	Sarah Duenwald-Kuehl
P15	Alterations in Transverse and Longitudinal Mechanical Properties of Artificially Aged Tendon	Gion Fessel

Poster Sessions

15:33-16:03

Poster Session II

Chairs: Catherine K. Kuo, PhD, Wei-Hsiu Hsu, MD

<u>Code</u>	<u>Title</u>	<u>Speakers</u>
P16	Three-dimensional Geometrical Changes of Knee Soft Tissues during Flexion by Anatomical-Based Fibre Mapping. An in-vitro Study	Claudio Belvedere
P17	Anatomical and Biomechanical Concepts in Achilles Tendon Pathogenesis	Toni Arndt
P18	Trigger Finger, Tendinosis and Gene Expression	Pernilla Eliasson
P19	“Failure with Continuity”-- A Common Mechanism of Rotator Cuff Repair “Healing”	Kathleen Derwin
P20	Systemic Administration of Oxytetracycline Induces an Age-Dependent Decrease in the Viscoelastic Properties of Rat Tail Tendons	Keri Gardner
P21	Substance p Enhances Collagen Gel Remodeling and MMP-3 Expression by Human Tenocytes	Gloria Fong
P22	Bone Tunnel Healing of Tissue Engineered Scaffold-less Bone Ligament Bone constructs and Patellar Tendon Autografts used for Anterior Cruciate Ligament Replacement in Sheep	Michael J. Smietana
P23	Tendon Mechanical Compromise after Partial Tear Simulation	Jackie Kondratko
P24	Protective Effects of Adipose-Derived Mesenchymal Stem Cells on Tendon Fibroblasts	Cionne Manning
P25	Do Mast Cells Play a Role in Ligament Healing?	Kelsie Brannagan
P26	A 6 Months Follow-up Study of T2 Value of Substituted ACL	Shota Katsumata
P27	Cell Interaction Distance Modulates Chondrocyte Response on Stratified Scaffolds	Xinzhi Zhang
P28	Dose-dependent Effect of 2-phosphoascorbate on Material Properties of 3D Porcine Tenocyte-populated Bioartificial Tendon	Jie Qi
P29	A Magnesium-Based Ring for Mechanical Augmentation of a Torn Anterior Cruciate Ligament—A New Experimental Animal Model	Kathryn F. Farraro
P30	Tenomodulin Promoted Tendon-derived Stem Cell Proliferation and Inhibited Angiogenesis – A Possible Molecular Mechanism of Tendinopathy	Qi Tan

Savio L-Y. Woo Young Researcher Award Winner

Biological Research

CHRONIC ROTATOR CUFF TEAR CHANGES THE EXPRESSION OF SEVERAL SMALL NON-CODING RNA MOLECULES THAT REGULATE MUSCLE ATROPHY, FIBROSIS AND AUTOPHAGY

Gumucio J.P., Lynch E.B., Davis M.E., Stafford P.L., Bedi A., Mendias C.L.
Department of Orthopaedic Surgery, University of Michigan, Ann Arbor

INTRODUCTION

Rotator cuff tears are among the most frequent conditions treated by shoulder surgeons, but our ability to fully restore mobility and function remains limited despite a structurally intact repair. A common pathophysiological change that occurs in torn rotator cuff muscles is atrophy of muscle fibers and an accumulation of fat in the muscle.¹ These changes are collectively referred to as "fatty atrophy." Previous studies in humans have failed to demonstrate a reduction in fatty atrophy following surgical repair.¹

The molecular etiology of fatty atrophy following rotator cuff tears remains unknown, and gaining greater insight into the mechanisms that lead to the development of fatty atrophy will likely improve the recovery of patients who undergo surgical repair of a torn rotator cuff. Many studies to date surmise that the fat accumulating in torn rotator cuff muscles is a result of adipogenesis, and the formation of mature adipocytes within the muscle.² However, the molecular mechanisms behind the formation of fat and proposed adipogenesis has yet to be elucidated.

MicroRNAs (miRNAs) are small non-coding RNA molecules that play important roles in the post-transcriptional regulation of many protein-coding mRNA molecules. miRNAs are typically either transcribed from the introns of protein-coding genes or from intergenic regions of DNA. miRNAs recognize complementary sequences in the 3'UTR regions of target genes and, in association with the RNA-induced silencing complex (RISC), target specific mRNAs for rapid degradation. miRNA molecules play important roles in the pathogenesis of several diseases including cardiovascular disease and various skeletal muscle myopathies. They also make important contribution to the remodeling of skeletal muscle in response to exercise training. As miRNAs play central roles in muscle pathogenesis and adaptation, we tested the hypothesis that a chronic tear of the rotator cuff change the expression of miRNA molecules with known or suspected roles in muscle atrophy, fibrosis, lipid accumulation and autophagy.

METHODS

This study was approved by the University of Michigan IACUC. Six-month old male Sprague Dawley rats (N=6) were used in this study. A tenectomy was performed on the supraspinatus and infraspinatus tendons of the right shoulder, while the left shoulder served as the sham-operated control. One month following the tear, muscles were harvested and prepared for histology or RNA isolation using an miRNeasy kit (Qiagen). RNA was reverse transcribed into cDNA using a miScript RT kit, and using miRNA qPCR arrays the expression of 88 of the most well known miRNA molecules was measured in a real-time thermal cycler. The expression of target genes was normalized to Rnu6, and expression of the torn side was further normalized to the control side. The combination of all miRNA transcripts that were significantly upregulated were analyzed with DIANA-miRPath software³ to identify molecular pathways that are potentially altered by the expression of these miRNAs. Based on the results of the DIANA-miRPath results, we examined the expression of macrophage and autophagy markers by reverse transcribing mRNA into cDNA using a RT² First Strand Kit (Qiagen) and analyzing the expression of target genes in a real-time thermal cycler. Values presented are mean±SEM and differences between sides were tested using paired t-tests ($\alpha=0.05$).

For histology, muscles were frozen in TissueTek OCT and sectioned at 10µm. Light microscopy sections were stained with hematoxylin and oil red O to measure fat content of the muscle. Fluorescent microscopy sections were labeled with DAPI to identify nuclei, WGA-lectin to identify extracellular matrix (ECM), BODIPY to identify lipid, and F4/80 to identify macrophages. Sections were imaged on a Zeiss Axioplan 2 microscope equipped with an 8MP camera.

RESULTS AND DISCUSSION

As previously described, the tear induced substantial muscle atrophy and fat accumulation as visualized by oil red O staining (Figure 1).

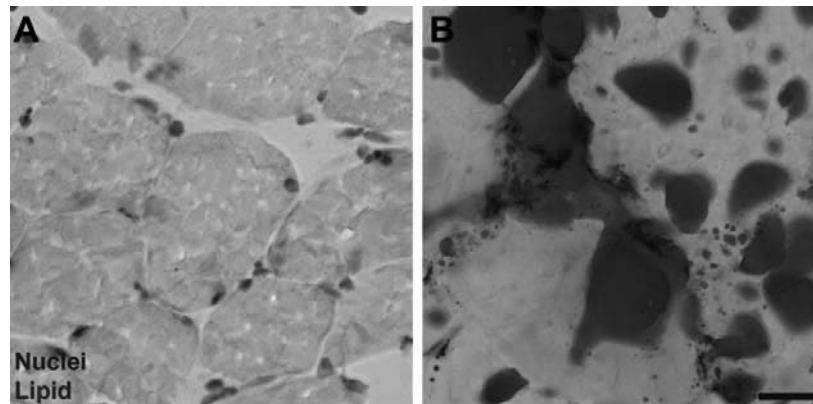


Figure 1. Compared with uninjured rotator cuff muscles (A), rotator cuff tear (B) induces dramatic accumulation of lipid. Hematoxylin, blue; oil red O, red. Scale bar = 25 μ m.

After validating that fatty atrophy was indeed present in the samples, we examined the expression of 88 common miRNA molecules from control and torn muscles. Compared with control muscles, 31 of these miRNA transcripts were upregulated ($P < 0.05$) in torn muscles (Figure 2). We did not identify any miRNAs that were downregulated.

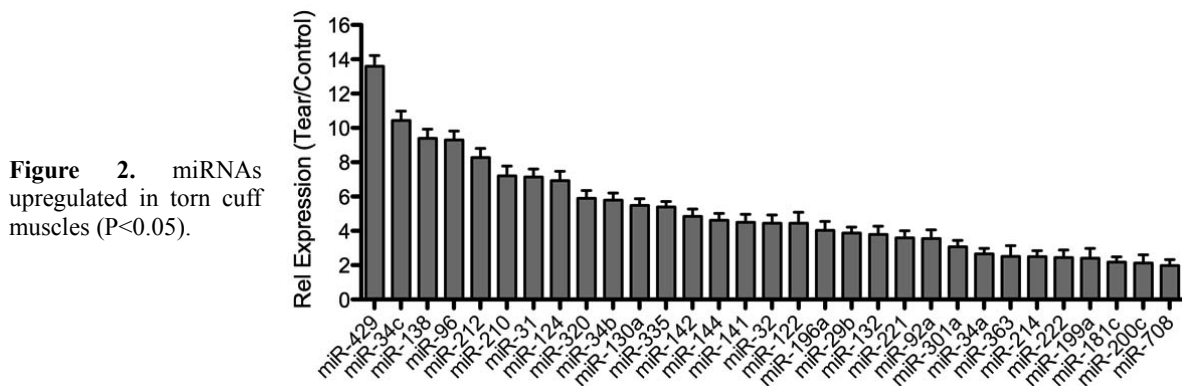


Figure 2. miRNAs upregulated in torn cuff muscles ($P < 0.05$).

We then used DIANA-miRPath to determine which molecular pathways were activated in torn rotator cuff muscles. Pathways that were predicted to be activated in the torn rotator cuff muscles include the ephrin/semaphorin, MAPK, focal adhesion, autophagy, TGF- β , HIF-1 α and ubiquitin-proteasome pathways. The activation of these pathways is consistent with the induction of muscle fiber atrophy and fibrosis, and macrophage recruitment. Interestingly, the leptin, fatty acid synthesis and lipid signaling pathways were predicted to not be activated in the torn rotator cuff muscles.

Based on the results from the DIANA-miRPath analysis, we investigated the expression of genes involved in the regulation of macrophage recruitment and autophagy^{4,5}, F4/80, ApoE, CIDEA and Vps34. F4/80 is a transmembrane protein that is a specific marker for macrophages. ApoE is critical for the breakdown of triacylglyceride residues in lipoproteins, and is highly enriched in a type of fatty macrophage called a foam cell. CIDEA is an important mediator of apoptosis, is involved in lipid droplet formation and is also highly enriched in foam cells. Vps34 is a PI3-kinase that is critical for vesicular formation during autophagy, budding, and required for autophagy in many cells. All four transcripts are upregulated following rotator cuff tear (Figure 3). Consistent with these results, using immunohistochemistry, we identified that all areas of extramyocellular lipid accumulation in torn rotator cuff muscles also had high levels of macrophage infiltration (Figure 4).

CONCLUSIONS

While we found substantial lipid accumulation in torn cuff muscles, all areas of extramyocellular lipid accumulation also displayed substantial evidence of macrophage infiltration. Using a bioinformatics approach, we demonstrate here that the canonical adipogenic pathways are unlikely contributors to the accumulation of fat in torn rotator cuff muscles. This is confirmed by the upregulation of several genes important in the regulation of autophagy. Combined, these results suggest that the lipid accumulation present in torn rotator cuff muscles may not be due to bona fide adipogenesis, but rather might be due to autophagy and infiltration of macrophages and foam cells.

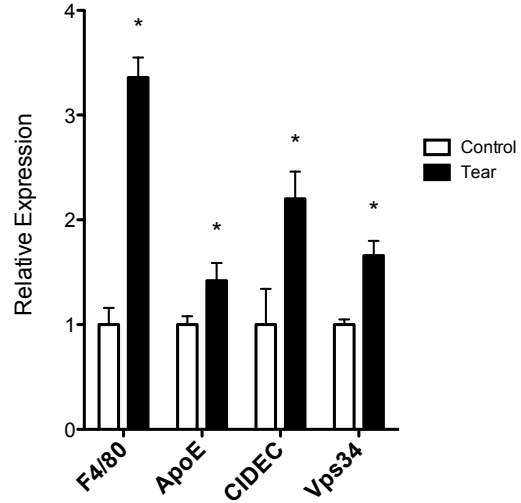


Figure 3. Expression of various mRNA transcripts involved in the regulation of autophagy and macrophage recruitment in control and torn rotator cuff muscles. *, $P < 0.05$.

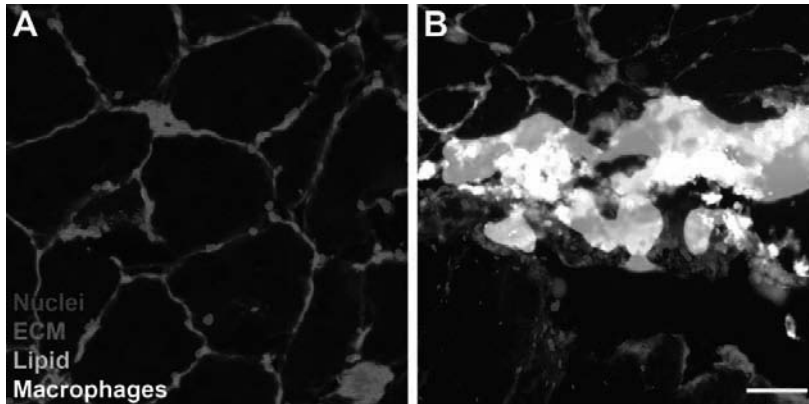


Figure 4. Compared with uninjured rotator cuff muscles (A), rotator cuff tear (B) induces a pronounced atrophy of muscle fibers and accumulation of lipid. Additionally, macrophages are noted to be present in areas of lipid accumulation. Nuclei (DAPI), blue; ECM (WGA-lectin), red; lipid (BODIPY), green; macrophages (F4/80), white. Scale bar = 50 μ m.

ACKNOWLEDGEMENTS

This work was supported by grant AR058920 from NIAMS.

REFERENCES

1. Gladstone J.N. et al. *Am J Sports Med.* 2007 May;35(5):719-28.
2. Kim HM, Galatz L.M., Lim C, Havlioglu N, Thomopoulos S. *J Shoulder Elbow Surg.* 2011
3. Papadopoulos G.L. et al. *Bioinformatics.* 2009 Aug 1;25(15):1991-3.
4. Li H. et al. *Int J Mol Med.* 2010 Aug;26(2):231-9.
5. Frost R.A., Lang C.H. *Physiology.* 2011 Apr;26(2):83-96.

**ACL INJURY AND TUNNEL LENGTH
-TRANSTIBIAL VERSUS FAR ANTEROMEDIAL PORTAL TECHNIQUE
FOR POSTEROLATERAL FEMORAL TUNNEL DRILLING
IN ANATOMIC DOUBLE-BUNDLE ANTERIOR CRUCIATE LIGAMENT RECONSTRUCTION-**

Mitsuo Ochi, Atsuo Nakamae, Nobuo Adachi, Masataka Deie,
Department of Orthopaedic Surgery, Graduate School of Biomedical Science, Hiroshima University,
Hiroshima, Japan

INTRODUCTION

In double-bundle anterior cruciate ligament (ACL) reconstruction, the far anteromedial portal technique allows more flexibility in accurate anatomical positioning for femoral tunnel drilling than the transtibial technique. However, recent cadaveric studies have identified several potential risks of femoral tunnel drilling for posterolateral (PL) bundles utilizing the far anteromedial portal technique for double-bundle ACL reconstruction; these risks include limited tunnel depth, interposition of soft tissues between the EndoButton and femoral cortex, iatrogenic damage to the peroneal nerve, and blowout of the posterior cortex of the lateral femoral condyle. The purpose of this study was to compare the clinical results of the transtibial and far anteromedial portal techniques for PL femoral tunnel drilling in double-bundle ACL reconstruction. In addition, in cadaveric knees, we evaluated the length of femoral tunnel for PL bundle prepared with the far anteromedial portal technique in varying degrees of knee flexion.

METHODS

The first study involved 50 patients who underwent double-bundle ACL reconstruction and were followed-up for more than 2 years. The anteromedial bundle was reconstructed using the far anteromedial portal technique in all patients. However, the PL bundle was reconstructed using the transtibial and far anteromedial portal techniques in 22 (group T) and 28 (group F) patients, respectively. The follow-ups included evaluation of Lysholm knee scores, measurement of anterior knee laxity using an arthrometer (KT-2000), the pivot-shift test, and radiography.

In the second study, we used ten human cadaveric knees (5 matched pairs). Femoral tunnels for PL bundle were prepared by the far anteromedial portal technique. Guidewires for femoral tunnel drilling were advanced in varying degrees of knee flexion (90°, 110°, and 130°). Intraosseous tunnel length was measured in each knee.

RESULTS

In the clinical study, the length of the PL femoral tunnel in group F (32.2 mm) was significantly shorter than that in group T (39.0 mm). Lateral knee radiographs showed that the positions of the EndoButtons for the PL bundles were significantly more posterior (12.8 mm) and distal (3.1 mm) in group F than in group T. The average KT-2000 side-to-side difference in group T (0.9 mm) and F (0.7 mm) did not significantly differ. In addition, no significant difference was noted between the groups with respect to Lysholm knee scores and the pivot-shift test results.

In the cadaveric knee study, the average length of the PL femoral tunnel was 25.4 mm in 90° of knee flexion, 31.7 mm in 110°, and 32.8 mm in 130°. The tunnel length in 90° of knee flexion was significantly shorter than those in 110° and 130° of knee flexion.

DISCUSSION

Although recent cadaveric studies identified several potential risks of femoral tunnel drilling for PL bundles utilizing the far anteromedial portal technique, this study showed that the far anteromedial portal technique is as effective as the transtibial technique and results in good restoration of joint stability and knee scores in spite of shorter femoral tunnel length and inferoposterior position of the EndoButton.

In the far anteromedial portal technique, more than 110° of knee flexion is desirable with respect to the femoral tunnel length for the PL bundle.

REFERENCE

Nakamura M, Deie M, Shibuya H, Nakamae A, Adachi N, Aoyama H, Ochi M. Potential risks of femoral tunnel drilling through the far anteromedial portal: a cadaveric study. *Arthroscopy* 2009;25(5):481-7.

BIOLOGY OF HEALING AND BIOMECHANICS AFTER ACL RECONSTRUCTION

C.B. Frank and N. G. Shrive

McCaig Institute for Bone and Joint Health, University of Calgary, Calgary, AB

CLINICAL PROBLEM: Injuries to the anterior cruciate ligament (ACL) are common and it is well known that a complete tear of the ACL in a high risk individual can lead to on-going instability, meniscal tears, secondary progressive cartilage degeneration, and osteoarthritis (OA). Surgical reconstruction of the ACL using various autograft or allograft tendons has evolved as the best surgical solution for “restoring” normal ligament functions. However, in spite of apparently clinically successful ACL reconstruction, there is still a significant incidence of secondary OA. As of this 2012 ISL&T symposium, the combination of biomechanical or biological changes that are actually responsible for OA development in ACL deficient or ACL reconstructed joints, remains to be determined.

BIOMECHANICAL CHANGES AFTER ACL RECONSTRUCTION: It is well established clinically that surgical replacement of the ACL with tendon autografts or allografts can restore functional joint stability in the majority of patients. Meniscal tears in particular appear to have major consequences to the unstable knee, so it is hoped that reconstruction will protect the menisci by virtue of relative normalization of kinematics. Some have shown that surgical repair after ACL injury does appear to protect the knee from developing abnormal knee motion (e.g.: Isberg et al. 2011). However, others have demonstrated some on-going kinematic abnormalities following ACL-reconstruction in comparison to the intact contralateral knee (e.g.: Papannagari et al. 2006). Recent studies have demonstrated that the simple mechanics of walking leads to continual loading/unloading cycles on the articular cartilage (Koo et al. 2011). Furthermore, Andriacchi et al. (reviewed in 2009) have reported that peak knee adduction moment during normal walking influences the variations observed in medial and lateral cartilage thickness in healthy and osteoarthritic subjects. In addition, regional wearing of cartilage has been observed in subjects with ACL injuries due to the anterior-posterior translation or internal-external rotation (Andriacchi et al. 2009). Moreover it has been demonstrated that individuals with ACL reconstructive surgery exhibit an increased peak knee-abduction moment that may lead to the earlier onset of knee OA in this population (Butler et al. 2009). Animal models of ACL reconstruction can be used as an alternative to defining the biomechanical effects of ACL grafting. Our recent studies using an ovine animal model have demonstrated that in spite of identical combined ACL and medial collateral ligament (MCL) injuries, some interesting inter-animal variations in instability, inflammation and OA were noted. Inflammation of the synovium appears to be implicated in this individuality in some way. Moreover, significant kinematic abnormalities in medial-lateral (ML) translation appear to correlate best with early OA in sheep. We have also found that what we consider to be "idealized ACL reconstructions" (anatomic reconstruction using the native ACL cored out at one end only) do not totally prevent OA for reasons that we are still exploring.

BIOLOGICAL CHANGES AFTER ACL RECONSTRUCTION: The biological changes following tendon autografting include a variety of interesting effects. Remodeling of the grafts appears to take place over many months, beginning with some cell death and repopulation with some new cells that include revascularization. The increased blood flow observed in the initial period after the surgery gradually returns to normal levels with time. Although increased angiogenesis is essential for providing nutrients to the remodeling ligament, it is also associated with enhanced tissue degradation caused by the elevated expression of matrix metalloproteinases. There is growing evidence that cytokines such as tumor necrosis factor (TNF) α , interleukin (IL) 1 β , IL-6, bone morphogenetic proteins and nitric oxide play an important role in the remodeling of grafted tendons following ACL reconstruction. Furthermore, increases in both oxidative stress markers and pro-inflammatory cytokines have been observed in the synovial fluid following ACL surgery. Some of these cytokines have also been shown to induce oxidative and nitrative stress thereby mediating muscle atrophy (Zysk et al. 2004; Barker et al. 2009) and therefore possibly also contributing to the results of ACL grafts in other ways.

CONCLUSIONS: Changes in the biology of grafts (including their inflammation and degradation) may be responsible for subtle mechanical changes to the graft tissue and perhaps to other joint tissues as well, even in perfectly placed grafts, and this combination of abnormalities may contribute to the development of OA - even after "successful" ACL reconstruction.

REFERENCES:

- Isberg J, et al. (2011). *Knee Surg Sports Traumatol Arthrosc*, 19(10):1634-42.
- Papannagari R, et. al. (2006). *Am J Sports Med*. 34(12):2006-12.
- Koo S et al. (2011) *J Biomech*. 29;44(7):1405-9.
- Andriacchi TP et al. (2009) *J Bone Joint Surg Am*. 2009 Suppl 1:95-101
- Butler RJ et al. (2009). *Br J Sports Med*.;43(5):366-70.
- Zysk SP et al. (2004). *Knee Surg Sports Traumatol Arthrosc*..12(2):98-103.
- Barker, T. et al. (2009). *Free Radic Biol Med*. 46(5):599-606..

LOCAL ADMINISTRATION OF ALENDRONATE REDUCED PERI-TUNNEL BONE LOSS AND PROMOTED GRAFT-BONE TUNNEL HEALING IN ACL RECONSTRUCTION

*^{1,2}Yuk Wa Lee, *^{1,2,3}Pauline Po Yee Lui, ^{1,2}Tsui Yu Mok, ^{1,2}Yau Chuk Cheuk, ^{1,2}Kai Ming Chan

¹Department of Orthopaedics and Traumatology, The Chinese University of Hong Kong.

²The Hong Kong Jockey Club Sports Medicine and Health Sciences Centre, Faculty of Medicine, The Chinese University of Hong Kong.

³Program of Stem Cell and Regeneration, School of Biomedical Science, The Chinese University of Hong Kong

*Lee YW and Lui PPY have equal contribution in this study.

INTRODUCTION

Peri-tunnel bone loss was commonly observed after ACL reconstruction both clinically and in animal model. We have reported that systematic administration of alendronate reduced peri-tunnel bone resorption and promoted graft-bone tunnel healing at early stage post-ACL reconstruction. However, we observed systematic increase in bone mineral density in the contralateral intact knee, particularly at the tibial metaphysis. While we did not observe any negative effect of this increase and the administration of alendronate is only for limited time post-reconstruction, we asked if local administration of alendronate into the bone tunnel during ACL reconstruction could achieve similar benefits yet without the systematic effect on bone. This would also reduce the frequency of alendronate administration and increase the compliance of patients to the treatment in the future. This study therefore aimed to investigate the effect of local administration of alendronate on the reduction of peri-tunnel bone loss and promotion of tendon graft to bone tunnel healing in a rat ACL reconstruction model.

METHODS

ACL reconstruction was performed in 72 male Sprague Dawley rats with flexor tendon autograft. The rats were divided into 3 groups: mid dose, low dose alendronate and saline. For local administration, alendronate at 6µg/kg (low-dose group) or 60µg/kg (middle-dose group) was applied to the tibial and femoral bone tunnels, respectively, for 2 minutes before graft insertion and repair. At week 2 and 6, the reconstructed complex was harvested for vivaCT imaging, followed by biomechanical test (n=9/time point) or histology (n=3/time point).

RESULTS

Similar to systematic administration of alendronate, there was significant increase in BMD and BV/TV at the femoral tunnel and metaphyseal region of tibial tunnel at week 2 and week 6 after local administration of alendronate. Local administration of alendronate significantly increased the peri-tunnel BMD and BV/TV at the metaphyseal region of tibial tunnel at week 2 and all tunnel regions at week 6. Local administration of low-dose of alendronate significantly increased the pull-out strength of the reconstructed complex at week 2 but not at week 6 when the failure mode changed from graft pull-out from femoral tunnel to graft mid-substance failure. There was no significant increase in BMD in the knee region in the contralateral limb.

DISCUSSION

Local administration of low-dose alendronate reduced peri-tunnel bone loss, promoted bone tunnel mineralization and increased pull-out strength of reconstructed complex at early stage after ACL reconstruction.

ACKNOWLEDGEMENT

This project is supported by the GRF (project no. 470808, 08/001/ERG) from the University Grant Council and the Hong Kong Jockey Club Charities Trust.

EFFECTS OF ALTERING GRADE ON VERTICAL GROUND REACTION FORCES AND ACL FORCES IN THE SHEEP MODEL

¹R.J. Nesbitt, ¹S.T. Herfat, ²M.T. Galloway, ¹C. Gooch, ¹D.L. Butler, ¹J.T. Shearn

¹Department of Biomedical Engineering, University of Cincinnati, Cincinnati, OH ²Cincinnati Sports Medicine, Cincinnati, OH

INTRODUCTION. Functional demands placed on the human knee's anterior cruciate ligament (ACL) vary with activity but remain impossible to measure directly in-vivo¹. Our lab is characterizing these demands in the sheep model by reproducing recorded in-vivo knee kinematics during activities of daily living (ADLs) and measuring the 3D forces in the ligament. However, these ADLs must be carefully chosen to challenge the knee and capture a broad range of ACL forces. In this study, we sought to determine how varying ADLs (level, inclined, and declined walking) influence vertical ground reaction forces (VGRFs) and ACL force, as indicated by an arthroscopically implantable force probe (AIFP, Microstrain, Burlington, VT). We hypothesized that while declined walking should lower hind limb VGRFs, ACL forces will increase due to the stabilizing effect of the knee's extensor mechanism.

METHODS. Four (4) skeletally mature, female Suffolk sheep (age: 3-6 yrs; weight: 150-200 lbs) were used in this IACUC approved study. Pre-surgery VGRFs were recorded at one speed (1 m/s) during level (0°), inclined (+6°), and declined (-6°) walking conditions using an instrumented treadmill (Kistler Gaitway, Amherst, NY). One author (MG) then surgically exposed the left hind limb ACL, longitudinally split its fibers, and implanted an AIFP into a small pouch in the midstance. VGRFs and AIFP activity (expressed as % maximum activation) were then simultaneously recorded for all grades (N=2). All data for each animal were normalized over a full gait cycle using at least 5 consecutive strides.

RESULTS. Vertical Ground Reaction Forces (N=4): Compared to level walking (42.05±1.40%BW), inclined walking significantly increased average hind limb VGRFs (46.66 ± 0.45 %BW; p<0.001) while declined walking significantly decreased average hind limb VGRFs (37.45 ± 2.11 %BW;p<0.05) (Fig 1A). In the right hind limb, inclined walking also significantly increased peak VGRFs (59.85 ± 1.65 %BW) compared to declined walking (53.91±3.81 %BW; p<0.05). **Force Probe Voltages (N=2):** Compared to level walking (15.33 ± 0.51 %), inclined walking decreased average AIFP activity levels (8.92 ± 0.63 %), while declined walking increased these values (25.36 ± 1.11 %) (Fig 1B).

DISCUSSION. Each grade condition affected both hind limb VGRFs and AIFP activity, demonstrating that these conditions provide unique challenges to the knee. Our current VGRF values during level and inclined walking are consistent with previous data from our lab². These preliminary results suggest that declined walking does result in higher ACL force despite resulting in lower VGRFs, supporting our hypothesis that declined walking is a greater challenge for the ACL. Trends in ACL probe activity are apparent across the gait cycle for all three inclinations. Most notable is the large spike in activity at left limb heel strike during declined gait, implicating the aforementioned stabilization effect imposed by the knee's extensor mechanism. Also of note is the small rise in activity as the left limb loses contact with the treadmill, possibly marking push off forces at left limb toe-off. Surgical effects on response measures were minimized by implanting sensors through the medial aspect of the joint, avoiding major tendon and ligament groups. Comparisons of pre- and post-surgery VGRFs showed that average hind limb values were restored to at least 90%, and peak values of the operated limb to at least 80% (data not shown). However, hind limb stance duration was significantly affected, with the left (operated) limb maintaining stance for a shorter time, as can be observed by comparing the distances between the first and last dashed lines in each figure. Ongoing studies aim to expand our data set and to quantify the 3D forces and torques on the ACL by reproducing measured in vivo motions on a 6-DOF robot, using AIFP data for external validation.

ACKNOWLEDGEMENTS. Support from NIH grant AR056660-01.

REFERENCES: [1] Butler et al. CORR, 2004; [2] Herfat et al. J Biomech Eng, 2011

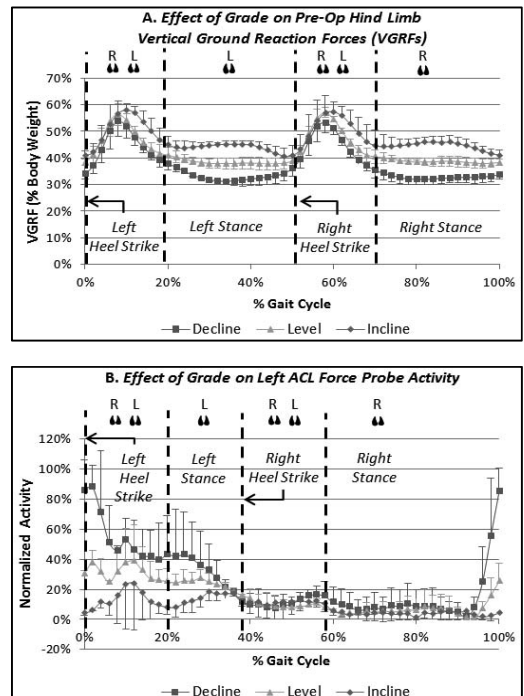


Figure 1 A. (Pre-Surgery VGRFs) Compared to level, inclined gait increases VGRFs while declined gait decreases VGRFs. **B.** (Post-Surgery AIFP activity) During declined gait, AIFP activity of the left ACL peaks at left heel strike. Values for level and inclined gait are lower throughout the gait cycle.

EFFECT OF COMBINED ACL AND MENISCUS INJURIES ON KNEE JOINT KINEMATICS

Guoan Li; Jing-Sheng Li; Ali Hosseini; Hemanth Gadikota; Thomas Gill
Orthopaedic Bioengineering Laboratory
Harvard Medical School and Massachusetts General Hospital, Boston, MA 02114, USA

INTRODUCTION

Although ACL reconstruction has been widely accepted as an efficient surgical treatment of the ACL injured knees, long term joint degeneration has been observed in up to 62% of the patients [1]. While various ACL reconstruction techniques have been shown to be efficient in restoration of knee stability in AP translation [2], few data has been reported on the effect of combined injuries of other soft tissues on knee joint function [3]. This study investigated the rotational stability of the knee after injury of the ACL with or without a combined medial or lateral meniscus injury during stair ascending activity.

METHODS

With IRB approval, 21 ACL injured patients (with contralateral side intact) were recruited in this study before undergoing ACL reconstruction, where 5 had isolated ACL injuries; 8 had combined medial meniscus injuries; and 8 had combined lateral meniscus injuries. Both knees of each patient were MRI scanned for construction of 3D anatomic knee models; and were then scanned during stair ascending (Fig. 1) using a dual fluoroscopic image system. The 6DOF knee kinematics during stair ascending was reproduced using the 3D knee models. The kinematics of the injured knee was compared to that of its intact contralateral side. In this study, we specifically examined the axial rotation of the knee during the stair ascending extension.

RESULTS

Joint rotation at the second 50% of the stair ascending cycle (knee extended from $\sim 30^\circ$ to full extension) were different among the ACL injured patients with different injury conditions of the meniscus (Fig. 2). The knee has reduced internal tibial rotation (by $\sim 5^\circ$) compared to the intact contralateral side if only has isolated ACL injury. The change of tibial rotation was small if the knee has a combined medial meniscus injury. When there is a combined lateral meniscus injury, the knee has an increased internal tibial rotation during the stair ascending.

DISCUSSION

The data revealed that the knee joint rotation was affected differently if the knee had combined ACL and meniscus injuries. Most of current sports medicine research has been focused on the knee with isolated ACL injuries. Accordingly, contemporary ACL reconstructions have been mostly designed based on the knowledge on isolated ACL injuries. Considering the different effect of meniscus injuries on knee joint kinematics, future studies should focus on specific treatment of combined ACL and meniscus injuries in order to protect the joint from post-operative degeneration.



Figure (1) Subject during the stair ascending exercise in a dual fluoroscopic image system.

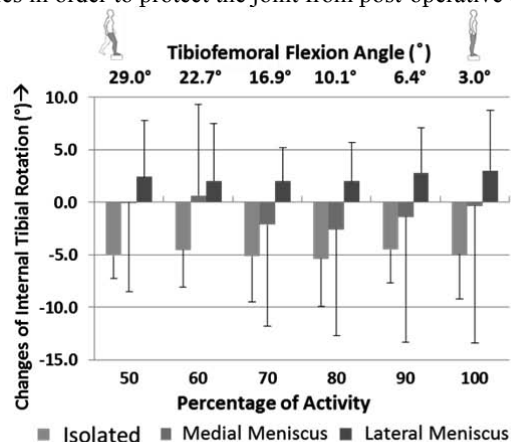


Figure (2) Internal tibial rotation during the second-half of stair ascending exercise in isolated ACL injured knees and combined medial or lateral meniscus injured knees.

REFERENCES

- [1] Keays SL et al., Am J Sports Med. 2007;35(5):729-39.
- [2] Sim JA et al., Am J Sports Med. 2011 Sep 9
- [3] Chhadia AM et al., Am J Sports Med. 2011;39(9):1984-9.

CHARACTERIZATION OF INFLAMMATION FOLLOWING ACL INJURY

C.M. Haslauer, B. Proffen, and M.M. Murray
Children's Hospital Boston, Boston MA

INTRODUCTION

The anterior cruciate ligament (ACL) is the most commonly injured ligament of the knee, requiring surgery to restore it to near-normal kinematics. Surgical techniques employ the use of autografts or allografts, however, primary repair of the ACL has regained interest as it potentially reduces donor site morbidity. Previous studies have shown promising results in a large animal model when primary repair is combined with an enhanced suture technique (1). Yield load and linear stiffness were improved with the addition of a collagen-platelet composite scaffold. In a follow-up study, primary repair following a delay of 2 or 6 weeks was compared to primary repair immediately following injury (2). The results indicated a significant decrease in yield load, maximum load, and linear stiffness in the animals subjected to a clinically relevant delay period. Therefore, we hypothesize there exist several mechanisms which promote inflammation, and consequently catabolic changes, in the ACL, preventing the healing process observed following immediate repair.

METHODS

Complete ACL transection was performed unilaterally on 12 adolescent Yucatan minipigs. C-reactive protein (CRP) concentration in serum was measured prior to transection and 1h, 3h, 1, 3, 5, 7, 9, 12, and 14 days following ACL injury (n=3 per time point). Minipigs were sacrificed at 1, 5, 9, and 14 days (n=3) and tissue harvested from the ACL and synovium. Quantitative real-time PCR analysis performed to quantify changes in expression of several genes of interest, including matrix metalloproteinase-1 (MMP-1), macrophage inflammatory protein (MIP-1), interleukin 1 receptor antagonist (IL-1RA), and Col 1 and 3.

RESULTS

Results indicate a significant increase in CRP in serum at day 1 (**Figure 1**). CRP levels remain elevated, though slightly decreased, on days 3 and 5. By day 7, CRP levels returned to pre-injury values. MMP-1 expression in the ligament decreased initially; however, an upregulation in expression was observed by day 14 (**Figure 2**). An increase in MMP-1 expression was observed at all time points in synovium. A significantly increased fold change was observed for IL-1RA expression in both ligament and synovium tissue at 1 day when compared to tissue obtained from intact knees (data not shown). This change was diminished by 5d and remained near normal levels.

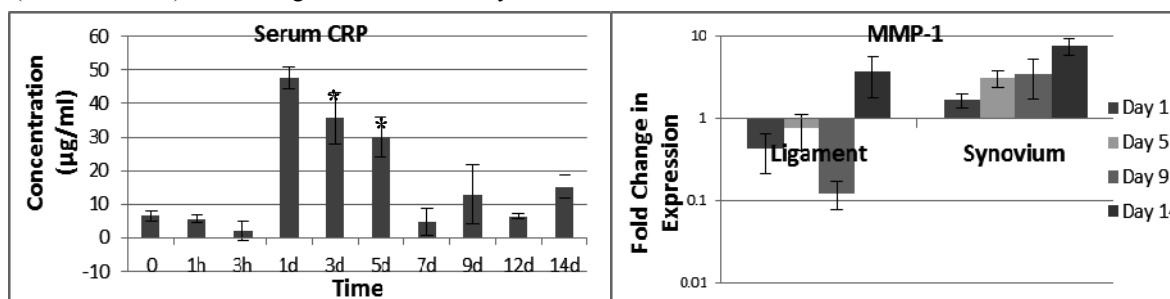


Figure 1. Serum CRP levels following ACL injury. Significant differences are specified by * ($p < .05$). *

Figure 2. Fold change in MMP-1 expression over 14d following ACL injury compared to uninjured control.

DISCUSSION

C-reactive protein is an acute-phase protein found in the blood whose levels increase in response to both acute and chronic inflammatory changes, including tissue injury. Baseline porcine CRP levels typically range from 5-30 µg/ml and may increase 10-25 fold in response to inflammation (3). Results indicate a significant increase in CRP in serum occurs within 24 h following ACL injury, and remain significantly elevated through day 5. IL-1RA is a natural inhibitor of the pro-inflammatory effects of IL-1 β (4) and exhibited at least a 10 fold increase in expression at day one in both the ligament and synovium before returning to normal expression levels by day 5. MMP-1 plays an important role in tissue remodeling, and breaks down type I and III collagen when activated. Following an initial decrease in MMP-1 expression in the ligament, levels are increased at 14d. MMP-1 expression levels increase immediately following injury in the synovium and remain elevated through the 2wk period. These results indicate an inflammatory condition is initiated by ACL injury and can be characterized by protein and gene expression changes.

ACKNOWLEDGEMENTS This work was supported by a grant from the NIAMS AR054099 (MMM).

REFERENCES: 1. Joshi et al. Am J Sports Med 2009. 2. Magarian et al. Am J Sports Med 2010. 3. Martinez-Subiela et al. Luminescence 2007. 4. Perrier et al. FEBS Lett 2006.

BIPLANAR X-RAY DERIVED ACL EXCURSIONS DURING A JUMP-CUT MANEUVER ASSOCIATED WITH ACL INJURY

D.L. Miranda, M.J. Rainbow, J.J. Crisco, B.C. Fleming

Department of Orthopaedics, Warren Alpert Medical School of Brown University, Providence, RI

INTRODUCTION

Activities involving jumping and cutting are commonly associated with non-contact ACL injury. High-speed biplanar x-ray provides a means to accurately quantify joint kinematics and ligament length changes during dynamic activities. The purpose of this study was to compare how ACL length and knee kinematics change across three phases of a jump-cut maneuver.

METHODS

After granting their informed consent, 10 healthy volunteers (5M, 25±4.2 yrs; 5F, 26±2.3 yrs) were instructed to perform a jump-cut maneuver associated with a non-contact ACL injury. Three targets were placed in the testing environment for the subject to land on and jog toward: one on the center of a force plate and the other two 45° and 1 m from the landing target [1]. For each trial, the subject stood 1 m from the force plate with their knees bent at 45°. When the subject jumped toward the landing target, a visual prompt instructed the subject to perform a sidestep cut (L or R) and jog toward the respective angled target. Ten trials were performed and the subject was unaware of the directional prompt prior to each trial. 3-D femur and tibia models were created (Mimics 13) and their respective ACL insertion sites were outlined (Geomagic 11). Biplanar x-ray (<http://www.xromm.org>) data was collected at 250Hz during 3 trials. Ground reaction forces (GRF) were time synchronized and collected at 5,000Hz. CT scans were obtained for each subject's imaged leg. The biplanar x-ray data were processed using custom markerless tracking software (Autoscooper; Brown University, Providence, RI). The center of each insertion site was then tracked using the biplanar x-ray motion data, and the ACL length was determined as the distance between the insertion site centroids. Percent ACL elongation was calculated as: $[L_{ACL_i} - L_{ACL_{ref}}] / L_{ACL_{ref}}$, where L_{ACL_i} is the length of the ACL at a given time-point and $L_{ACL_{ref}}$ is the ACL length as determined from the CT scan. Knee joint add/abd and int/ext rotations were determined using Visual3D. All data were separated into three periods: flight phase to contact (A), contact to peak GRF (B), and following peak GRF (C). All trials were time normalized within each period and ensemble averaged across each subject's trials. The total excursions of the ACL (max-min), add/abd, and int/ext rotations were determined for each subject across each period. Kruskal-Wallis and Dunn's multiple comparison tests were used to test for significant differences between periods.

RESULTS

The median ACL excursion values varied significantly across the three periods ($P=0.026$). The ACL lengthened to the greatest extent (Fig.1.i) after peak ground reaction force (period C). Median add/abd excursion (Fig.1.ii) was not found to be statistically significant across periods ($P=0.117$). However, the median int/ext rotational excursion varied significantly across the three periods ($P<0.0001$). External rotation of the tibia occurred prior to contact. Internal rotation of the tibia began after contact and through peak GRF (Fig.1.iii).

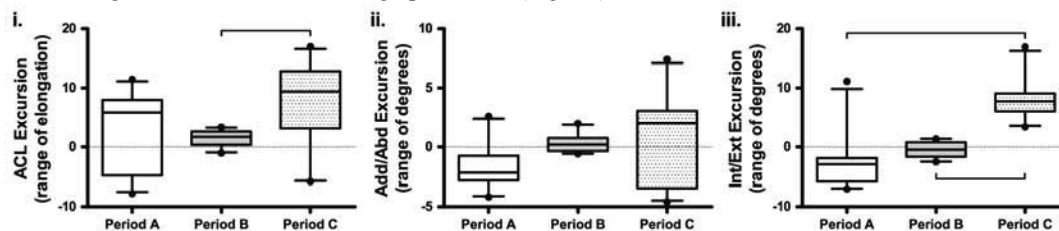


Fig.1: Signed ACL excursion (i), add/abd excursion (ii), and int/ext excursion for periods A, B, and C. The bracketed lines connecting box plots denotes that a pairwise statistical differences was found.

DISCUSSION

An increase in ACL elongation and internal rotation of the tibia occurred after ground contact, most notably after the peak GRF. This is consistent with results of Tashman et al., where the ACL lengthens and the tibia internally rotates after foot strike during downhill running [2]. Additionally, these results support the proposition that excessive internal tibial rotation could produce strains contributing to ACL failure. While this study is limited by subject number, it provides insight into how knee rotations affect ACL biomechanics during an activity associated with non-contact ACL injury. It is our intent to use biplanar x-ray to elucidate differences between gender and injury condition (ACL deficiency and reconstruction).

ACKNOWLEDGEMENTS

This study was funded by grants from the W.M. Keck Foundation and the NIH (R01-AR047910-07; P20-RR02484).

REFERENCES: 1. Ford et al. Med Sci Sports Exerc 2005. 2. Tashman et al. Am J Sports Med 2004.

EFFECT OF GRAFT FIXATION ANGLES ON KNEE KINEMATICS, GRAFT TENSION CURVES AND LOAD SHARING IN DOUBLE-BUNDLE ANTERIOR CRUCIATE LIGAMENT RECONSTRUCTION

¹Koga, H; ¹Muneta, T; ¹Sekiya, I
¹Tokyo Medical and Dental University, Tokyo, Japan

INTRODUCTION

In double-bundle anterior cruciate ligament (ACL) reconstruction, no consensus exists on an optimal setting of anteromedial bundle (AMB) and posterolateral bundle (PLB) graft fixation angles.¹⁻³ The objective of this study was to evaluate the effect of different graft fixation angles on knee kinematics and graft tension in the AMB and PLB, especially focusing on the fixation angle of the PLB graft.

METHODS

Twenty-four patients who underwent double-bundle ACL reconstruction were included in this study. The AMB and PLB grafts were provisionally fixed to a graft tensioning system during surgery. The graft fixation settings were as follows: 1) AMB at 20° and PLB at 0° (A20P0), 2) AMB at 20° and PLB at 20° (A20P20), and 3) AMB at 20° and PLB at 45° (A20P45). All the grafts were tensioned at a constant stress level. Anterior tibial translation (ATT), internal rotation (IR) and external rotation (ER) at 30° and 90° of knee flexion applied with manual maximum load were measured before graft insertion and in each setting using a navigation system. Bundle tension was recorded during knee flexion-extension and in response to the applied anterior or rotatory loads. A pivot shift test, as well as factors affecting the residual pivot-shift, was also evaluated.

RESULTS

A20P0 was less constrained than A20P45 in IR at 30° and in ER at 30° (Table 1). A20P45 created reciprocal tension curves and load sharing with the tensions of both bundles equivalent during flexion-extension and each loading test at 30°. In A20P0, tension of AMB was constantly higher than that of PLB (Table 2). Seven cases showed grade 1 pivot shift phenomenon in A20P0, while no case showed positive pivot shift in other settings. Larger tension reduction of the PLB between 0° and 30° and smaller load sharing of the PLB were significant factors affecting residual pivot-shift.

DISCUSSION

In double-bundle ACL reconstruction, Fixation of the AMB at 20° and the PLB at 45° created reciprocal tension curves and load sharing between the bundles, and restored better stability than that of the AMB at 20° and the PLB at 0° at the time of surgery, when grafts were tensioned at a constant stress level. Fixation of the AMB at 20° and the PLB at 0° is not recommended, as it would lead to insufficient tension in the PLB and fail to restore reciprocal tension curves and load sharing, resulting in residual pivot shift phenomenon in cases where tension reduction of the PLB near extension was too large.

Table 1. Knee Kinematics Before graft insertion and in Each Graft Fixation Setting (Mean ± SD)

Fixation setting	ATT30 (mm)	IR30 (°)	ER30 (°)	ATT90 (mm)	IR90 (°)	ER90 (°)
Before insertion	13.2 ± 1.4	18.0 ± 4.5	14.2 ± 4.6	7.6 ± 1.6	18.2 ± 3.9	17.0 ± 4.7
A20P0	5.2 ± 1.1 ^a	14.4 ± 3.4 ^a	11.2 ± 2.6 ^a	4.1 ± 2.0 ^a	17.0 ± 4.3	13.3 ± 3.1 ^a
A20P20	5.0 ± 1.4 ^a	13.1 ± 3.5 ^a	9.7 ± 3.2 ^a	3.5 ± 1.9 ^a	16.4 ± 3.9	11.8 ± 3.0 ^a
A20P45	4.7 ± 1.4 ^a	10.6 ± 3.1 ^{ab}	9.2 ± 3.1 ^{ab}	3.3 ± 1.3 ^a	14.7 ± 3.7 ^a	12.1 ± 3.3 ^a

^aSignificant difference compared with Before graft insertion. ^bSignificant difference compared with A20P0.

Table 2. Load Sharing of the PLB Graft^a

setting	30°			90°		
	ATT	IR	ER	ATT	IR	ER
A20P0	38.6 (5.0)	38.7 (5.8)	38.2 (6.3)	33.0 (7.3)	35.8 (6.7)	38.6 (8.1)
A20P20	46.4 (3.5) ^b	47.4 (4.0) ^b	47.6 (4.5) ^b	40.5 (6.2) ^b	43.3 (6.3) ^b	46.4 (6.7) ^b
A20P45	49.1 (3.8) ^{bcd}	49.7 (3.9) ^{bd}	50.0 (5.6) ^{bd}	43.2 (4.4) ^b	45.0 (5.4) ^b	47.5 (7.0) ^{bd}

^aData are presented as mean (SD), expressed as percentages of the total load generated in both bundles in each setting. ^bSignificant difference compared with the A20P0 setting. ^cSignificant difference compared with the A20P20 setting. ^dNo significant difference compared with the AMB graft.

REFERENCES: 1. Miura et al. Am J Sports Med 2006. 2. Murray et al. Arthroscopy 2010. 3. Anderson et al. Am J Sports Med 2010.

INTRA-OPERATIVE SUPPLEMENTATION OF VITAMIN C IMPROVED KNEE LAXITY RESTORATION IN ANTERIOR CRUCIATE LIGAMENT RECONSTRUCTION

W.H. Cheng, S.C. Fu, Y.C. Cheuk, T.Y. Mok, S.H. Yung, L.K. Hung, K.M. Chan

Department of Orthopaedics and Traumatology, The Chinese University of Hong Kong, Hong Kong SAR, China.

INTRODUCTION

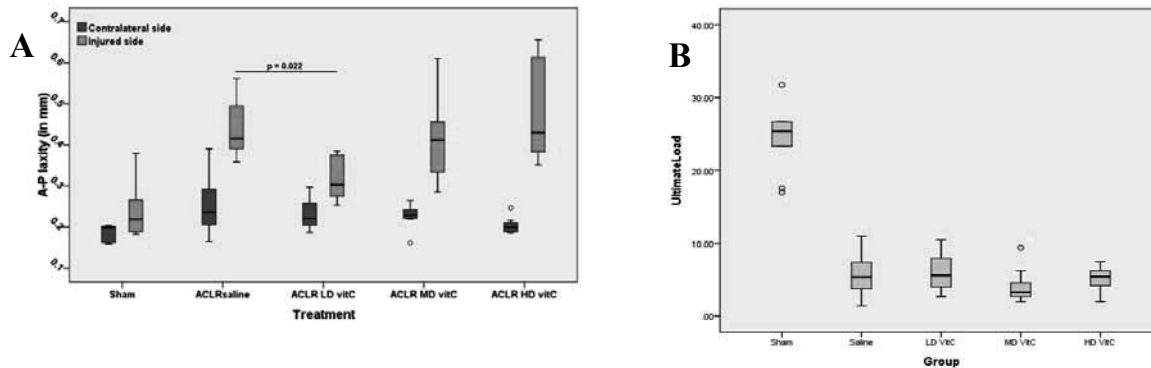
Anterior cruciate ligament (ACL) reconstruction is the standard treatment to ACL tear. However, the healing process after ACL reconstruction (ACLR) is often compromised, and the surgically-restored antero-posterior (AP) laxity is deteriorated at early healing stages and regains very slowly. As oxidative stress at early inflammatory phase can exert unfavorable influences on graft healing, we propose to investigate the effect of intra-operative supplementation of vitamin C on the mechanical restoration after ACLR.

METHODS

Sixty male Sprague Dawley rats were used. After the ACL was transected, ACLR was performed using flexor digitorum longus tendon grafts and fixation to periosteum under constant tension (4N) according to our previous study (Fu et al., 2011). During operation, the wounds and ACL grafts were continually irrigated with normal saline or isotonic solutions (10 ml in total) containing 3 mg/ml (LD), 10 mg/ml (MD) or 30 mg/ml (HD) vitamin C (n=12). A sham operation group with saline irrigation served as control. At week 6, the rats were sacrificed for knee antero-posterior (AP) laxity test and graft pullout test (n=8). The remaining rats from each group were sacrificed at week 1 or week 6 post-op for histological examination (n=2).

RESULTS

At week 6 post-op, increased knee AP laxity was observed in ACLR knees with saline irrigation as compared to sham group. Intra-operative irrigation of low dose vitamin C irrigation saline (LD) significantly restored knee AP laxity as compared to saline group ($p=0.022$) (A), but MD and HD groups did not show significant improvements. With respect to failure load of femur-graft-tibia complex, all vitamin C groups did not show differences as compared to saline group (B). Histological examination showed that cell recruitment in the intra-articular space around the graft was less extensive at day 7 in LD group, and the graft integrity was better preserved. However, the extents of graft remodeling were similar among different groups at week 6 post-op.



DISCUSSION

Our results showed that intra-op supplementation of low dose vitamin C improved knee AP laxity, probably by reducing cell infiltration into graft at early healing stages, thus the release of initial graft tension due to graft degeneration was prevented. However, higher doses of vitamin C did not show positive effects, suggesting an intricate modulation of reactive oxygen species is essential. On the other hand, the tensile strength of the graft complex at week 6 post-op was not affected by intra-op vitamin C irrigation. As knee laxity was restored immediately post-op but graft incorporation was gradually improved, the effect of intra-op redox modulation was limited to early healing stages and only affected graft tension. Further study is necessary to elucidate the dose and time of redox modulation to promote biological augmentation in ACLR.

REFERENCES

Fu SC et al. (2011) Effect of graft tensioning on mechanical restoration in a rat model of anterior cruciate ligament reconstruction using free tendon graft. ISL&T XI, 12 J anuary 2011, Long Beach, California.

DISCLOSURE

The data presented in this poster are used for patent application in US and China.

KNEE KINEMATICS AFTER ACL RECONSTRUCTION USING TRANSTIBIAL AND ANTEROMEDIAL PORTAL SURGICAL TECHNIQUES

¹Hongsheng Wang, ²James E. Fleischli, and ¹Nigel Zheng

¹University of North Carolina at Charlotte, NC, USA; ²OrthoCarolina, Charlotte, NC, USA

INTRODUCTION

Residual kinematic changes still retain in ACL-reconstructed (ACL-R) knees, which could cause abnormal cartilage contact during daily activities and would contribute to a higher prevalence of osteoarthritis (OA) among ACL-R knees in a long term [1-3]. To restore the knee stability, it is important to drill an ACL graft tunnel close to its natural insertion site. In the mostly used transtibial tunnel technique, the femoral tunnel is drilled through the tibial tunnel, in which the tunnel location is often anteriorly and superiorly shifted [4] (Fig. 1). Thus, the graft is usually too vertical in transtibial technique. In anteromedial portal technique, the femoral tunnel is drilled through anteromedial portal and the surgeon has more control at the drilling location, thus it yields an anatomically placed tunnel placement. Anatomically placed grafts are believed to more likely restore the function of the ACL. In this study, we aimed to evaluate the postsurgical knee kinematics of two different surgical techniques during a gait cycle.

METHODS

Thirty-nine patients with unilateral ACL reconstruction using transtibial technique (n=30), anteromedial portal technique (n=9), and 20 healthy controls were recruited and tested by following IRB approved protocol. At the time of testing, they completed rehab (> 4 months after surgery). And there was no significant difference in post-surgery time, body weight and height between the two ACL groups. Skin marker-based motion analysis was performed to measure the knee joint motion following the previous published procedures [3, 5]. The knee joint rotations and translations were expressed in 3 anatomical planes of tibia. Comparisons were made between 3 groups by using one way ANOVA (SPSS, IL, USA), and significance level was set at 0.05. The *pos-hoc* analysis test was performed using Turkey's honestly significant difference (HSD) procedure.

RESULTS

The anteromedial portal knees had more flexion during stance phase compared to other two groups (Fig. 2); both ACL-R groups had less valgus rotation and superior translation at the peak knee flexion (FP2) than healthy group. The anterior translation of anteromedial portal knees was almost the same as the healthy group, while the transtibial knees exhibited significantly greater anterior tibial translation during swing phase.

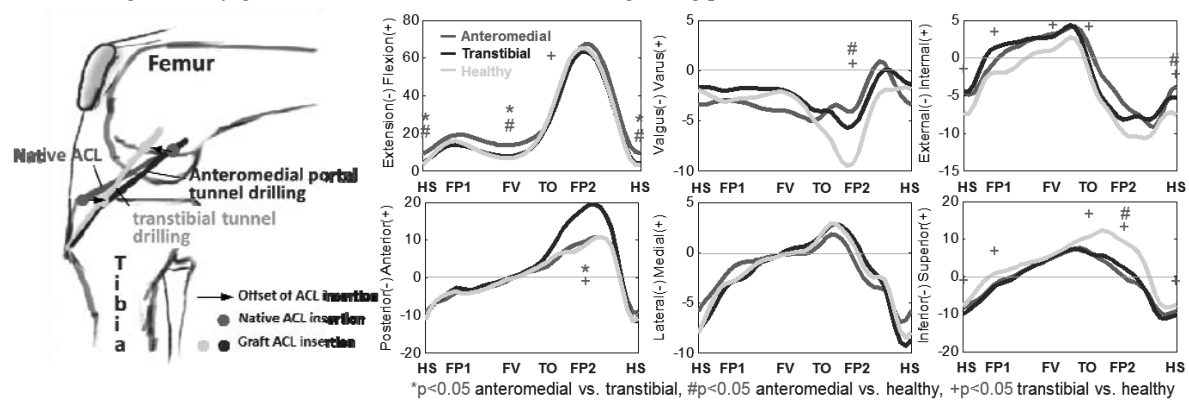


Fig. 1 Tunnel locations in different techniques

Fig. 2 Knee rotations and translations during a gait cycle. HS-heel strike, FP1-flexion peak during stance phase, FV-flexion valley, TO-toe off, FP2-flexion peak during swing phase

DISCUSSION

In anteromedial portal knees, the anatomically placed grafts may have length and orientation closer to native ACL than those in transtibial knees [4, 6]. As a result, it could exert enough constraint to the anterior tibial translation. The more vertical ACL graft in transtibial knees failed to restore the anterior stability. On the other hand, the higher knee flexion angle among anteromedial portal knees might be caused by the posteriorly shifted tibial tunnel location compared to the natural ACL insertion site on tibial plateau. Significantly reduced valgus rotation and superior translation during swing phase may indicate that the ACL grafts were tighter than natural ACL; it may also be caused by a self-protective strategy that flexor muscles constrain the knee motion during swing phase.

REFERENCES: 1. Andriacchi T.P. et al. CORR 2006. 2. Daniel D.M. Am J Sports Med 1994. 3. Gao and Zheng, Clic Biomech 2010. 4. Dargel J. et al. Knee Surg Sports Traumatol Arthrosc 2009. 5. Wang H. et al. Clin Biomech 2011. 6. Abebe E.S. et al. J Biomech 2011.

INTRA-OPERATIVE ASSESSMENT OF JOINT LAXITY IN THE ACL-DEFICIENT AND CONTRALATERAL HEALTHY KNEES

¹P. Imbert, ²C. Belvedere, ²A. Leardini

¹Department of Knee Surgery, Clinique Notre Dame De La Merci, Saint-Raphaël, France.

²Movement Analysis Laboratory, Istituto Ortopedico Rizzoli, Bologna, Italy

INTRODUCTION

Surgical techniques for the reconstruction of the anterior cruciate ligament (ACL) allowed a satisfying correction of the antero-posterior laxity (APL) and of rotational instability. Post-operative recurrence of giving way and unphysiological kinematics were reported in these operated knees. Deeper investigations on this altered joint laxity in the ACL deficient knee (ADK) is therefore essential to comprehend the biomechanical changes occurring after ACL injury. In particular, the quantification of joint laxity also at contralateral healthy knee (CHK), and the analysis of different evaluation tests would offer good references in understanding these alterations (1). The current surgical navigation systems for ACL reconstruction are suitable for carrying out these assessments during operation.

The aim of this study was to point out the extent to which joint laxity is found immediately before surgery, in comparison with the corresponding in the CHK. Navigated techniques were applied on a large patient cohort, through several evaluation tests and considering subject specific skeletal dimensions.

METHODS

Thirty-two consecutive primary ACL reconstructions were performed in patient with a single ADK. During surgery, a navigation system for ACL reconstruction (Praxim, La Tronche, France) was used only for intra-operative measurement. This allows assessment of antero-posterior laxity (APL) and axial rotation range (ARR) by means of marker clusters on the femur and the tibia and a pointer-like cluster used for landmarks digitations. All patients provided written informed consent for intra-operative data collection on both CHK and ADK.

At the beginning of surgery, the CHK was analysed. Anatomical landmarks were digitized percutaneously after careful external palpation. On the thigh, these were the medial and lateral epicondyles; on the shank, these were the medial and the lateral malleoli, the tibial tuberosity, and the most medial and most lateral points of the ridge of the medial and lateral tibial plateau. The tibial anatomical reference frame was based of the digitised landmarks with the origin in the midpoint between the digitized ridges (2). The following laxity tests were then performed: the AP Drawer and the Lachmann test, the internal-external rotation tests, the varus-valgus test, and the pivot-shift test.

Afterwards, the surgeon removed the clusters from CHK, and moved these to the ADK, on which the same procedures were repeated. Once all the data were collected, the surgeon proceeded with the ACL reconstruction surgery according to the standard, i.e. not navigated, procedure.

The relevant stored data were: 1) the medial and lateral APL, defined as the AP translation of the medial and lateral epicondyles on the tibial transverse plane; 2) the internal and external ARR; 3) the varus/valgus ranges. To consider possible differences in skeletal size across specimens, APL data were reported in terms of percentage of the AP tibial dimension (%AP-tib), being this the distance between the centre of the tibial plateau and the tibial tuberosity projected on the tibial transverse plane.

RESULTS

Significantly higher ($p < 0.01$) medial and lateral APL of about 4.7 ± 4.4 %AP-tib and 9.8 ± 7.9 %AP-tib, respectively, were observed in ADK with respect to the CHK in the AP Drawer test; the lateral APL was larger than the medial both in CHK and ADK. These values were found doubled in the Lachmann test.

No relevant differences were observed between the knee laxity in the CHK and in the ADK in the rotation tests at 20° and 90° knee flexion. A significant larger varus-valgus range was observed in ADK.

The positivity to the pivot-shift test in the ADK was confirmed by the higher laxity, almost twice the value of that observed in the CHK, the difference being ($p < 0.01$) 12.3 ± 11.3 %AP-tib and $5.2^\circ \pm 4.7^\circ$ for APL and ARR.

DISCUSSION

These results confirm that the translational instability in the ADK is larger than that in the CHK. Particularly, this is test-dependant but associated to a higher rotational instability only in the pivot-shift test. This, therefore, seems highly valuable in revealing the most real knee laxity status.

This study offers a contribute to the much controversial knowledge on knee joint instability by means of a thorough assessment of the knee joint laxity in the injured and contralateral healthy knees. The knee size normalization and the large patient cohort allows for a reliable statistical analysis of these measurements.

REFERENCES: 1. Miura et al. Arthroscopy 2010. 2. Colombet et al. Clin.Orthop.Relat Res. 2007.

BIOMECHANICAL EVALUATION OF BIOABSORBABLE POLYMER INTERFERENCE SCREWS FOR ACL RECONSTRUCTION AT TIME ZERO AND 12 WEEKS OF HEALING IN A GOAT MODEL

K.E. Kim, M.M. Tei, A.N. Pickering, K.F. Farraro, and S.L-Y. Woo
Musculoskeletal Research Center, Department of Bioengineering,
Swanson School of Engineering, University of Pittsburgh, Pittsburgh, PA

INTRODUCTION: Metallic interference screws are often used for fixation of an ACL graft in the bone tunnel [1]. Despite their popularity, these devices have shortcomings including distortion of post-operative MRI images [2], complication during revision surgery, and so on [3]. Recently, bioabsorbable screws have been used as they are intended to degrade over time for better graft integration in the bone tunnel [4]. In this study, we assessed the in vitro performance of bioabsorbable screws in terms of graft slippage and fixation strength as well as in vivo performance in a goat model after 12 weeks of healing. We hypothesized that bioabsorbable screws would provide comparable resistance to graft slippage and initial fixation strength to those of the titanium screw. We further hypothesized that the comparable initial performance would translate to a positive outcome at 12 weeks of healing in terms of the joint stability and structural properties of the femur-graft-tibia complex (FGTC).

METHODS: For the in vitro ACL reconstruction, a 5-mm-wide BPTB graft was harvested from 4 goat stifle joints obtained from a local abattoir. Then, the ACL of the same stifle joint was surgically removed, and an osseous tunnel of 6 mm in diameter was drilled at the tibial and femoral footprints. Bone blocks were affixed using a polymer screw or a titanium screw in each tunnel. Three cyclic loading tests were performed, followed by a load-to-failure test, with a 1 hour restoration period after each test. For the in vivo surgery, a bone-patellar tendon-bone ACL reconstruction was performed on right stifle joints of 3 Spanish breed goats. A 5 mm wide graft was harvested and fixed in 6 mm diameter femoral tunnel. On the tibial side, the bone block was fixed on the tibia using a suture anchor with 35 N tension at 60 degree of flexion. The goats were allowed free cage activity for 12 weeks. After euthanasia, the harvested joints were tested on the robotic testing system for joint stability and a materials testing machine (Instron, Norwood, MA) for the structural properties of the FGTCs.

RESULTS: From the time zero evaluation, the total residual elongation (unrecoverable elongation of the FGTC) after the three cyclic loading tests was 1.9 ± 1.1 mm and 1.4 ± 0.4 mm for the bioabsorbable and Ti screws, respectively, ($p > 0.05$). The ultimate load values of the femur-graft-tibia complexes (FGTC) were 235 ± 71 N and 234 ± 13 N respectively, and they were also not significantly different ($p > 0.05$). After 12 weeks of healing, the in situ forces in the tendon graft were 20 ± 16 N, 8 ± 3 N, and 12 ± 11 N at 30° , 60° , and 90° flexion respectively. During tensile testing, one specimen failed through graft pulling out of the femoral tunnel, while the remaining two failed in the mid-substance. The ultimate load of the FGTCs reconstructed with bioabsorbable screws was 156 ± 42 N.

DISCUSSION: The amount of graft slippage following cyclic loading (residual elongation) was equivalent between the two groups, as was the ultimate loads of the FGTC, confirming our first hypothesis on the time-zero performance of bioabsorbable screws. However, after 12 weeks, the in situ forces and the ultimate load of the graft were significantly lower than those from comparable animal models [5,6]. Thus, our second hypothesis was not confirmed. These findings indicate loss of adequate initial fixation, which may have resulted in loss of tension in the graft over time due to either graft slippage or poor graft-tunnel healing or both. We believe that improving the design of bioabsorbable screws in terms of thread profile, overall length and so on may help achieving better outcome. Also, we are investigating screws made by a stronger metallic material, such as biodegradable/bioresorbable magnesium to potentially overcome some of the shortcomings of the current polymeric materials.

ACKNOWLEDGEMENTS: Financial support from Commonwealth of Pennsylvania and NSF Engineering Research Center Grant (#0812348).

REFERENCES: 1. Moissal, A.S., et al., *KSSTA*, 2008, 16(12):1080-6 2. Bowers, M.E., et al., *Osteoarth Cart*, 2008, 16(5):572-8 3. Yaremchuk, M.J. and J.C. Posnick, *JCS*, 1995, 6(6):525-538 4. Eppley, B.L., et al., *Plast and Recon Surg*, 2004, 114(4):850-856 5. Abramowitch, S.D., et al., *J Orthop Res*, 2003, 21(4):708-15 6. Ng, G.Y., et al., *J Orthop Res*, 1995, 13(4):602-8

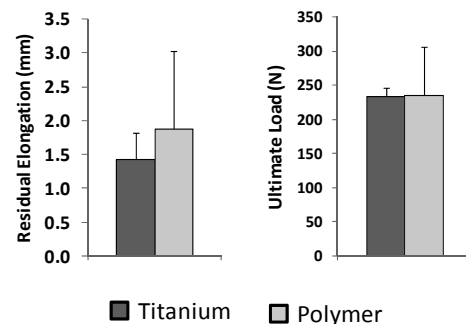


Figure 1. Time-zero comparison of residual elongation (graft slippage) and ultimate load of the FGTCs with titanium screws and polymer screws (* $p < 0.05$)

RELATIONSHIP BETWEEN MEDIAL-TO-LATERAL FEMORAL CARTILAGE THICKNESS RATIO AND PEAK ADDUCTION MOMENT DURING WALKING FOR ACL RECONSTRUCTED AND HEALTHY CONTRALATERAL KNEES

¹Zabala ME, ¹Favre J, ¹Scanlan SF, ^{1,2}Andriacchi TP

¹Stanford University, Stanford, CA; ²VA Palo Alto Health Care System, Palo Alto, CA

INTRODUCTION

Rupture of the anterior cruciate ligament (ACL) has been shown to result in increased risk for knee osteoarthritis (OA), despite reconstruction [1]. While several kinematic alterations have been described for ACL reconstructed (ACLR) knees, the pathway towards OA is still not fully understood. Recently, a study reported a reduction of the peak knee adduction moment during walking in ACLR knees [2]. This alteration of knee kinetics is of particular interest because the femoral cartilage thickness of healthy knees has been shown to adapt to ambulatory load. Specifically, the relationship between the ratio of medial-to-lateral (ML) cartilage thickness and peak knee adduction moment has been shown to be positive for healthy knees and negative for osteoarthritic knees [3]. The goal of this study was to investigate the relationship between ML thickness and adduction moment in knees following ACL reconstruction. Specifically, this study tested the hypothesis that the relationship between ML femoral cartilage thickness ratio and adduction moment in ACL reconstructed knees will have a reduced slope compared to the healthy contralateral knees suggesting that the alteration of knee adduction moment is an important factor in the initiation of knee OA after ACL reconstruction.

METHODS

Twenty-six subjects with clinically successful unilateral ACL reconstruction and no other history of serious lower limb injury (28.4±6.5 yrs, 1.7±0.1 m, 73.3±12.4 kg, 14 male, 2.6±2.0 mo injury to surgery, 27.1±3.8 mo post surgery, 92.5±6.2 Lysholm) were recruited after providing IRB-approved informed consent. An optoelectronic system and a force plate were used to record the peak knee adduction moment during walking at self-selected normal speed. Cartilage thickness of the central load-bearing regions of the medial and lateral femur [4] was determined from 3D femoral cartilage models created by segmentation of magnetic resonance images (3D SPGR, 1.5T) using custom software [5]. Paired t-tests were used to compare the adduction moment, cartilage thickness, and ML thickness ratio between the ACLR and contralateral knees. Linear regression was used to examine the relationship between ML cartilage thickness ratio and peak adduction moment for both knee conditions, and an ACOVA test was performed to compare the slope of both linear regressions. For all analyses, the level of significance was set to $p < 0.05$.

RESULTS

The peak adduction moment was significantly lower for the ACLR knees compared to the contralateral knees ($p=0.04$). No significant differences between knee conditions were noticed for the medial and lateral cartilage thickness or the ML thickness ratio. Both ACLR and healthy contralateral knees demonstrated a significant positive linear relationship between ML thickness ratio and peak adduction moment (Fig.1). Although the slope of the regressions were reduced by 25% for the ACLR knees compared to the contralateral knees, this difference was not statistically significant.

DISCUSSION

The results of this study did not support the hypothesis in the fact that the ML cartilage thickness ratio of the ACLR knees had the same positive relationship to peak adduction moment as the contralateral knees. It is important to note that no difference was observed for the cartilage thickness and the cartilage thickness ratio between knee conditions. All together this suggests that approximately two years after surgery, the femoral cartilage of the ACLR knees have not had enough time to respond to the presence of altered loading. Longer follow-up durations are required to determine whether the cartilage will adapt to the altered loading or whether the relationship will become weaker or even display a negative slope as seen in osteoarthritic knees [3].

REFERENCES: 1. Lohmander LS 2004 *Arthritis Rheum* 50:3145-3152. 2. Zabala MZ Rep Proc Am Soc Biomechanics Conf 2011 Long Beach, CA. 3. Andriacchi TP 2004 *Ann Biomedical Engr* 32(3):447-457. 4. Wirth 2008 *IEEE Trans Med Imaging* 27(6). 5. Koo S 2005 *Osetoarthritis Cartilage* 13(9)

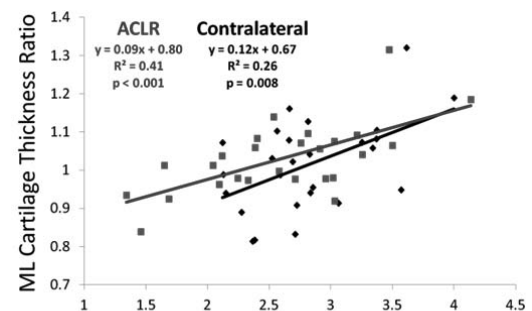


Figure 1. Relationship between ML cartilage thickness ratio and peak knee adduction moment for ACL reconstructed (ACLR) and healthy contralateral knees.

WORKING ACROSS MODEL SYSTEMS AT THE INTERFACE BETWEEN FUNCTIONAL TISSUE ENGINEERING AND DEVELOPMENTAL BIOLOGY TO IMPROVE ADULT TENDON REPAIR

¹Butler D; ²Dyment NA; ¹Shearn JT; ³Kinneberg K; ¹Breidenbach A; ¹Lalley A; ¹Gilday S; ¹Gooch C; ⁴Liu C-F; ⁴Wylie C
¹Biomed. Engineering Program, U Cincinnati, Cincinnati, OH; ²Center for Regenerative Med. & Skeletal Devel., U Conn. Health Center, Farmington, CT; ³University of Colorado, Boulder, CO; ⁴Cincinnati Children's Hospital, Cincinnati, OH

INTRODUCTION. Over 16 million patients present each year in the US with tendon, ligament, and joint injuries at a cost of \$30 billion per year [1]. To treat tendon injuries, our lab employs principles of functional tissue engineering (FTE) to first characterize normal *in vivo* tendon function during activities of daily living (ADLs) to then guide creation of cell-scaffold tissue engineered constructs (TECs) that meet these functional demands after surgery [2-5]. Much of our work has focused on repairing a central patellar tendon defect in the rabbit using mechanically-preconditioned TECs composed of mesenchymal progenitor cells (MPC) in collagen-based scaffolds. While these treatments have achieved many of our functional goals, further improvements require that we consider the tendon's biological design criteria in addition to the mechanical parameters. In this context, our strategy has been to understand how to mimic aspects of normal *murine* tendon development to better design TECs that improve tendon repair. Specifically, we are investigating cell signaling mechanisms and gene expression patterns during late embryonic and early postnatal development and translating these patterns to control MPC differentiation and improve TECs in culture [6-7]. Of course, these discoveries still need to be translated to larger animal models and ultimately to humans. However, translating this FTE-DB paradigm over a hierarchy of preclinical model systems remains a major hurdle and goal. While large-animal and human models are more clinically relevant and involve better-controlled surgeries, larger mechanical demands post-surgery can compromise repairs and the biological homology between species during repair is still unknown.

FTE CHALLENGES. Establishing mechanical design criteria and safety factors for a repair (e.g. matching normal tangent stiffness and exceeding a normal tendon's maximum *in vivo* force levels without damage) are obvious, but only if technologies exist to make these measurements! Transducers inserted in very small animals can damage a tendon, alter gait patterns, and create errors in force computations during calibration. Without actual forces and safety factors, investigators must estimate PT force ranges from similar *in vivo* forces [8] expressed as ratios of failure force from models such as rabbits (21%) [9] and goats (40%) [10] (Fig. 1). These data are essential if researchers are to link improved repair biomechanics across model systems.

BIOLOGICAL CHALLENGES. The biological advantages of conducting murine research are numerous, including the

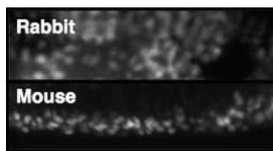


Fig. 2. ECFP-expressing articular chondrocytes from (top) juvenile rabbit and (bottom) adult murine patella [11].

wide array of biologic tools available to study mechanisms important in development. Numerous reporter, knockout and conditional knockout mice are available to study developmental and natural healing events *in vivo* and factors affecting murine TEC maturation in culture. For example, chondrocytes from Col2ECFP transgenic mice and rabbits both display increased Col2ECFP signal in response to compressive load in culture [11] (Fig. 2). However, size constraints in mice limit the surgeon's ability to reproducibly implant TECs to assess treatments to improve healing in larger species.

Instead, we have used the murine model to directly compare natural healing of defects in murine and rabbit models [8,12] and showed their similar responses over time.

As we continue to identify novel murine markers of tendon development, such as Indian Hedgehog signaling in the insertion site [7] (Fig. 3), we can then seek homologous and specific gene or protein markers that lead to new treatment candidates in larger species. Coordinated studies between laboratories can speed development.

FUTURE DIRECTIONS FOR TENDON TISSUE ENGINEERING. Numerous challenges and opportunities face tissue engineers seeking to commercialize their biological devices. 1) Tissue engineers will need to conduct preclinical animal studies using more realistic surgical environments that challenge their novel TECs. Animal models of realistic injury (e.g., rotator cuff and graft insertion), inflammation, and degeneration are needed if TECs are to be adequately challenged after surgery. 2) Tissue engineers also need to develop better *in vitro* predictors of *in vivo* outcome. TEC and repair tissue properties (e.g. stiffness and modulus) may be correlated [2,4,5] but other sensitive mechanical and biological markers are needed to more rapidly create effective TECs for surgery. 3) Tissue engineers must find more rapid and cost-effective methods to manufacture their biologic products while not compromising their unique features that improve repair outcome. 4) Scale up from the laboratory to clinical usage requires consideration of factors like biocompatibility, sterility, and ensuring that surgeons can easily handle and prefer to use the product to treat their patients.

REFERENCES 1. Praemer A, *Musculoskel. Condition US*, 1999; 2. Juncosa-Melvin N, *Tissue Engr*, 2006; 3. Juncosa-Melvin N, *Tissue Engr*, 2005; 4. Butler D, *J Orthop Res* 2008; 5. Shearn et al, *JBME*, 2007; 6. Liu et al, *Tissue Engr (B)* 2011a; 7. Liu et al, *Tissue Engr* 2011b; 8. Dyment et al, *JOR* 2011; 9. Juncosa et al, 2003; 10. Korvick et al, *JOR*, 1996; 11. Chokalingam et al, *TE*, 2008; 12. Awad et al, *JOR*, 2003.

ACKNOWLEDGMENTS NIH Grants AR46574-10 and AR56943-02.

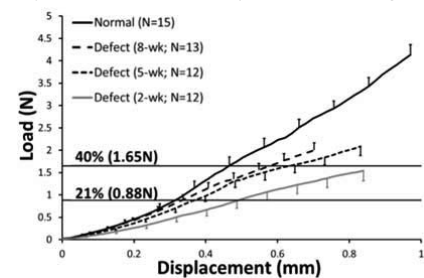


Fig. 1. Previously-recorded peak *in vivo* loads were used to estimate functional healing of murine PT defects. [8-10]

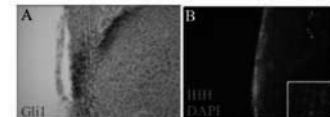


Fig. 3. Activated hedgehog signaling pathway in tibial insertion at P1. (A) Cells respond to hedgehog (blue stain) using Gli1-LacZ reporter line. (B) Note Indian Hedgehog in insertion site. Insert shows representative IHH positive cells.

TYPE I COLLAGEN SYNTHESIS IN SCAFFOLD-FREE, SINGLE FIBERS FOR ENGINEERED TENDON

N.R. Schiele, and D.T. Corr

Department of Biomedical Engineering, Rensselaer Polytechnic Institute, Troy, NY

INTRODUCTION

We have developed a cell-based and scaffold-free method to direct fibroblast cells to form single fibers [1]. This approach replicates a few key aspects of embryonic tendon development, such as high cellularity and cells that are in direct cell-cell contact through the adhesion molecule, cadherin-11 [2]. Our scaffold-free approach toward tendon tissue engineering is unique, as there is no three-dimensional scaffold or extracellular matrix present initially, rather matrix synthesis is dependent on the cells that form the fiber. As an important step towards better understanding fiber development and matrix synthesis in our system, the objective of this study was to evaluate fiber structure and cellular synthesis of type I collagen within the first 72 hours of development.

METHODS

Fiber formation: Growth channels were micromachined into 2% agarose gel by a computer-controlled UV laser system (TeoSys, Crofton MD). The linear channels were machined to a 1.65-cm length, ~275- μ m width, and ~300- μ m depth. Human fibronectin (BD Bioscience, Bedford, MA) was pipetted (30 μ l of 0.3 mg/ml) into the growth channels and dried for one hour. Type I collagen sponge disks (4-mm diameter, Kensey Nash, Exton, PA) were inserted into each end of the growth channel to act as anchor points for the developing fibers. (**Fig1.**) Human dermal fibroblast cells (1.0 ml of $\sim 2 \times 10^5$ cells/ml) in culture media (89.5% DMEM, 10% FBS, 0.5% penicillin-streptomycin, 50 μ g/ml L-ascorbic acid) were introduced to the growth channels using a pipette and then placed in a standard cell culture incubator (37 °C, 5% CO₂, 95% RH).

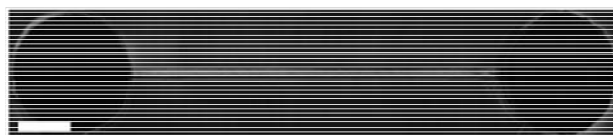


Fig1. Laser-micromachined growth channel assembly (scalebar=2mm).

Immunocytochemistry: Fibers were removed from the growth channels using tweezers following 4, 24, and 72 hours of development. For antibody labeling, the extracted fibers were incubated for 1 hour at room temperature with type I collagen antibody (Millipore, Temecula, CA) diluted in PBS, then incubated for an additional 1 hour at room temperature with FITC-conjugated secondary antibody, Hoescht, and phalloidin in 2% BSA. All time points were examined in triplicate, and imaged using the same camera exposure time for qualitative evaluation of collagen content. Controls with primary antibody excluded showed minimal background fluorescence.

RESULTS

Scaffold-free, single fibers exhibited a three-dimensional and highly cellular structure at all three time-points. Fibers that had developed for 72 hours were consistently removed from the channels intact; whereas 4- and 24-hour fibers proved less structurally stable, and at times only fiber fragments could be extracted. Cells within the fibers quickly become organized, as cell nuclei are seen to align in the direction of the fiber long-axis at both 24 and 72 hours (**Fig2c,e**). At 4 hours the cell nuclei appear disorganized and randomly orientated within the fiber (**Fig2a**). Type I collagen is at a minimum at 4 hours with only a slight increase in intensity by 24 hours (**Fig2b,d**). At 72 hours, a significant increase in type I collagen is observed compared to both 4 and 24 hours (**Fig2f**).

DISCUSSION

During embryonic and post-natal tendon development, collagen content is minimal (~2.8% at 4 days post-natal [3]). In an effort to replicate the high cellularity and minimal collagen matrix found in developing tendon we have developed a scaffold-free, single fiber model. Herein, we find that type I collagen content is minimal early (4 and 24 hours) in fiber development, as there is no outside source of collagen within the fiber. However, by 72 hours the cells within the fibers have synthesized collagen, and collagen begins to accumulate within the fibers. While yet to be fully investigated, this increase in collagen may correspond to the decrease in cadherin-11 we have observed at 72 hours. Future work will further investigate cadherin-11 content, effects of mechanical stimulation, and single-fiber mechanical properties.

ACKNOWLEDGEMENTS

This work was supported by NSF CAREER CBET-0954990 (DTC).

REFERENCES: 1. Schiele et al. Proceeding ISLT-XI 2011. 2. Schiele et al. Proceeding USNCB 2011. 3. Ansoorge et al. Ann Biomed Eng 2011.

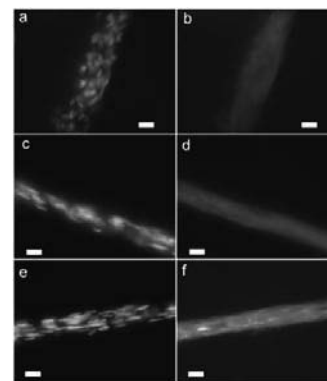


Fig2. Cell nuclei in a fiber at a) 4 hrs, c) 24 hrs, and e) 72 hrs. Type I collagen at b) 4 hrs, d) 24 hrs, and f) 72 hrs with a significant increase in intensity (scalebars=20 μ m).

FABRICATING SCAFFOLDS OF ELECTROSPUN NANOFIBRES FROM SYNTHETIC BIOPOLYMERS FOR TENDON REPAIR

⁺¹Bosworth, LA; ²Wong, J; ¹Cartmell, SH; ¹O'Brien, M; ²McGrouther, DA; ¹Downes, S
⁺¹School of Materials, The University of Manchester, Manchester, UK
²School of Medicine, The University of Manchester, Manchester, UK

INTRODUCTION

Tendons are susceptible to wear and tear and even spontaneous rupture. With autologous tendon grafting creating secondary sites of tissue morbidity, there remains an unmet clinical need for the development of an alternative intervention. We have developed synthetic, degradable scaffolds using electrospinning, which possess architectures similar to tendon tissue as a potential “off-the-shelf” therapy.

Here we report the material properties of electrospun scaffolds fabricated from different synthetic biopolymers and the subsequent assessment of the selected scaffold *in vivo*.

METHODS

Four polymer/solvent solutions (concentration 10 %w/v) were investigated; poly(ϵ -caprolactone) (PCL) (M_n 80,000; Sigma) dissolved in Acetone (Fisher Scientific); PCL dissolved in 1,1,1,3,3,3-Hexafluoroisopropanol (HFIP; Apollo Scientific); poly(lactic-*co*-glycolic acid) (PLGA_{85:15}; Sigma) dissolved in HFIP; and PCL/PLGA_{85:15} blend (50:50) dissolved in HFIP. Each solution was electrospun using pre-determined parameters: voltage – 20 kV, flow-rate – 1 ml/hr, distance to collector – 20 cm, spin-time 15 mins. Aligned fibres were collected on a fine-edged mandrel (width 1.5 mm) rotating at 600 RPM. Collected fibres were removed as ribbons and cut into 3 cm lengths. Fibre strips were briefly submerged in distilled water and manually twisted along their length to create 3D scaffolds (\varnothing ~200 μ m). Scanning electron microscopy was used to visualise the fibres. Scaffold tensile properties were determined by loading to failure using an Instron 2211 with 5 N load cell and 5 mm/min crosshead speed (n=5).

The optimal scaffold was implanted into a purpose-made defect in the left flexor digitorum tendon of a mouse (length 3 mm). The graft was held in place by surrounding tissues. The excised tendon tissue was used as an autologous graft within the right flexor digitorum tendon of the same mouse. Histological staining was performed on the grafts after 21 days post-operatively (n=5 per time-point).

RESULTS

All four polymer/solvent combinations were readily electrospinnable (Fig. 1(A-D)). However, significant beading was present in amongst the PCL (Acetone) fibres. Tensile properties varied for the four scaffold types (Fig. 1 (E and F)). Greatest Modulus was observed for PLGA_{85:15}, whereas PCL (HFIP) yielded highest tensile strength at break and reasonable stiffness. PCL (Acetone) resulted in overall lowest strength and stiffness.

The synthetic graft was clearly visible from H&E staining after 21 days post-implantation and a dense layer of cells encapsulating the outer edge was observed (Fig. 1(G)). Cell infiltration into the scaffold core had also occurred during this time. Tissue remodeling had occurred for the autograft control and surrounding tendon tissue (Fig. 1(H)).

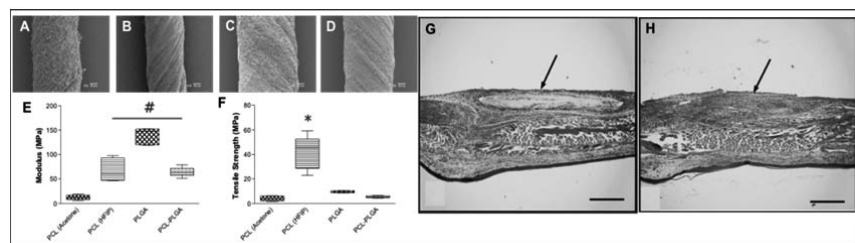


Fig.1 – micrographs of electrospun scaffolds for (A) PCL (Acetone), (B) PCL (HFIP), (C) PLGA_{85:15} (HFIP) and (D) PCL-PLGA (HFIP) (scale bar – A&B 50 μ m; C&D 20 μ m). Young's Modulus (E) and Tensile stress (F) of all four scaffold types (# - not significant; * - $p < 0.05$). H&E staining 21 days post-operative for PCL (HFIP) graft (G) and autograft (H) (scale bar – 500 μ m).

DISCUSSION

Smooth, bead-free fibres were obtained for polymers electrospun in HFIP. Acetone promoted the formation of beads, which had a detrimental effect on tensile properties. Overall, PCL (HFIP) yielded most promising tensile properties being significantly stronger compared to the other three scaffolds and demonstrated reasonable stiffness. This scaffold type was selected for implantation and after 21 days post-implantation an inflammatory reaction surrounding the scaffold was apparent. However, cell infiltration into the scaffold core had occurred, which is necessary for the long-term success of the implant.

ACKNOWLEDGEMENTS

The Authors' thank RegeNer8 and the MRC (grant code G1000788-98812) for funding.

FIBRIN HYDROGELS EXHIBIT IMPROVED BIOLOGICAL AND MECHANICAL PROPERTIES COMPARED TO COLLAGEN HYDROGELS IN TISSUE-ENGINEERED CONSTRUCTS *IN VITRO*

¹Andrew P. Breidenbach, ²Yinhui Lu, ¹David L. Butler, and ²Karl E. Kadler

¹Biomedical Engineering Program, University of Cincinnati, Cincinnati, OH

²Wellcome Trust Centre for Cell-Matrix Research, University of Manchester, Manchester, UK

INTRODUCTION Tendon and ligament injuries account for nearly half of all musculoskeletal injuries costing \$30 billion annually in the United States [1]. Understanding how cells interface with the tissue-engineered construct (TEC) material and remodel the extracellular environment is integral in elucidating methods that can lead to improved biological and mechanical function of tissue-engineered repairs. This study sought to compare TEC mechanical properties, TEC structure and gene expression of cells seeded in fibrin and type I collagen gels over time in culture. Due to the presence of exogenous collagen fibrils in collagen gels, we hypothesized that collagen TECs would have increased fibrillogenesis gene expression (Col1a1, Col3a1, Fmod, Dcn) and improved fibril organization near the cell surface. Further, we hypothesized that collagen TECs would exhibit greater linear modulus than fibrin TECs at all time points.

METHODS Experimental Design. TEC mechanical properties (n=9), gene expression (n=3) and scaffold structure (n=2) were examined on the day that the gel contracted into a linear construct (T0) and three days later (T3). TEC Preparation. Fibrin (3.4mg/ml) and collagen (2.6mg/ml) TECs were made using chick tendon fibroblasts (passage 6-7) as previously described [2]. Gene Expression (qPCR). RNA was isolated, converted to cDNA, and amplified in triplicate using primers and SYBR Green detection for Col1a1, Col3a1, Fmod, Dcn, FN, Scx, integrins α 11 and β 1, and 18S. Scaffold Structure. TECs were prepared for transmission electron microscopy (TEM) and analyzed for fibril diameter as previously described [3]. Mechanics. TECs were failed in tension at a 10%/s strain rate and material properties were determined as previously described [3]. Statistics. Response measures were compared either via two-way ANOVA (mechanics and scaffold structure) or MANOVA (gene expression) with time and material as fixed factors ($p < 0.05$).

RESULTS Gene Expression. Fibrin TECs exhibited greater expression of Col3a1 and integrins α 11 and β 1 than collagen at T3 (Fig. 2). Material did not affect the remaining genes, and time did not affect any genes investigated. Scaffold Structure. Collagen fibrils located near the cell surface are aligned along the axis of the construct in both TEC materials, but average fibril diameter is greater in fibrin at T3 ($p < 0.05$). Mechanics. Time increased linear modulus (LM), with collagen TECs increasing from 0.37 ± 0.09 MPa (mean \pm SD) at T0 to 0.99 ± 0.26 MPa at T3 ($p < 0.01$), while fibrin TECs increased from 0.32 ± 0.12 MPa at T0 to 2.39 ± 0.67 MPa at T3 ($p < 0.01$). Although material did not affect LM at T0, fibrin TECs showed higher LM than collagen at T3 (Fig. 1).

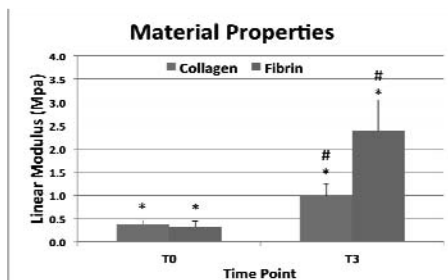


Figure 2: Comparing TEC material properties showing significant differences ($p < 0.01$) with respect to time (*) and material (#)

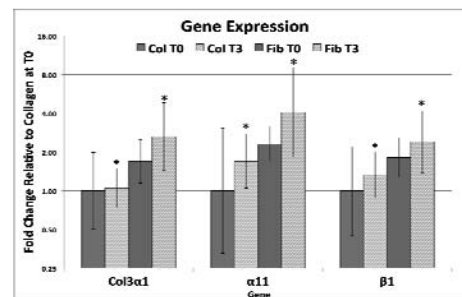


Figure 2: Gene expression data showing significant differences ($p < 0.05$) with respect to material (*)

DISCUSSION Increased expression of matrix synthesis and cell adhesion genes in fibrin TECs at T3 suggests increased synthesis and interaction of fibroblasts with the surrounding extracellular matrix. TEM reveals improved matrix alignment and fibril characteristics in fibrin TECs at T3. These findings translate to improved mechanical properties in fibrin, as fibrin TECs exhibited 2.4 fold greater increases in LM than collagen TECs from T0 to T3. Fibroblasts did not appear to efficiently remodel the type I collagen gel to resist tensile forces during the time period of this study. Future work will focus on identifying how cell-material interactions affect mechanical and structural properties at later time points and how this translates to repair response in an *in vivo* tendon injury model.

ACKNOWLEDGMENTS The Wellcome Trust (KK), Helen-Muir Fund (KK), NIH grant 56943-02 (DB), NSF IGERT 0333377 (DB).

REFERENCES 1) Praemer et al, AAOS, 1999; 2) Kapacee et al, Matrix Biol, 2008; 3) Kalson et al, Matrix Biol, 2010.

ADDITION OF COLLAGEN FIBERS TO MPC-COLLAGEN GELS TO PROMOTE TISSUE ENGINEERED CONSTRUCT STIFFNESS AND MATRIX PRODUCTION

⁺¹Lalley, A L; ¹Dyment N A; ¹Butler D L; ¹Shearn J T

⁺Biomedical Engineering Program, University of Cincinnati, Cincinnati, OH

INTRODUCTION Soft tissue musculoskeletal injuries pose a large burden on the US economy with over 16 million patients presenting with soft tissue injuries at a cost of \$30 billion per year [1]. The prevalence of these injuries, and limited successful therapies available, has led to the emergence of tissue engineering approaches for tendon and ligament repair. Our lab has focused on improving tendon repair by designing and implanting tissue engineered constructs (TEC) into a rabbit central third patellar tendon (PT) defect. Previous work indicates that adding a lyophilized collagen sponge to a mesenchymal progenitor cell (MPC)-collagen gel improved repair biomechanics at 12 weeks post-surgery [2]. Examining previous in vivo PT repair studies also shows a positive correlation exists between TEC linear stiffness, total collagen content, and in vivo repair outcome [3]. In this study, we investigated the effect of incorporating type I collagen fibers on gene expression and biomechanics of our MPC-seeded collagen gel TECs with the goal of promoting extracellular matrix organization and linear stiffness in vitro. We hypothesized that incorporating collagen fibers would promote expression of genes involved in matrix organization and lead to a subsequent increase in TEC linear stiffness in vitro.

METHODS TEC Creation. TECs were created using rabbit MPCs (P2) at 0.10×10^6 cells/mL mixed with bovine-derived collagen gel (3.1 mg/mL, Advanced BioMatrix PureCol) at a concentration of 2.625 mg/mL and collagen fibers at a concentration of 5mg/construct (n = 5). Two collagen fiber sizes were evaluated: 0.5-1.0mm and 1.0-1.4mm. TECs with no fibers (NF) served as the control. TECs remained in an incubator (37°C, 95% RH, and 5% CO₂) under static tension and fed every other day with DMEM (Gibco BRL/Life Technologies, Inc., Gaithersburg, MD) supplemented with 5% ascorbic acid/5% FBS. Gene Expression. Gene expression levels were measured for collagen type 1 alpha 1 (Col1a1), collagen type 3 (Col3), decorin (Dcn), fibromodulin (Fmod), matrix metalloproteinase 13 (MMP-13), and tissue inhibitor of metalloproteinase 1 (TIMP-1) for day 6 (D6) and day 12 (D12) samples using qPCR with TaqMan® probes, normalized to GAPDH. Biomechanics. TECs were failed in tension at a strain rate of 10%/s at D6 and D12. Statistics. Gene expression data was compared using a two-way MANOVA and biomechanics data was compared using two-way ANOVA with time in culture and fiber size as fixed factors.

RESULTS Gene Expression. The addition of small and large fibers had no effect on gene expression. Time significantly decreased small fiber TECs Col1a1 (p=0.032) and TIMP-1 (p=0.004) expression (Fig.1). Biomechanics. Time significantly increased the linear stiffness for NF (p=0.007) and the addition of small fibers significantly decreased stiffness compared to NF at D12 (p=0.019) (Fig. 2).

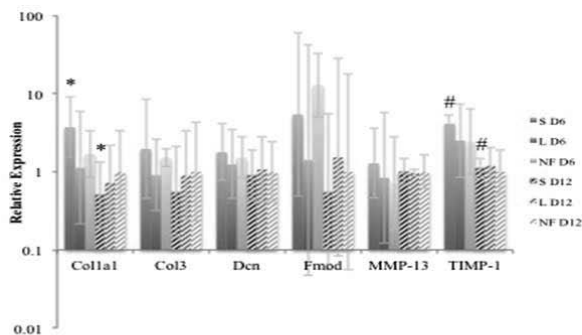


Figure 1: Adding collagen fibers produced no significant effect in gene expression; however, time had a significant effect on Col1a1 and TIMP-1 for small fiber TECs (p<0.05).

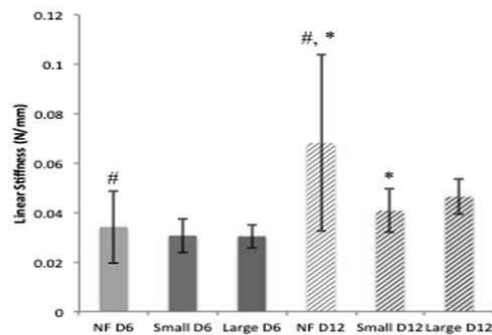


Figure 2: The addition of small fibers significantly decreased linear stiffness compared to NF D12 and time produced a significant increase in stiffness for the NF TECs (p<0.05).

DISCUSSION The results of this study indicate that the addition of collagen fibers did not improve linear stiffness; however, the gene expression trends show that the small fiber TECs may have increased activity at D6 compared to both NF and large fiber TECs. We will increase the sample size to determine the significance of this trend. Despite potential increased activity, the small fiber TECs had the lowest linear stiffness value at D12. This may imply that there are additional genes that must be investigated to understand the mechanism through which extracellular matrix organization, and subsequent TEC stiffening, occurs. The NF TECs at day 12 had the largest linear stiffness compared to all other treatments, and this may be attributed to the 10-fold increase in fibromodulin expression at D6, a gene implicated in regulating ECM assemblage and maturation. We will continue to investigate the effects of fibromodulin on stiffness as the study continues. Future studies will include optimizing collagen content through the addition of collagen fibers and adding mechanical stimulation as an input parameter to improve matrix formation and organization.

REFERENCES 1. Praemer A, Musculoskel. Condition US, 1999; 2. Juncosa-Melvin N, Tissue Engineering, 2006; 3. Juncosa-Melvin N, Tissue Engineering, 2005.

ACKNOWLEDGEMENTS NIH Grants AR46574-10 and AR56943-02.

EFFECT OF NANOFIBER ALIGNMENT AND MECHANICAL LOADING ON HMSC DIFFERENTIATION

S. D. Subramony, B. R. Dargis, M. Castillo, E. U. Azeloglu, M. S. Tracey, A. Su and H. H. Lu
Department of Biomedical Engineering, Columbia University, New York, NY, USA

INTRODUCTION

The anterior cruciate ligament (ACL) is the most frequently injured ligament of the knee, with over 100,000 reconstructions performed annually[1]. Due to limitations associated with current grafts[2], there is a significant interest in ACL tissue engineering. To this end, nanofiber scaffolds are advantageous as the fiber dimensions mimic that of the collagen ultrastructure, and scaffold fabrication parameters can be tailored to match nanofiber organization to that of the ACL[3]. In addition, human mesenchymal stem cells (hMSC) represent an attractive cell source for tissue engineering, though the challenge there lie in systematically controlling and directing hMSC differentiation towards the ligament fibroblast phenotype. **It is hypothesized** that both mechanical loading and nanofiber organization are essential for the induction and maintenance of the ligament fibroblast phenotype, and **the objective of this study** is to elucidate the relative contribution and coupled effects of dynamic tensile loading and nanofiber alignment on the fibroblastic differentiation of hMSC on nanofiber-based scaffolds.

METHODS

The hMSCs (Lonza, 30,000 cells/cm²) were seeded on aligned or unaligned nanofiber scaffolds (PLGA 85:15) fabricated by electrospinning[3]. With the exception of alignment, fiber diameter, pore size and porosity are similar between both scaffold types. Following five days of static culture, the experimental groups were subjected to 1% uniaxial tensile strain for 90 minutes (2x/day, 1Hz) in a custom bioreactor. The loaded and unloaded samples were analyzed at 1, 7, 14 and 28 days. Cell attachment and morphology were assessed (Live/Dead), and cell alignment was quantified (n=3) using circular statistical analysis[5]. Cell number (n=5, PicoGreen) and collagen synthesis (n=5, hydroxyproline) was measured. Collagen distribution (n=2, immunohistochemistry) and the expression (n=5, qPCR) of ligament fibroblast markers (collagen I & III, fibronectin, tenascin-C, scleraxis, tenomodulin) and integrins ($\alpha 2$, αV , $\alpha 5$, $\beta 1$) were tested. **Statistical Analysis:** ANOVA and the Tukey-Kramer *post-hoc* test (*p<0.05).

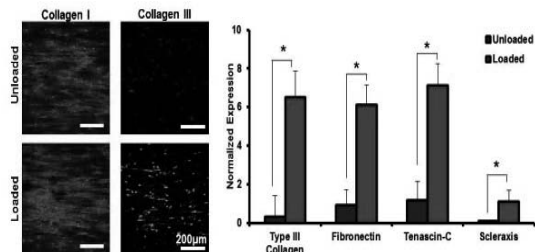


Fig. 1. **ALIGNED:** Loading resulted in collagen III production in addition to the upregulation of several key ligament fibroblast markers after 28 days.

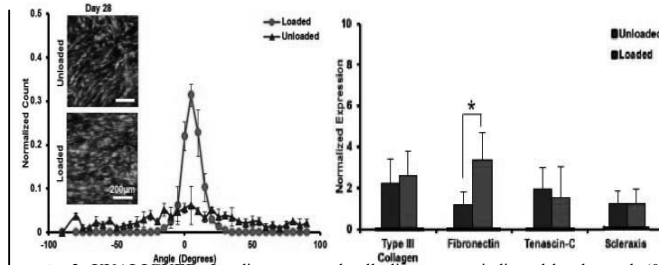


Fig. 2. **UNALIGNED:** Loading promoted cell alignment as indicated by the peak (0° aligned horizontally). In terms of markers, only fibronectin upregulation was observed after 28 days.

RESULTS

On **aligned scaffolds**, mechanical loading resulted in no differences in cell alignment but increased collagen synthesis, including the production of collagen III (Fig.1), as well as deeper infiltration into scaffolds as compared to control samples. Loading also upregulated the expression of collagen III, fibronectin, tenascin-C and scleraxis (Fig.1) as well as integrins $\alpha 2$, $\alpha 5$, and $\beta 1$ after 14 days of stimulation (p<0.05). On **unaligned scaffolds**, quantitative analysis of cell alignment after loading revealed a significant increase in the number of cells aligned in the direction of applied strain (0°, Fig.2). Mechanical stimulation also resulted in a significant increase in total cell number and total collagen production after 28 days as compared to unloaded controls. In terms of fibroblastic markers, only fibronectin was upregulated after 14 days and maintained after 28 days of culture (Fig. 2). The expression of integrin $\alpha 5$ at day 7 and the upregulation of $\alpha 2$ and $\beta 1$ at day 14 were also observed.

DISCUSSION

The results of this study collectively suggest that hMSC differentiation is modulated by both mechanical stimulation and scaffold architecture. On *aligned scaffolds*, upon seeding, cells displayed an elongated, fibroblastic, morphology in the direction of fiber alignment. While mechanical loading resulted in no change in cell alignment, it increased total collagen synthesis including both collagen I and III, along with significant upregulation of all ligament fibroblast-related markers. The ratio of collagen I:III expression was similar to that of the native ligament (7:1)[6]. In contrast, on unaligned scaffolds, cells were randomly oriented upon seeding and mechanical stimulation rescued cell alignment as well as enhanced cell proliferation and matrix production. As such, cells on unaligned scaffolds failed to differentiate towards a fibroblastic lineage, likely progressing to scar tissue formation. In summary, the results of this study demonstrate that physical stimulation coupled with biomimetic scaffold alignment is essential for fibroblastic differentiation of hMSCs. It is anticipated these findings have broad applications towards both ligament/tendon tissue engineering as well as guided wound healing or connective tissue repair.

ACKNOWLEDGEMENTS: NIH(AR056459-02, AR055280-02), NYSTEM(C024335), NSF GRFP(SDS), K. D. Costa, Ph.D.

REFERENCES: 1. Brown and Carson. Clin Sports Med 1999. 2. Beynon *et al.* JBJS 2002. 3. Moffat *et al.* Tissue Eng 2009. 4. Altman *et al.* FASEB J 2002. 5. Costa *et al.* Tissue Eng 2003. 6. Amiel *et al.* JOR 1984.

BMP-2 ELUTING BIPHASIC HYBRID SILK SCAFFOLD FOR LIGAMENT AND BONE TUNNEL REGENERATION

Thomas K.H. Teh, Pujiang Shi, Siew-Lok Toh, James C.H. Goh

Division of Bioengineering and Department of Orthopaedic Surgery, National University of Singapore, Singapore

INTRODUCTION

The current gold standard for ACL reconstruction has been with the use of tendon autografts. However, problems persist in this solution, primarily due to the inherent limitation of donor site morbidity and poor graft integration. The dysfunction of this integration site or enthesis, has led to 3000 - 10000 revision surgeries annually in the United States alone [1]. In view of the morbidity issue due to graft harvesting and the need for robust graft integration, we propose the use of a functionalized biphasic silk scaffold for complete regeneration of the ligament and bone tunnel tissues. The ends of this hybrid silk scaffold system are incorporated with hydroxyapatite nanoparticles (n-HA) and loaded with bone morphogenetic protein 2 (BMP-2) to stimulate bone tunnel and enthesis regeneration, while the central one-third supports ligament regeneration. It is hypothesized that the osteoinductive BMP-2 will synergistically complement the osteoconductive n-HA to encourage bone and enthesis regeneration.

METHODS

Knitted scaffolds (60 × 20 mm) were fabricated from raw *Bombyx mori* silk (240 fibroins, Thailand) and degummed with mechanical agitation to obtain knitted silk fibroin (SF) [2]. Scaffold fabrication was completed upon lyophilization and methanol treatment of cast SF-based solutions with the knitted SF. Two groups of biphasic scaffolds, distinguished by the different composition at the scaffold ends, were fabricated: SF/n-HA (0.78mg/end, control) and SF/n-HA/BMP-2 (0.78mg/end and 29µg/end respectively, experimental). The blank scaffolds were characterized for scaffold morphology, mechanical properties at the two phases and elution kinetics. For *in vitro* characterizations, the different phases of the scaffolds were characterized using rabbit bone marrow derived MSCs (P3, 1×10^6 /scaffold) over 28 days static culture for cellular viability, proliferation, cell morphology, gene expression, collagen synthesis levels, alkaline phosphatase (ALP) activity, calcium deposition via Alizarin red staining, ECM morphology and specific ECM deposition levels (n = 3 each). For *in vivo* characterizations, the two groups of biphasic scaffolds were each seeded with rabbit MSCs (P3, 3×10^6 /scaffold) and statically cultured for a day prior to implantation via ACL reconstruction procedure on forty-eight New Zealand White rabbits (12 weeks old, 2.5–3.0 kg). The animal experiments were approved by Institutional Animal Care and Use Committee of National University of Singapore. The rabbits were sacrificed at 8, 16, and 24 weeks postoperatively with the knee joints collected immediately and kept at -80°C. The samples were then scanned using micro-CT prior to histological preparations (n = 3) and mechanical tests (n = 5).

RESULTS

The biphasic scaffolds were shown to be porous with interconnected pores. n-HA and BMP-2 were observed to be securely incorporated in the lyophilized SF sponges. The bioactivity of BMP-2 was ascertained after the fabrication process and was shown to be eluting with an initial burst release, followed by a lowered sustained release. MSCs were observed to be viable and proliferative in all three groups of the *in vitro* study. It was determined that an up-regulation of osteogenic genes persisted in the SF/n-HA and SF/n-HA/BMP-2 groups compared with the pure SF group. This was further substantiated by the increased deposition of calcium in these two groups. Gross observation of the excised knee joints showed no signs of osteoarthritis and that the ligament portion was regenerated. Bone tunnel narrowing was observed in the experimental group as compared to the control group. Histological characterizations further indicated presence of new bone formation in the experimental group with development of Sharpey's fibers in the earlier post-implantation stages. Better graft to bone integration was also observed from the superior pull-out strength of the experimental group compared to the control.

DISCUSSION

The BMP-2 eluting biphasic silk scaffold was able to release BMP-2 in a manner that resembled the physiological conditions, whereby a high concentration of BMP-2 would be present at the bone defect site at the first instance, which would subsequently deplete to a lower maintenance level for continued osteogenic stimulation. From the *in vitro* characterization, it was conclusive that BMP-2 and n-HA synergistically complemented each other in stimulating osteogenic differentiation of MSCs. This was further exemplified in the small animal study, whereby the biophysical cues of the implantation site further stimulated the construct to lead to bone formation within the bone tunnel and a limited degree of fibrocartilage regeneration. The BMP-2 eluting biphasic silk scaffold was thus shown to be promising as a tissue engineering solution to regenerate the complete ACL tissue and the bone tunnels. It can serve as an advanced treatment modality for ACL reconstruction by avoiding limitations, such as donor site morbidity and lack of graft integration, of current methods.

REFERENCES: 1. Ferretti et al. J Bone Joint Surg Am 2006, 2. Teh et al. Biomed Mater 2010.

LOCALIZED CONTROLLED RELEASE OF HUMAN PDGF FROM HIGHLY ALIGNED COLLAGEN-NANOPARTICLE FIBER FOR TENDON REPAIR

XingGuo Cheng, Christopher Tsao, Thomas B. Potter
Department of Microencapsulation and Nanomaterials
Southwest Research Institute, 6220 Culebra Rd
San Antonio, TX, 78238

INTRODUCTION

To enhance the repair and regeneration of tendon/ligament, we propose a functional tissue engineering approach which involves advanced biomaterials - highly aligned collagen fibers, growth factors (human platelet derived growth factor (PDGF) and stem cells (adipose derived stem cells, ADSCs). In year 1 of this project, we have fabricated PDGF-containing nanoparticles (NPs) which can be co-assembled with collagen to form aligned collagen-NP fibers. This might lead to the production of a tendon/ligament repair medical product which minimizes the burst release of PDGF and fast clearance of PDGF from implantation site, thus providing significant potential for dense soft connective tissue regeneration.

METHODS

Two types of NPs were fabricated. Liposome-PDGF NPs were fabricated by an extrusion method, while PLGA-based NPs are prepared by a standard water-oil-water double emulsion technique. PDGF loading was characterized by human PDGF Quantikine ELISA assay (R&D Systems, Inc). Aligned collagen-NPs fibers were formed by an electrochemical process as previously described^{1,2}. Drug release from the fiber was achieved by collagenase (type I, Worthington Biochem Inc.) digestion which was followed by the ELISA assay.

RESULTS

NPs provide a localized, controlled release mechanism for PDGF. After co-assembly of NPs with collagen, collagen remained in alignment, as confirmed by the blue interference color (Figure 1A). SEM image confirmed NPs were loaded inside the highly aligned fiber (Figure 1A inset). The dosage and release profile of PDGF can be controlled by using different NP-PDGF formulation and crosslinking densities (Figure 1B).

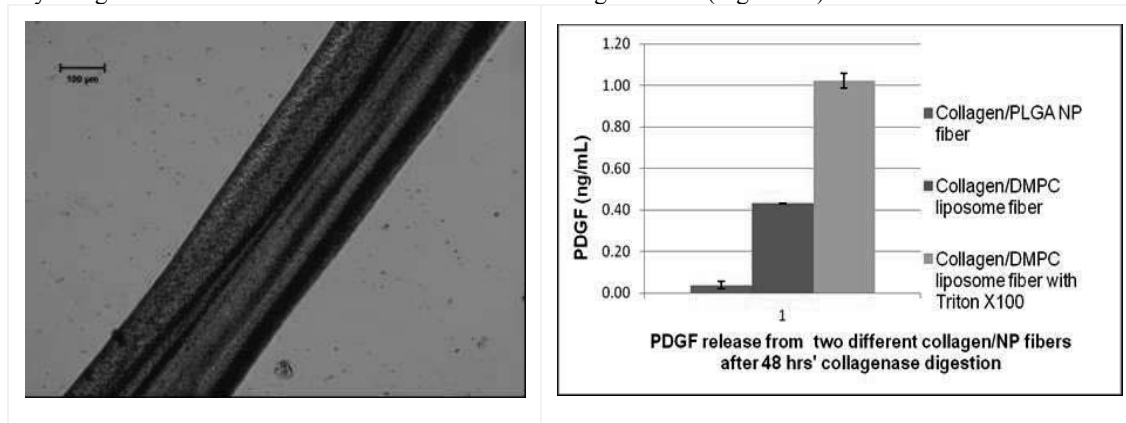


Figure 1 A) Aligned Collagen-NP fiber (optical and SEM) images. B) PDGF release from collagen fiber.

DISCUSSION

Our results indicate that it is feasible to co-assemble NPs with collagen to form composite fiber by the electrochemical process. NPs incorporated inside aligned collagen fiber provide a novel localized, controlled release mechanism of growth factors. The aligned collagen-NPs biomaterial will be evaluated for cell and tissue response towards tendon repair in year 2 and 3.

ACKNOWLEDGEMENTS

Funding from USAMRAA (oppW81XWH-09-PRORP-IDA) is acknowledged.

REFERENCES

1. Cheng XG et al. Biomaterials 2008; 29(22):3278-3288.
2. Cheng XG, Poenitzsch V. US patent application, 12/813,834. 2010.

LOW OXYGEN TENSION PROMOTES PROLIFERATION AND ENHANCES THE STEMNESS OF HUMAN TENDON STEM CELLS

Jianying Zhang, James H-C. Wang[#]

MechanoBiology Laboratory, Departments of Orthopaedic Surgery and Bioengineering
University of Pittsburgh, Pittsburgh, PA, [#]wanghc@pitt.edu

INTRODUCTION

Tendons are frequently injured, especially in athletic settings. However, due to the lack of understanding of tendon biology, the restoration of normal structure and function to injured tendons is one of the most challenging problems in orthopaedic medicine. The new discovery of tendon stem cells (TSCs) may offer a hope for more effective repair of injured tendons [1, 2, 3]. For in vitro research, TSCs are typically cultured at atmospheric conditions with 21% oxygen (O₂). This culture condition nevertheless is less physiological, as tendons in vivo exist in a much lower oxygen environment [4]. It is known that oxygen levels in vitro affect the proliferation and differentiation capacities of mesenchymal stem cells [5]. Therefore, this study was designed to determine the effects of a hypoxia condition (5% O₂) on TSCs in terms of their proliferation and stemness.

MATERIALS AND METHODS

Human TSCs (hTSCs) were isolated from the patellar tendons of six donors from 26 to 49 years of age using our published protocol [2]. The cells were seeded in 6-well plates at a density of 40,000/well and grown in DMEM supplemented with 20% FBS. The plates were placed either in a regular incubator with 21% O₂ and 5% CO₂ or in a tri-gas incubator with 5% O₂ and 5% CO₂. New medium was pre-incubated in the regular or tri-gas incubator for 30 min each time and was then used to replace old medium every 2 days. Cell proliferation was determined by cell counting. In addition, the stemness of hTSCs was tested by measuring the expression of stem cell markers Nanog and Oct-4 using real time quantitative RT-PCR (qRT-PCR). In separate experiments, hTSCs were seeded into two 12-well plates at a density of 20,000/well and placed in a regular or tri-gas incubator for 3 days. Then immunocytochemistry was performed to determine the protein expression of stem cell markers nucleostemin, Oct-4, Nanog, and SSEA-4. The staining results were quantified by semi-quantitative analysis. Finally, a *t*-test was used for statistical data analysis.

RESULTS

We found that hTSCs at 5% O₂ significantly increased in proliferation compared to those at 21% O₂ (Fig. 1). Moreover, the expression of two stem cell marker genes, Nanog and Oct-4, was upregulated in the cells cultured in 5% O₂ (Fig. 2). However, no significant changes in the expression of tenocyte and non-tenocyte related genes were noticed between the two O₂ concentrations (data not shown). Finally, in cultures under 5% O₂, more hTSCs were found to express the stem cell markers nucleostemin, Oct-4, Nanog, and SSEA-4 (Fig. 3).

DISCUSSION

This study showed that compared to normoxia culture condition (21% O₂), hTSCs under hypoxia (5% O₂) culture condition self-renewed more quickly, as evidenced by increased cell proliferation and upregulated stem cell gene expression as well as an elevated percentage of cells expressing all four stem cell markers (Fig. 3). In light of the fact that tendons are in a hypoxic condition in vivo, the findings of this study suggest that hTSCs mainly undergo self-renewal at normal physiological conditions in vivo. Finally, our findings indicate that less oxygen should be used to better maintain TSCs in culture.

References: [1] Bi et al., 2007; [2] Zhang et al., 2010; [3] Rui et al., 2010; [4] Rempel et al., 2001; [5] Lennon et al., 2001.

Acknowledgement: This work was supported in part by NIH AR049921 and ARAR061395 (JHW).

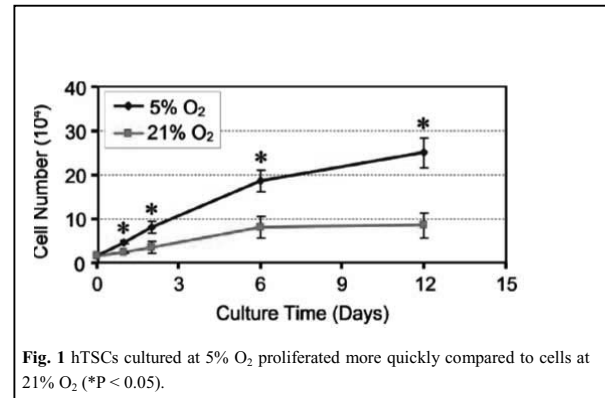


Fig. 1 hTSCs cultured at 5% O₂ proliferated more quickly compared to cells at 21% O₂ (*P < 0.05).

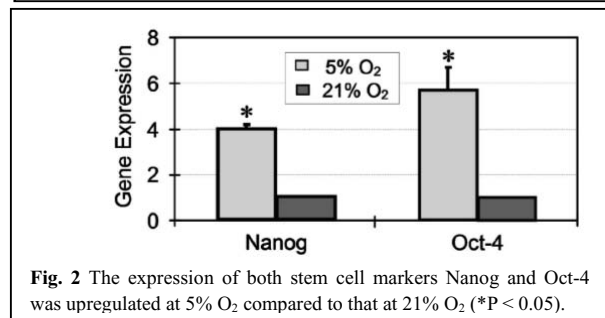


Fig. 2 The expression of both stem cell markers Nanog and Oct-4 was upregulated at 5% O₂ compared to that at 21% O₂ (*P < 0.05).

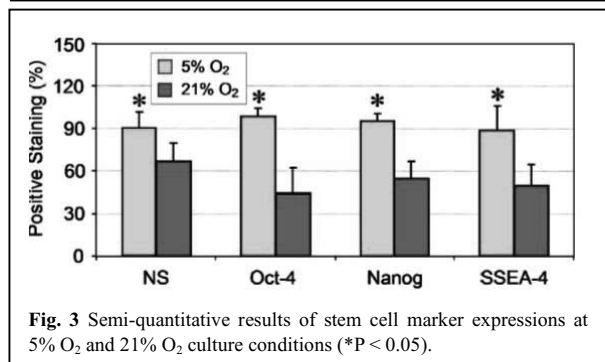


Fig. 3 Semi-quantitative results of stem cell marker expressions at 5% O₂ and 21% O₂ culture conditions (*P < 0.05).

ALGINATE ENCAPSULATED PLATELET-RICH PLASMA AND SYNOVIAL FLUID MESENCHYMAL STEM CELLS PROVIDED POTENTIAL TO REPAIR THE PARTIAL LIGAMENT TEAR

¹Ying-Chih Wang, ¹Chih-Hwa Chen, ^{1,2}Shu Wen Wu, ¹Kun-Chung Wang, ¹Chun-I Su, ¹Hsien-Tao Liu, ¹Chung-Ming Yu, ¹I-Chun Wang, ³Hsia-Wei Liu, ¹Shi-Hui Chen, and ⁴Ching-Lin Tsai

¹Department of Orthopaedic Surgery, Chang Gung Memorial Hospital-Keelung, Keelung, College of Medicine, Chang Gung University, Taouang, ² Department of Medical Device, Medical and Pharmaceutical Industry Technology and Development Center, New Taipei, ³Department of Life Science, Fu Jen Catholic University, New Taipei, ⁴ Department of Orthopaedic, National Taiwan University Hospital, Taipei, Taiwan

INTRODUCTION

Partial ligament tear usually treats by a conservative therapy and ligament recovers itself by healing ability. It causes long recovery time, inconvenient for patients, and the sequels, including adhesion, hyperplasia, calcification and laxation.¹This study utilized autologous synovial mesenchymal stem cells (SFMSCs) conjugate platelet-rich plasma (PRP), which contains plenty growth factors, mix with alginate, and coat onto the partial tear ligament by ion exchange.(Figure 1) The PRP concentration affect on growth of SFMSCs in alginate beads is evaluated first. The results could demonstrate the potential of SFMSCs-PRP-alginate mixture to repair partial ligament tear in the future.

MATERIALS AND METHODS

All porcine procedures were conducted according to the Guide for the Care and Use of Laboratory Animals and approved by the Committee of Experimental Animal Sciences of Chang Gung University. Synovial fluid was harvested from female black small ear pigs (weight about 40Kg). The synovial fluid was centrifuged to remove the supernatant, and the SFMSCs were obtained. PRP was collected by drawing the whole blood of black small ear pig via neck vessel penetration. The whole blood was centrifuged to harvest the PRP. The same alginate concentration (1%), different concentrations of PRP 0, 20, 50, 70 and 90% solution was prepared. The 5×10^4 cells/ml of SFMSCs was prepared in above five kinds of the PRP alginate solution. The SFMSCs-PRP-alginate solution dropped into 0.1M of calcium chloride solution for 2 minutes to form cell beads-like alginate beads. The cell alginate beads were cultured for 0, 3, 7, 14 and 28 days. At each time point, 10 cell alginate beads were took out, and dissolved with lysis buffer to determine DNA content.

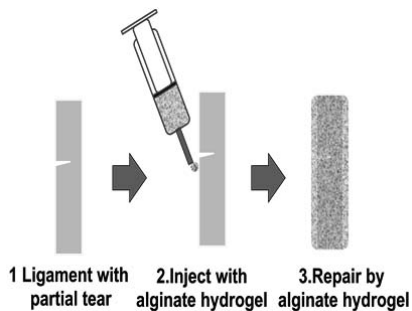


Figure 1. Alginate hydrogel repair partial tear ligament

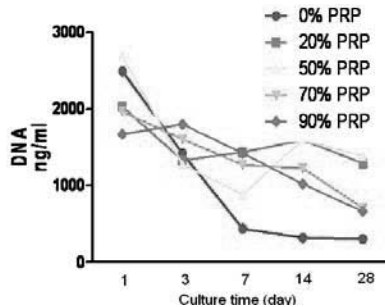


Figure 2. The DNA content of SFMSCs vs. concentration of platelet-rich plasma in alginate beads

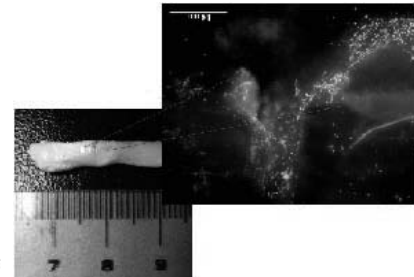


Figure 3. SFMSCs-PRP-alginate complex repaired partial tear ligament

RESULTS

The concentration of platelets in whole blood was $4.5 \pm 0.8 \times 10^8$ platelets/ml, and that in PRP was $1.9 \pm 0.6 \times 10^9$ platelets/ml (422% more in PRP than in whole blood). The DNA content increased with culture time when concentration of PRP greater than 50% in alginate beads was shown in figure 2. The DNA content of 0% PRP in alginate beads decreased with time was observed. The DNA content of 20% PRP in alginate beads decreased before 3 days and increased after 3 days was observed. The DNA content did not increase with the concentration of PRP in alginate beads was found. All PRP concentration of SFMSCs-PRP-alginate complex beads expressed good viability during culture time. Therefore, 20% and 50% PRP in alginate hydrogel was suitable concentration for cell proliferation at 14 and 28 day. The 20% of PRP enhanced cell proliferation in alginate beads for long time culture was proved.

CONCLUSION

SFMSCs-PRP-alginate complex provided good proliferation and viability. The complex is feasibility for healing partial tear of cruciate ligament.

REFERENCES

[1] Maeda A, Shino K, Horibe S, Nakata K, Buccafusca G. Am J Sports Med 24: 504-509, 1996.

**LONG HEAD OF THE BICEPS TENDON IS DAMAGED
FOLLOWING A ROTATOR CUFF TEAR IN A RAT MODEL:
INITIATION OF DAMAGE AND POSSIBLE MECHANISM OF INJURY**

L.J. Soslowsky and C.D. Peltz*

McKay Orthopaedic Research Laboratory, University of Pennsylvania, Philadelphia, PA
(*presently at Bone and Joint Center, Henry Ford Health System, Detroit, MI)

INTRODUCTION

Rotator cuff tears are painful and disabling conditions that result in joint loading changes and functional deficiencies. With rotator cuff tears, damage to the long-head of the biceps tendon occurs and tear size correlates with advanced biceps tendon lesions. However, there is debate over the role of the biceps tendon at the shoulder following a rotator cuff tear with some believing that the biceps plays a significant role as a humeral head depressor, while others believe the biceps plays essentially no functional role. As a result, controversy exists regarding its optimal treatment, with physicians relying mostly on anecdotal experience. Unfortunately, most clinical studies are not able to address the underlying causes in a controlled manner and cadaveric studies cannot monitor the injury process with time. Therefore, the first objective of this study is to demonstrate that the well-established rat model of rotator cuff injuries can be used for studying biceps damage through development and characterization of biceps pathology in this model. Importantly, tendon degeneration and inflammation are both thought to play a role in biceps tendon damage; however, the mechanisms responsible remain unknown. Therefore, the second objective of this study was to examine the location along the biceps tendon where pathologic changes initiate; where extra-articular changes would support a role for inflammation as a possible mechanism and intra-articular changes would support a role for increased loading. For our third objective, we determined the effect of alterations in loading on the initiation of pathological changes in the biceps tendon in order to determine its role as a possible mechanism for these changes.

METHODS

To evaluate our first objective, we created rotator cuff tendon injuries of different sizes in the rat model and evaluated the changes in the long head of the biceps tendon as a result of these injuries. To evaluate our second objective, we performed a time-course study compared to a sham surgery to determine where along the length of the tendon pathological changes initiated. To evaluate our third objective, we created experimental groups with decreased and increased biceps tendon loading to assess the role of altered loading as a mechanism of biceps pathology.

RESULTS

For our first objective, we determined that the rat and human have similar biceps anatomy and that the biceps tendon is indeed damaged in the presence of a rotator cuff tear, and that damage increases with increasing tear size. For our second objective, we determined that biceps pathology in the presence of a rotator cuff tear initiates intra-articularly, before proceeding extra-articularly with time. Changes were seen in the biceps as early as one week following rotator cuff injury which continued through eight weeks. For our third objective, changes with altered loading were present, with these changes beginning at the biceps insertion site at the superior glenoid. In general, increased loading resulted in further detrimental changes while decreased loading resulted in improved properties.

CONCLUSIONS

In conclusion, this rat model of biceps pathology compares well with the human condition and demonstrates that the biceps tendon is detrimentally affected by rotator cuff tendon tears. Results illustrate that changes in the biceps tendon occur gradually over time, with histological changes preceding area and mechanical changes, and that these changes represent degenerative changes rather than inflammatory changes alone. Additionally, changes occurred first in the intra-articular space indicating that the biceps tendon likely plays an increased role as a load bearing structure against the humeral head in the presence of rotator cuff tears and these changes proceed along the tendon length with time. These results indicate that increased compressive loading on the biceps tendon in the presence of a rotator cuff tear may play a role in the development of pathology and therefore, rotator cuff repair may help to resolve these changes.

EFFECT OF THE ADIPOSE-DERIVED STEM CELL FOR THE IMPROVEMENT OF FATTY DEGENERATION OF THE ROTATOR CUFF MUSCLE IN RABBIT MODEL

Seok Won Chung, Joo Han Oh, Sae Hoon Kim, Joon Yub Kim, Yeun Ho Kim, Byung Wook Song,
Seoul National University College of Medicine, Korea

INTRODUCTION

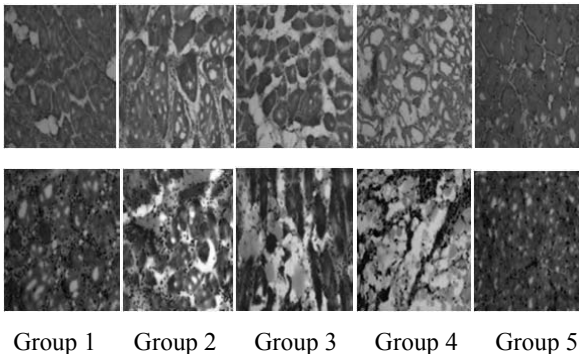
Chronic rotator cuff tears cause fatty degeneration, which may profoundly affect the postoperative shoulder function and the longevity of the repair. Even though rotator cuff repair has been shown to decrease pain and to increase shoulder function, the failure rate for anatomical cuff healing is considerably high. The purpose of this study is to verify the effect of the adipose-derived stem cell (ADSC) on tendon healing and reversal of fatty degeneration in chronic rotator cuff tear model using rabbit subscapularis (SSC) muscle.

METHODS

We randomly allocated 40 mature New Zealand white rabbits (weight, 3.5 to 4.0 kg) into 5 groups (8 rabbits per each group): group 1 (repair + stem cell injection), group 2 (repair only), group 3 (stem cell injection only), group 4 (chronic tear model without subsequent procedures), and group 5 (normal control group). For group 1, 2, 3, and 4, chronic tear model was created in both shoulders by severing SSC tendon at the insertion site and by leaving alone for 6 weeks after wrapping the torn tendon with a silicone penrose drain. For group 5, we performed sham operation. After 6 weeks, we repaired the torn SSC tendon to the lesser tuberosity in a matrix fashion using two mini-suture anchors for group 1 and 2, and injected the ADSCs (1×10^7) which had previously cultured using the abdominal fat of rabbits to the SSC muscle adjacent to musculotendinous junction area for group 1 and 3, and performed sham operation for group 4 and 5. Again after 6 weeks, we measured the compound muscle action potential (CMAP) five times by using a portable electrostimulator (1 HZ frequency, 0.1 ms stimulation duration, 30 mA stimulus intensity) under anesthesia, and calculated the average of areas under negative phase of CMAP which indicates the recruitment of motor unit. After EMG examination, we sacrificed rabbits and took out the entire SSC muscle of right shoulder along with the humeral head, then evaluated the mode of tear and the load to failure at a rate of 1mm/s with a preload of 5 N using a custom fixture clamping system attached to an Instron materials testing machine. In addition, we harvested the SSC muscle 1 cm proximal to the musculotendinous junction of left shoulder, and assessed the proportion of fat to muscle from H&E stain and the degree of fat cell staining from Oil Red O stain.

RESULTS

One rabbit in group 1 and another one rabbit in group 2 showed active infection with pus discharge, so they were excluded in this study. All SSC tendons in group 3 and 4 failed to heal with no connection between tendon and bone, therefore, we performed the EMG and mechanical test only for group 1, 2, and 5. For EMG evaluation, group 1 showed larger area in CMAP than group 2 (11.86 ± 2.97 ms*mV vs. 9.42 ± 3.57 ms*mV, $p = 0.03$), and almost reached to the level of normal control (13.17 ± 6.63 ms*mV, $p = 0.46$). For mechanical evaluation, the ratio of insertional tear to mid-substance tear was 4:3 in group 1, 5:2 in group 2, and 3:5 in group 5, and the load to failures were higher in group 1 (87.02 ± 29.81 N) than group 2 (59.85 ± 37.77 N) with marginal significance ($p = 0.09$). The load to failure of normal SSC tendon (group 5) was 122.97 ± 50.78 N and higher than that of the other group (all $p < 0.01$). For histological evaluation, the mean proportion of fatty degeneration in SSC muscle was as follows: $32.9 \pm 18.1\%$ in group 1, $38.6 \pm 10.3\%$ in group 2, $52.9 \pm 17.0\%$ in group 3, $60.0 \pm 12.6\%$ in group 4, and $18.7 \pm 10.3\%$ in group 5 ($p = 0.001$). In addition, when we assessed the stained portion qualitatively in Oil Red O stain, there was a tendency of a more increased fat stain from group 1 (unclear or weak) to group 4 (strongly present) (Fig. 1).



Group 1 Group 2 Group 3 Group 4 Group 5
Fig. 1 Fatty degeneration in H&E stain and Oil Red O stain (x200, Olympus BX51 microscope, AxioCamMR5)

DISCUSSION

The local administration of ADSCs might have the possibility to improve tendon healing and decrease muscle atrophy and fatty degeneration after cuff repair through the current study. This result could suggest another solution to increase the cuff healing rate and to reverse the fatty degeneration of rotator cuff muscle which still remain unsolved even after successful cuff repair.

BIOMECHANICAL FACTORS PREDISPOSING TO PROPAGATION OF ROTATOR CUFF TEARS: TEAR SIZE, SHOULDER ELEVATION AND ROTATION, AND ROTATOR CUFF MUSCLE STRENGTH

^{1,2}Teruhisa Mihata, ¹Bong Jae Jun, ¹Ryan Quigley, ¹Michelle H. McGarry, ²Mitsuo Kinoshita, ¹Thay Q Lee

¹Orthopaedic Biomechanics Laboratory, VA Long Beach Healthcare System and UC Irvine

²Department of Orthopaedic Surgery, Shoulder&Elbow Biomechanics Laboratory, Osaka Medical College, Japan

INTRODUCTION

Previous studies of the natural history of rotator cuff disease have shown that rotator cuff tear size progresses over time, and there is a trend toward a correlation between tear size progression and the development of shoulder symptoms. However, the factors that promote tear progression during daily activities are not known. We assessed the biomechanical factors promoting tear propagation after full-thickness rotator cuff tear.

METHODS

Seven cadaveric shoulders were tested in a custom shoulder-testing system. From the results of clinical studies, a point 15 mm posterior to the bicipital groove was chosen as a center point (CP) for rotator cuff tear creation. A small tear was created by making a 5-mm incision in both a posterior and an anterior direction from the CP and a 10-mm incision medially from the lateral footprint. The end result was a small tear 10 × 10 mm. The medium-sized tear was created by extending the small tear another 5 mm posteriorly and 5 mm anteriorly, and the large tear was created by extending the medium tear 5 mm posteriorly and 5 mm anteriorly. Rotator cuff tendon strain was measured with a Microscribe 3DLX by digitizing the position of bone markers, consisting of screws placed in the bone just lateral to the rotator cuff footprint, and soft tissue markers, consisting of glass beads, each sutured to the tendon with 4-0 silk at each testing position. Strain was calculated for markers at the tear edge, 5 mm from the tear edge, and 10 mm from the tear edge, in both the anterior and posterior directions, giving six total strain measurements under four rotator cuff conditions: intact, small tear (10 mm), medium tear (20 mm), and large tear (30 mm). Data were collected at three glenohumeral elevations (0°, 30°, and 60°) and five glenohumeral rotations (maximum internal rotation, max IR; 30° of internal rotation, 30 IR; neutral rotation, NR; 30° of external rotation, 30 ER; and maximum external rotation, max ER) with two subsequent loading conditions: (1) passive loading of rotator cuff, deltoid, pectoralis major, and latissimus dorsi to simulate residual muscle tension, and (2) increased loading to simulate strengthening rotator cuff. Statistical comparisons were made by using Tukey's post hoc test and a t-test.

RESULTS

Tensile strain adjacent to the torn tendon decreased with increasing distance from the torn edge. Tendon strain and distance from the torn edge were significantly correlated ($P < 0.05$, $r = -0.46$). At the tear edge on both the anterior and posterior sides, tendon strain increased with increasing tear size in all positions ($P < 0.05$). Tendon strain at the tear edge, 5 mm, and 10mm from the tear edge on the anterior side in the internally rotated position (30 IR and max IR) was significantly greater than that in the externally rotated position (30 ER and max ER), whereas on the posterior side the tendon strain at the tear edge and 5 mm from the tear edge in the externally rotated position was significantly greater than that in the internally rotated position. In the case of the medium and large tears on both the anterior and the posterior side of the torn tendon, tendon strain at the tear edge and 5 mm from the tear edge in 0° of glenohumeral elevation was significantly greater than that in 60° of elevation ($P < 0.05$). In the medium and large tears, tendon strain at the tear edge, 5 mm, and 10mm from the tear edge decreased significantly with increasing rotator cuff muscle loading ($P < 0.05$).

CONCLUSION

Tendon strain increased with increasing tear size, suggesting that tear propagation accelerates with extension of the rotator cuff tear. Rotator cuff tear may tend to propagate posteriorly in the externally rotated position, and anteriorly in the internally rotated position. Tendon strain at a low abduction angle was significantly greater than that at a high abduction angle, indicating that rotator cuff tears may propagate whether or not patients are engaged in work or sports that require extreme abduction of the shoulder. Residual cuff muscle strengthening may be effective in preventing tear propagation, specifically in the case of medium and large tears.

THE ARTHROSCOPIC BONE NEEDLE. A NEW, SAFE AND COST-EFFECTIVE TECHNIQUE FOR ROTATOR CUFF REPAIR

Stehle, J H; Frick, H; Volz, M; Haag M
Clinic for Sports Medicine, Ravensburg, Germany

INTRODUCTION

Reconstruction of a rotator cuff tendon tear using transosseous sutures has been time proven when surgery was done open or mini-open and has the advantage of no implants and cost effectiveness [1]. Arthroscopic rotator cuff repair is less invasive, but suture anchors are expensive. A Giant needle technique [2] was introduced, but this technique is technically difficult and has some disadvantages. This article will evaluate a modified technique using an improved design of the needle (Figure 1) and a different method for passing the sutures through the tendon (Figure 2) compared to the Giant needle technique allowing multiple usage of the same needle, combining the advantages of an arthroscopic procedure and transosseous sutures. The purpose of the study was to evaluate the clinical results, patient satisfaction, re-rupture rate and hardware costs of this procedure.

METHODS

66 patients with a tear of the supraspinatus tendon were treated with the Arthroscopic Bone Needle from 08/2008 to 11/2009. 60 patients were evaluated about one year after surgery with the Constant Score (CS). Additionally, patient satisfaction and complications were evaluated. The hardware costs of a supraspinatus reconstruction using the Arthroscopic Bone Needle were documented and compared in each case to the hardware costs using the estimated number of suture anchors that would have been necessary.

A separate study was performed to evaluate the re-rupture rate after supraspinatus reconstruction: 20 consecutive patients (operated from 07/2010 to 01/2011) had a MRI 3 months postoperatively and were evaluated by independent radiologists.

RESULTS

The average CS at follow up was 73 (SD 12) which equals a normalized CS for age and gender of 92% (SD 15). This represents a very good clinical result. 56 patients (93%) were satisfied or very satisfied with the surgery. One adhesive capsulitis occurred in this series but no axillary nerve injury or fracture of the greater tuberosity occurred. 2 patients (10%) had a re-rupture of the reconstructed tendon in the MRIs. The hardware costs of a supraspinatus reconstruction were reduced by 80% by using the Arthroscopic Bone Needle compared to suture anchors (\$ 121 vs \$ 600)

DISCUSSION:

The Arthroscopic Bone Needle technique proved to be a new, safe and cost-effective method with good clinical results and low re-rupture rate for the repair of rotator cuff ruptures.

REFERENCES

1. Post, M., R. Silver, and M. Singh, Rotator cuff tear. Diagnosis and treatment. Clin Orthop Relat Res, 1983(173): p. 78-91.
2. Fleega, B.A., Arthroscopic transhumeral rotator cuff repair: Giant needle technique. Arthroscopy, 2002. 18(2): p. 218-23.

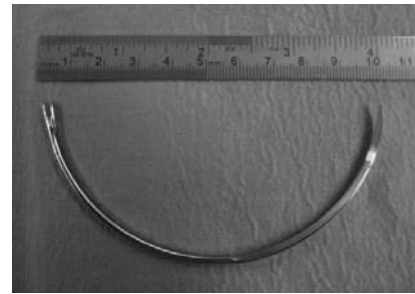


Figure 1: The Arthroscopic Bone Needle

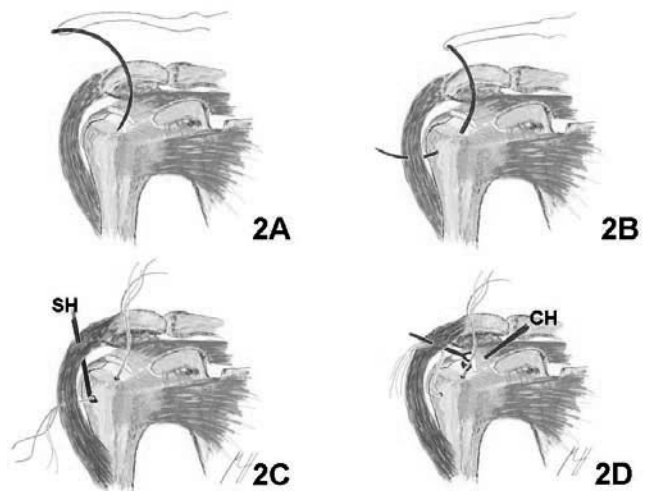


Figure 2: Schematic drawing of all steps how to reconstruct a rotator cuff tear with the Arthroscopic Bone Needle: SH= suture hook to retrieve the distal limb of the suture, CH=CleverHook® suture passer

BIOCHEMICAL CAUSES OF TENDINOPATHY?

^{1,2}P. Danielson

¹Dept. of Integrative Medical Biology, Anatomy, Umeå University, Umeå Sweden (1)

²Dept. of Ophthalmology and Ophthalmic Surgery, University Hospital of Umeå, Umeå, Sweden

In the course of the last decade, increasing attention has been directed towards the biochemical micromilieu of human tendons. Encouraged by the lack of information on the causality of tendinopathy, much contemporary research has been focused on the possible roles of biochemical agents in the development of tendon symptoms and tendon tissue changes (tendinosis). Although the functional importance of such biochemical mediators in tendinopathy is still not completely elucidated, evidence of a drastic metamorphosis in local cell signaling within chronically painful tendons exists. Studies on human tendinopathy patients have shown that there is a local, non-neuronal production in tendon cells (tenocytes) of signal substances traditionally confined to neurons. These substances include acetylcholine [7,10,13], catecholamines [6,11,12], substance P [2], and glutamate [15]. Furthermore, the receptors for several of these substances have been found on nerve fascicles and in blood vessel walls, as well as on the tenocytes themselves, of the tendon tissue. These findings provide the basis for locally produced signal substances to influence pain signaling, vascular regulation, and/or tenocyte-mediated tissue changes in tendinopathy [9].

Recent experimental studies on both *in vivo* [3] and *in vitro* [5] models of tendinopathy have further confirmed that the neuropeptide substance P (SP) is of importance, as the tendon production of SP is significantly increased after mechanical load [4,5] and as SP has been found to contribute to tissue phenomena seen in tendinosis; phenomena such as tenocyte hypercellularity and angiogenesis [1,5].

The new studies reinforce a previously presented “biochemical hypothesis” for tendinopathy [14], suggesting that biochemical mediators in the tendon tissue might influence/irritate nociceptors, in or around the tendon, to elicit chronic tendon pain, and that the cause of tendinosis is primarily of biochemical, rather than mechanical, nature. The evidence for biochemical involvement in tendinopathy development that has recently emerged might complement, rather than replace, existing theories on the pathogenesis. It furthermore fits a theoretical model in which tendon pathology exists on a continuum which, at various points, involves abnormalities in blood vessels, nerves, tenocytes, and extracellular matrix [8].

The aim of this key note lecture is to present the evidence that supports this biochemical model of tendinopathy.

REFERENCES

1. Andersson G, et al. *Br J Sports Med*, 2011. 45: 1017-22
2. Andersson G, et al. *Regul Pept*, 2008. 150: 81-7
3. Andersson G, et al. *Br J Sports Med*, 2011. 45: 399-406
4. Backman LJ, et al. *J Musculoskelet Neuronal Interact*, 2011. 11: 133-40
5. Backman LJ, et al. *PLoS ONE*, 2011. 6: e27209. doi:10.1371/journal.pone.0027209
6. Bjur D, et al. *Histol Histopathol*, 2008. 23: 197-208
7. Bjur D, et al. *Cell Tissue Res*, 2008. 331: 385-400
8. Cook JL, et al. *Br J Sports Med*, 2009. 43: 409-16
9. Danielson P. *Br J Sports Med*, 2009. 43: 265-8
10. Danielson P, et al. *Microsc Res Tech*, 2006. 69: 808-19
11. Danielson P, et al. *Microsc Res Tech*, 2007. 70: 908-11
12. Danielson P, et al. *Microsc Res Tech*, 2007. 70: 310-24
13. Danielson P, et al. *Life Sci*, 2007. 80: 2235-8
14. Khan KM, et al. *Br J Sports Med*, 2000. 34: 81-3
15. Scott A, et al. *J Orthop Res*, 2008. 26: 685-92

ACKNOWLEDGEMENTS

This work was primarily funded by the national Swedish Research Council, the J.C. Kempe and Seth M. Kempe Memorial Foundations, the Swedish Society of Medicine, and the Swedish National Center for Research in Sports.

Contributing current and former PhD-students in the project are Dr. Gustav Andersson, Mr. Ludvig Backman, and Ms. Gloria Fong. Research partners Assist. Prof. Alexander Scott, the University of British Columbia, Vancouver, Canada, and Prof. Sture Forsgren, Umeå University, Umeå, Sweden, are furthermore acknowledged for their scientific contributions.

DICLOFENAC AND TRIAMCINOLONE ACETONIDE IMPAIRS MESENCHYMAL STEM CELL GROWTH AND THEIR DIFFERENTIATION TO TENOCYTES

Maritha Fredriksson, Anders Stålman, Lars-Arne Haldosén, Li Felländer-Tsai
Dept of Orthopaedics, CLINTEC, Karolinska Institutet, Stockholm, Sweden
Dept of Biosciences and Nutrition, NOVUM, Karolinska Insitutet, Stockholm, Sweden

INTRODUCTION

Tendons and ligaments provide joint stability, enable movement and distribute power of the muscle. They comprise not only of extracellular matrix (mainly collagen I and IIIa) but also of differentiated mesenchymal stem cells (MSC), i.e tenocytes producing matrix. Tendons have their own vascularization, unlike cartilage which receives nourishment from passive diffusion of the joint fluid.

Previous experiments have shown that patellar fibroblasts mature into tendon cells when exposed to GDF-7/BMP-12, a growth factor from the TGF- β super family. Maturation is analyzed with several gene specific markers; Scleraxis, Tenomodulin and Collagen 1a1.

Several reports have shown that anti-inflammatory drugs affect the components of the synovial joint, which originate from the mesenchymal stem cell, in a negative direction with deleterious effects such as cartilage death.

We hypothesized that these two commonly used drugs, often prescribed to reduce pain and facilitate physical activity, had negative impact on mesenchymal growth and differentiation into tenocytes.

METHODS

Murine MSC were cultivated in an incubator, 5 % CO₂ in 37 C°. Growth was analyzed with WST-1-kit (Roche®). Cells where exposed to diclofenac 100nM-100 μ M and triamcinolon acetonide 1nM-1 μ M with ten-fold increase of concentration. Growth was analyzed on day 0,1,3 and 5 and gene expression was analyzed with samples from day 0,3,6 and 9. Gene expression of collagen 1a1 and scleraxis was analyzed as markers for differentiation into tenocytes. Runx2 and osteocalcin were analyzed to confirm the absence of osteogenesis. We also analyzed the expression of aP2 which is a gene for fatty-acid binding protein (FABP) and a marker for adipocytogenesis. Cellular microscopic changes and appearance were photo-documented.

RESULTS

MSC growth showed a concentration dependent reduction when exposed to either triamcinolone acetonide or diclofenac. MSC differentiated with GDF-7 and exposed to trimacinolone acetonide or diclofenac also showed an impaired growth. Gene expression of aP2 was higher in MSC exposed to higher concentrations of both diclofenac and trimacinolon acetonide over time.

DISCUSSION

Periarticular administration of triamcinolone acetonide results in locally high concentrations and some passive diffusion to surrounding tissues might be expected. Diclofenac has previously been reported to accumulate in paratendinous tissues when given orally though plasma-concentrations were lower.

The aim is to restore the patient's physical activity and reduce pain as soon as possible, however, some local inflammation might be necessary. Altering the natural course of healing with anti-inflammatory drugs, may deteriorate the vital healing process. For the first time, to our knowledge, our results show that these commonly used drugs should be used with caution since they impair growth of MSC and also affects differentiation of tenocytes negatively by promoting adipocytogenesis.

REFERENCES

- Wong MW et al (2009). "The effect of glucocorticoids on tendon cell viability in human tendon explants". *Acta Orthop.* **80**(3):363-7.
- Fu SC et al (2003). "The roles of bone morphogenetic protein (BMP) 12 in stimulating the proliferation and matrix production of human patellar fibroblasts." *Life Sci.* **72**(26):2965-74.
- Rolf C et al (1997). An open randomized study of ketoprofen in patients in surgery for Achilles or patellar tendinopathy. *J Rheumatol.* **24**(8):1595-8.
- Miyatake S et al (2009). "Randomized clinical comparisons of diclofenac concentration in soft tissues and blood plasma between topical and oral applications". *Br J Clin Pharmacol.* **67**(1):125-9.
- Syed HM et al (2011). "Bupivacaine and triamcinolone may be toxic to human chondrocytes: a pilot study". *Clin Orthop Relate Res.* **469**(10):2941-7.
- Fu et al (2010). "Deciphering the pathogenesis of tendinopathy: a three-stage process". *Sports Med Arthrosc Rehabil Ther Technol.* **13**(2):30.

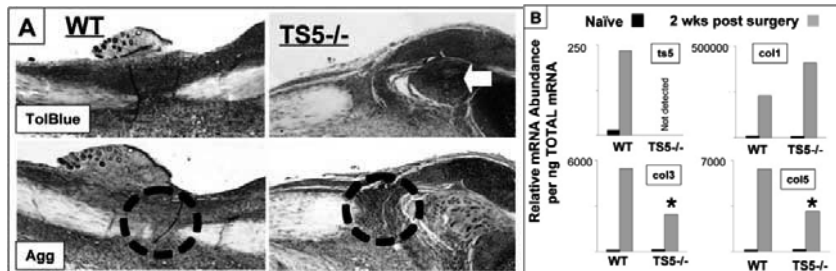
EVIDENCE THAT AGGREGAN-RICH DEPOSITS CAUSE TENDINOPATHIES BY BLOCKING FIBROGENESIS

^{1,2}R. Bell; ¹D. Gorski; ¹A. Bartels; ¹J. Li; ¹E.F. Shewman; ¹J.O. Galante; ¹J.D. Sandy; ¹A.H. Plaas; ^{1,2}V.M. Wang
¹ Rush University Medical Center, Chicago, IL, ² University of Illinois at Chicago, Chicago, IL

INTRODUCTION A major feature of tendinopathy is the accumulation of a glycosaminoglycan-rich matrix, or ARDs (Aggrecan-Rich Deposits). Gene expression studies of human Achilles tendinopathy [1] have shown an upregulation of aggrecan, suggesting that ARDs are associated with pathology, rather than with tissue compression that results in normal tendon fibrocartilages [2]. If ARDs *cause*, rather than *result from* pathology, then treatments to prevent formation or eliminate ARDs could be highly therapeutic. We recently found that equine degenerative ligament desmitis is also characterized by ARDs, which are apparently formed by progenitor fibroblasts diverted towards chondrogenesis [3]. To understand the mechanism by which ARDs might form, we next examined tendons in knockout mice lacking the most highly active aggrecanase, ADAMTS5 (TS5). These mice had earlier been shown to form ARDs within fibrous joint tissues following joint injury [4]. Furthermore, FDL and Achilles tendons in these mice [5] showed that the presence of ARDs is accompanied by a disturbance of tendon fibrillar architecture and inferior biomechanical properties. Analysis of dermal repair in TS5^{-/-} mice [6] has now uncovered a mechanism by which ARDs may cause tendinopathies. It appears that TS5-mediated removal of aggrecan from the surface of fibroblast progenitors is essential to maintain tendon fibrogenesis via the TGFβ1/Smad2/3 pathway. If the aggrecan is not removed (as in ARDs), the cells signal instead via the TGFβ1/Smad1/5/8 pathway to chondrogenesis and downregulate fibrogenesis. To test our hypothesis that ARDs can induce tendinopathies, we studied the healing response of Achilles tendons following a full-thickness punch defect.

METHODS 12-week old male C57BL/6 wild type (WT) and TS5^{-/-} mice received a 0.6 mm full-thickness punch defect of the right Achilles tendon. Mechanical testing (n=6 tendons/group) was conducted with the Achilles tendon-bone complex at 45° plantar flexion [5]. After preconditioning, specimens were loaded to failure at 0.05 mm/sec. Histologic sections (n=3 tendons/group) were stained with Toluidine blue or anti-aggrecan (DLS) [5] and finally methyl green. Quantitative PCR (n=24 tendons/group) was performed to assess collagen 1, 3, 5, and TS5 expression with Taqman primers (ABI) [6]. Data was calculated as 2^{-ΔΔCt} and further normalized to total mRNA. Student's t-test was used for statistical comparisons (p<0.05).

RESULTS Naive WT and TS5^{-/-} tendons showed similar (p>0.9) maximum stress values (9.0±3.2 MPa and 8.3±5.0



MPa, respectively), and at two weeks both genotypes exhibited an approximate 60% loss in maximum stress (to 3.4±2.0 MPa and 3.4±1.7 MPa, respectively, p>0.9). Toluidine blue and aggrecan IHC for WT (Fig. 1A), showed a contracted granulation tissue with little or no aggrecan across the punch wound and some ARDs in the peritenon. In contrast, TS5^{-/-} tendons showed a disorganized granulation tissue and both the wound area and peritenon had been remodeled to contain abundant ARDs (white arrow). QPCR (Fig. 1B) showed that in WT tendons, TS5 expression was elevated ~200-fold and both col3 and col5 increased ~6000-fold. Notably, for TS5^{-/-} tendons, both col3 and col5 expression were enhanced by less than 50% of that seen for WT.

DISCUSSION The current study demonstrates an accumulation of tendon ARDs following acute injury in TS5^{-/-} mice, which in an uninjured state exhibit pericellular aggrecan accumulation, a disturbance of tendon collagen architecture and inferior biomechanical properties [5]. The similar reduction of tensile properties at 2 weeks post wounding between WT and TS5^{-/-} mice parallels the results of our previous TGF-β1 injury model [7]; in the latter model, WT, but not TS5^{-/-} mice, demonstrated recovery of biomechanical properties at 4 weeks post-injury due to removal of ARDs by TS5 activity. Taken together, the results from these two injury models support the hypothesis that ARDs are *causative* agents in tendinopathy. It therefore seems possible that the removal of ARDs from diseased human tendons in the clinical setting may provide substantial therapeutic benefit.

REFERENCES [1] Corps AN+, *Rheumatology*. 2006 ; 45:291-294. [2] Vogel KG+, *JMNI*. 2005; 5:64-69.[3] Plaas A +, *J Orthop Res*. 2011; 29:900-6.[4] Li J +, *J Orthop Res*. 2011; 29:516-22 [5] Wang V.+, *J Orthop Res*. 2011, in press. [6] Velasco J +, *J Biol Chem*. 2011; 286:26016-27 [7] Bell R+, *Trans ORS*, 2012

LIPOXIN A₄ RECEPTOR MEDIATED INFLAMM-AGING IN FLEXOR TENDINOPATHY: A MECHANISM FOR IMMUNOSENESCENCE

¹S G Dakin, ¹R K W Smith, ¹D Werling, ¹D R E Abayasekara, ²N J Young, ¹J Dudhia
¹Royal Veterinary College, London, UK, ²National Institute for Biological Standards & Control, Herts, UK
sdakin@rvc.ac.uk

INTRODUCTION

The ability to resolve inflammation after injury is well documented for other body tissues¹, although the anticipated roles of specialized pro-resolving mediators such as lipoxins have not been investigated in tendinopathy. Our recent work has shown significantly increased expression of the inflammation resolving Lipoxin A₄ receptor (FPR2/ALX) in sub-acutely injured equine superficial digital flexor tendons (SDFT) compared to normal tendons (Dakin et. al, unpublished data). This study showed that although tenocytes were capable of mounting a FPR2/ALX response to counteract inflammation, this was of insufficient duration and magnitude in natural injury, thus potentiating chronic inflammation and fibrotic repair. Although tendon pathology and incidence of injury increases in aged humans and equids, the effect of age on the ability to resolve tendon inflammation is not understood. Our study aimed to investigate the effect of aging on the ability to resolve inflammation in tendinopathy. This was accomplished by assessing FPR2/ALX expression in natural injury and in an *in vitro* tendon explant model, in addition to determining Prostaglandin E₂ (PGE₂) levels in extracts from normal and injured SDFTs. We hypothesised that tendinopathic aged horses would exhibit elevated PGE₂ levels with reduced FPR2/ALX expression, and IL-1 β stimulated tendon explants from aged horses would show reduced FPR2/ALX expression *in vitro* compared to younger horses.

METHODS

Post mortem tissues were harvested from macroscopically normal (n=19, mean age 8 \pm 5 years) and diseased tendons, including sub-acute (3-6 weeks post injury, n=6, mean age 9 \pm 5 years) and chronic injury (>3 months post injury, n=9, mean age 13 \pm 4 years) in accordance with Institutional ethical guidelines. To determine endogenous PGE₂ levels with injury stage and age, tendon extracts were prepared as described by Zhang and Wang² and PGE₂ levels measured by radioimmunoassay. To assess FPR2/ALX expression with natural injury, tendons were snap frozen for cryosectioning and immunofluorescent staining performed whereby cryosections were probed with FPR2/ALX antibody (AbCam, UK). Expression levels were quantified by calculating the ratio of immunopositive cells to counterstained nuclei. To determine if age affected the ability of tenocytes to mount a counter-response to inflammation, we assessed the impact of 5 ng ml⁻¹ rhIL-1 β on tendon explants derived from horses <10 years of age (n=5) or \geq 10 years of age (n=8) on FPR2/ALX expression in an *in vitro* culture model. Vehicle-only samples served as controls for each horse. Explants were harvested 72 hours after stimulation, snap frozen and cryosections probed with FPR2/ALX antibody and quantitative analysis performed.

RESULTS

PGE₂ concentrations were significantly lower in extracts from sub-acutely injured tendons compared to normal and chronically injured SDFT ($P<0.001$ and $P=0.02$, respectively). In normal tendons PGE₂ levels were negatively correlated with increasing horse age ($P=0.01$) in contrast to the injured group where there was a positive correlation between PGE₂ levels and increasing age ($P=0.03$). Linear correlation analysis of tendons from horses with natural injury showed significantly reduced FPR2/ALX protein expression with increasing age ($P<0.001$). In explant cultures from normal tendons, FPR2/ALX expression was upregulated by IL-1 β in comparison to non-stimulated controls where expression was not detectable. FPR2/ALX expression was significantly reduced in stimulated explants derived from horses \geq 10 years of age compared to those <10 years of age (mean 10 fold; $P<0.01$).

DISCUSSION

A component of immunosenescence is 'inflamm-aging' whereby aged individuals exhibit diminished ability to cope with inflammation³. We demonstrate this is a feature of tendinopathy, with aged injured horses showing both increased PGE₂ levels compared to non-injured counterparts, with concurrent reduced expression of the inflammation resolving FPR2/ALX receptor. Thus it would suggest aged individuals are less able to mount a protective response to tendon inflammation by this mechanism compared to younger horses. In support of this we report significantly reduced FPR2/ALX expression in IL-1 β stimulated tendon explants from uninjured horses \geq 10 years old compared to those <10 years of age in an *in vitro* model of tendon inflammation. Inflamm-aging may therefore represent a potential mechanism for tendon re-injury and in the development of chronic injury with age. The influence of injury stage is of additional importance, as FPR2/ALX expression was significantly up-regulated in sub-acute tendon injuries which predominantly occur in younger horses, in contrast to chronic injuries which are more common in older horses due to re-injury.

REFERENCES

¹Diez-Roux et al. Development. 1997; 124, 3633-3638. ²Zhang & Wang. J Orthop Res. 2010; 28, 198-203.
³Franceschi et al. Ann N Y Acad Sci. 2000; 908; 244-254.

ACKNOWLEDGEMENTS

Biotechnology & Biological Sciences Research Council (UK) & Ceva.

VISUALIZATION OF COLLAGEN MATRIX DAMAGE IN A TENDON FASCICLE FATIGUE MODEL

S.J. Ros, N. Andarawis-Puri, E.L. Flatow

Leni and Peter W. May Department of Orthopaedics, Mount Sinai School of Medicine, New York, NY, USA

INTRODUCTION Tendinopathy is a common degenerative pathology of tendons and is a significant source of morbidity. Accumulation of matrix damage over-time is thought to lead to this pathology, however, little is known about the matrix-level changes associated with fatigue or their impact on the ability of tenocytes in damaged regions to mount a repair response. A fascicle model of fatigue damage was developed in a previous study and non-destructive mechanical parameters for damage induction were evaluated. The goal of the current study was to visualize and qualitatively describe the progression of matrix injury with increasing levels of fatigue loading. An understanding of damage progression is critical for the evaluation of cell and molecular responses to fatigue injury.

METHODS Rat tail tendon fascicles (RTTs) were harvested from 9 month old, female S-D rats (n=5) and immediately placed in PBS. RTTs were gripped between custom sandpaper grips for a 50mm gauge length and mounted in a materials testing system (Instron 8872, MA) equipped with a 10-lb load cell (Transducer Techniques, CA) and 37°C PBS bath. High speed imaging of fatigue tests confirmed no slippage. Data was acquired at 50Hz.

We have previously shown that loading of RTTs within the elastic region (1% strain, 0.5 Hz, 500 cycles) resulted in no damage as determined by the absence of changes in mechanical properties; however, loading of tendons in the plastic region (2.5% strain, 0.5Hz) showed measurable cycle-dependent changes in monotonic properties and the non-destructive parameter of elongation after 50 cycles. Based on these findings, the fatigue loading groups to be evaluated in this study were determined. Our fatigue loading protocol was as follows: A pre-load of 0.1N (~low toe-region) was first applied to remove slack and determine gauge-length. A non-destructive diagnostic test of 10 cycles, 0.5% strain was performed prior to fatigue. RTTs were then randomly subjected to 1% strain, 500 cycles (n=6) or 2.5% strain, 50, 300, or 500 cycles (n=6/group). Post-fatigue, tendons were loaded to 0.1N and a second diagnostic of 10 cycles, 0.5% strain was performed. All cyclic loading was sinusoidal at 0.5Hz. Tendons were unloaded and removed from the testing apparatus. RTTs were then fixed in tension overnight at a load of 0.1N by immersion in 10% neutral buffered formalin. Non-loaded controls (n=6) were included.]

Post-fixation, tendons were mounted on an imaging device and immersed in PBS. Structural damage to the collagen matrix was visualized by second harmonic generation (SHG) imaging at 60x magnification (LUMPFL W/IR, NA 0.90) using a multiphoton microscope (FV1000MPE, Olympus) tuned to 760nm laser excitation. Cell nuclei were visualized using ethidium homodimer and were imaged concurrently with the SHG signal. Image stacks were collected from the tendon surface to 60µm tissue depth at a 1µm step size. Stacks were qualitatively evaluated for matrix injury based on amount and severity of fibril deformations.

RESULTS SHG imaging of control specimens showed highly aligned collagen fibrils with no kink deformations (Fig. 1a). Loading to 1% strain for 500 cycles resulted in no discernable changes to the matrix. Loading to 2.5% strain resulted in progressive accumulation in both area/severity between 50 & 300 cycles. There was no evidence of further damage between 300 & 500 cycles. Cell nuclei exhibited similar deformations with kink patterns.

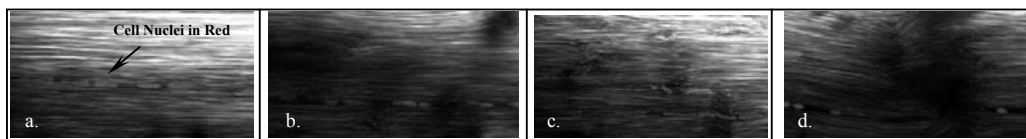


Figure 1: SHG images of RTTs with a) no damage, b) mild kink deformations, c) severe kinking, and d) micro-rupture

DISCUSSION The results confirm that loading within the linear elastic region of the monotonic load to failure curve for 500 cycles results in no collagen matrix injury, suggesting a possible physiological loading range in the RTT. Further, results provide evidence that loading to 2.5% strain results in progressive accumulation of kink patterns that progress from mild deformations to moderate kinking, which then progress to severe kink patterns and micro-rupturing. Further, the image stacks show that damage patterns propagate through the depth and along the width of the tendon. Interestingly, cell nuclei seemingly deformed along with collagen fibril deformations, which may alter cell signaling responses to loading and gap junction communication between cells. Future studies will quantify damage by the assessment of both damage area and severity. Ultimately, this model will be applied to an in vitro culture system that will evaluate the intrinsic tenocyte response to fatigue injury.

ACKNOWLEDGEMENTS: NIH: AR52743 (ELF) and GM00780 (SJR)

REFERENCES 1. Kastelic, J., 1980 2.Lavagnino, M., 2005. 3.Fung, D.T., 2008.

EFFECT OF DEGENERATIVE ROTATOR CUFF TEARS AND SUBACROMIAL BURSA STEROID INJECTION ON THE STRUCTURAL PROPERTIES OF THE SUPRASPINATUS TENDON

¹J.M.R. Tilley, ²R.J. Murphy, ²S. Chaudhury, ²A.J. Carr, ²J.T.Czernuszka

¹Department of Materials, University of Oxford, Oxford, U.K.

²Botnar Research Centre, Institute of Musculoskeletal Sciences, Nuffield Orthopaedic Centre, Oxford, U.K.

INTRODUCTION

Structure and composition of biological materials are intrinsically related to the loading environment. This is particularly relevant within the shoulder where tendon degeneration causes pain and mobility loss and often results in rotator cuff tears. Since these tears alter the loading environment of the cuff tendons [1], the structure of these tendons should differ from that of healthy tendons. To date, no studies have fully characterized the effect of rotator cuff tears on the structural properties of cuff tendons. Furthermore, while steroid injections have been shown to cause mechanical changes [2], their effect on tendon structure and how this treatment may translate to improved biomechanical properties and stronger tendons, has not been fully characterized. Previously, we demonstrated the structural adaptations of tendons exposed to different loading environments [3]. In this study we investigate the effect of tears and steroid treatment on the structural properties of human rotator cuff tendons.

METHODS

Specimens were collected from rotator cuff tendons containing small, medium, large or massive full thickness tears from patients undergoing rotator cuff surgery, and from partially torn supraspinatus tendons pre- and 7 weeks post-subacromial bursa steroid injection. Control specimens from patients < 35 years old and > 35 years old were obtained from normal rotator tendons during hemiarthroplasties and stabilizations. Specimens were fixed in 10% formalin prior to being embedded in paraffin wax. 10µm thick, deparaffinised, unstained sections were characterised using atomic force microscopy to assess tendon ultrastructure. 10µm thick, picrosirius red-stained samples were imaged using polarised light microscopy to assess fibre thickness distribution.

RESULTS

Control samples from patients < 35 years old exhibit smaller fibrils (Table 1) and a higher ratio of thinner fibres (Fig. 1) compared to control samples from patients > 35 years old. Fibril diameter (Table 1) and the proportion of thicker fibres (Fig. 1) decrease with tear size. Steroid injection increases fibril diameter (Table 1) but does not affect the fibre thickness distribution (Fig. 1). Repeat unit does not significantly differ between samples.

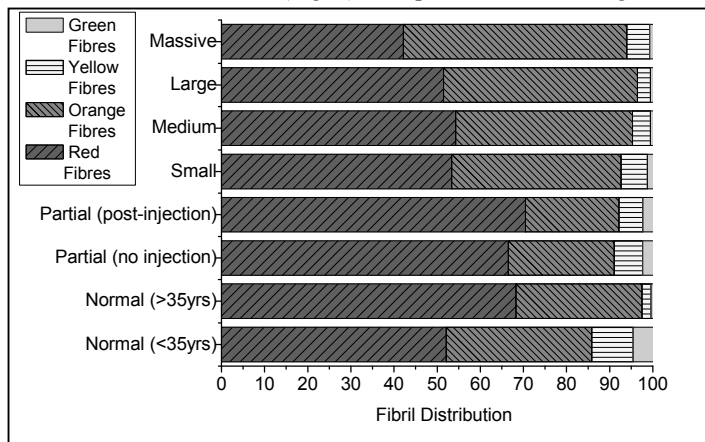


Fig. 3 Fibre thickness distribution of picrosirius red-stained samples

Table 1 Fibril dimensions assessed using AFM

	Fibril Diameter (nm)	Repeat Unit (nm)
Normal (<35yrs)	132.1	61.1
Normal (>35 yrs)	155.3	62.3
Partial (No injection)	100.9 * #	61.3
Partial (post-injection)	115.4 * #	60.8

* significantly different to Normal (<35 yrs) ($p < 0.05$)
 # significantly different to Normal (>35 yrs) ($p < 0.05$)
 § significantly different to small ($p < 0.05$)

DISCUSSION

Age influences tendon structure, with samples from older patients exhibiting larger fibrils and fibres than those from younger patients, suggesting that structural adaptation continues throughout life. Tendon structure is also affected by tear size, with smaller fibrils and fibres as tear size increases, indicating that the cuff tendons are adapting structurally to the altered loading environment caused by rotator cuff tears [1]. While steroid injection does not affect fibre thickness, steroid-treated samples do exhibit increased fibril diameters, indicating that post- injection, tendons are exposed to increased tensile stresses, possibly due to the increased mobility of the patient.

ACKNOWLEDGEMENTS

This work is funded by a doctoral training scholarship from the EPSRC and supported by the NIHR Biomedical Research Unit.

REFERENCES: 1. Sano et al. et al. J Shoulder Elbow Surg 2006. 2. Oxlund et al Acta Orthop 1980. 3. Tilley et al Micron 2011.

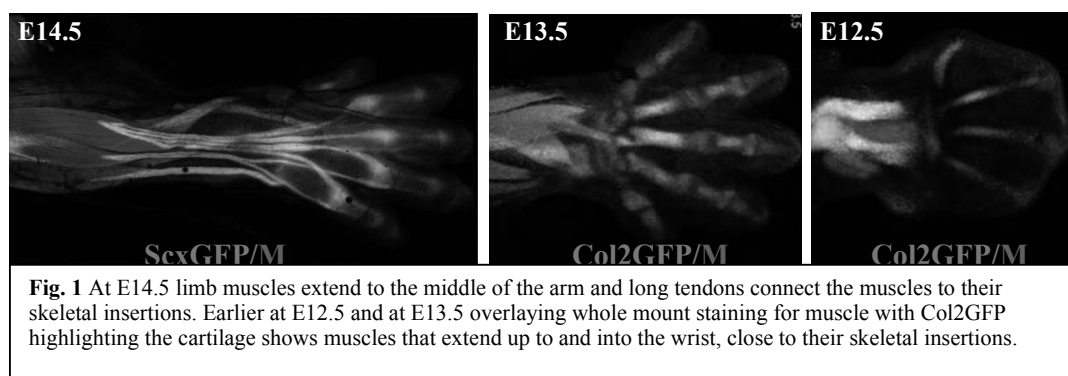
REGULATION OF TENDON ELONGATION BY STRAIN AND SCLERAXIS DEPENDENT TENOCYTES INDUCTION

Spencer S. Watson, Alice H. Huang, Ronen Schweitzer

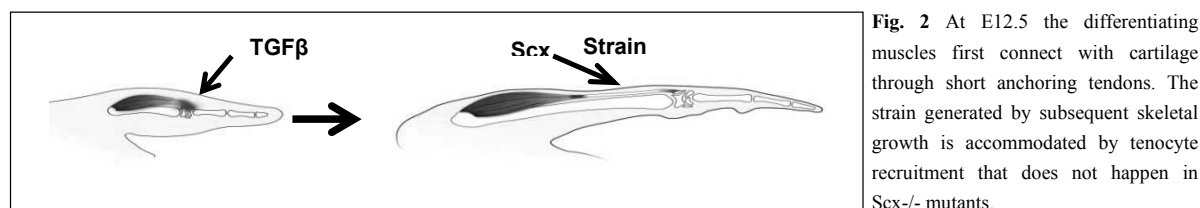
Shriners Hospital for Children, Research Department and Oregon Health and Science University, department. of Cell and Developmental Biology, Portland, Oregon

INTRODUCTION Organogenesis is a multidimensional process in which events of cell fate determination and tissue patterning combine with higher level interactions between tissues to generate fully integrated organs. The formation of the musculoskeletal system represents a unique and fascinating example involving heterotypic inductive interactions between tendons, muscles and cartilage, but almost nothing is known about patterning and integration of the musculoskeletal system. Models for musculoskeletal integration would have to address two key questions: What are the signals and cellular interactions that underlie the patterning and connections of musculoskeletal tissues? How is growth coordinated between musculoskeletal tissues in a system that maintains strain through the growth process?

INITIATION OF MUSCULOSKEETAL CONTACTS. An intuitive model for musculoskeletal connectivity would place the patterning information in tendons that use spatial queues to extend from muscles to the skeletal insertion point. By studying the early stages in tendon development we find, however, a different process. An organized musculoskeletal system is first observed at E13.5, but loosely organized tendon progenitors that align the differentiating muscles and cartilage elements are present already at E12.5 [1-3]. At this stage the muscles extend more distal than their eventual position in the limb reaching very close to their skeletal insertion. The first stage in musculoskeletal connectivity thus involves an interaction between muscle and cartilage that leads to induction of a short “anchoring tendon” (Fig.2). Interestingly, we previously showed dependence of tendon formation on TGF β signaling at the same stage [4], suggesting that induction of the anchoring tendon requires TGF β signaling.



TENDON ELONGATION. The anchoring of a muscle to a cartilage element at E12.5 generates a structural unit in which subsequent cartilage growth has is accommodated by growth of the soft tissues. Tendon growth from early embryonic stages thus occurs under and in response to strain. Using Cre mediated lineage tracing we show that tendon elongation does not occur by proliferation of the progenitors in the anchoring tendon but primarily by recruitment of new tenocytes [3]. Interestingly, we find that *Scx* function is essential for tenocyte recruitment and the tendons that do form in *Scx*^{-/-} mutant embryos are largely derived from the cells of the anchoring tendons. A fundamental question for future studies is whether tendon growth in later stages is also dependent on recruitment and if these mechanisms can be tapped to enhance treatments of injured tendons.



ACKNOWLEDGEMENTS This work was supported by NIH grant R01AR055973 from NIAMS.

REFERENCES [1] Schweitzer+ Dev 2001 [2] Murchison+ Dev 2007 [3] Schweitzer+ 2010 [4] Pryce+ Dev 2009

DIFFERENTIAL EXPRESSION AND CELLULAR LOCALIZATION OF NOVEL ISOFORMS OF THE TENDON BIOMARKER TENOMODULIN

^{1,2}J. Qi, J.M. ¹Dmochowski, ³A.N. Banes, ²M. Tsuzaki, ¹D. Bynum, ³M. Patterson, ³A. Creighton, ¹S. Gomez and ^{1,2}A.J. Banes

¹University of North Carolina, Chapel Hill, NC; ²Flexcell Int. Corp., Hillsborough, NC; ³North Carolina State University, Raleigh, NC.

INTRODUCTION

Tenomodulin (Tnmd, also called Tendin) is a type II transmembrane glycoprotein, which is highly expressed in tendons. Tnmd is also expressed in the eye in cornea, retina and sclera, where it is thought to act as an angiogenesis inhibitor. However, data from a Tnmd mouse knock-out did not support the involvement of Tnmd in anti-angiogenesis, although, in retrospect, only isoforms 1 and 2 were actually knocked out. Two recent reports also associated six single nucleotide polymorphisms (SNPs) in Tnmd with macular degeneration and with obesity. A report of a myostatin (MSTN^{-/-}, GDF-8) KO mouse model has indicated that expression of Tnmd, as well as collagen 1 and scleraxis (Scx) are decreased. Although Tnmd is accepted as a major tenocyte biomarker, its function in tendons is still disputed and unknown. In the present study, we showed the existence of multiple Tnmd isoforms in tendons. Intracellular localization and functional prediction suggest that each Tnmd isoform may play distinct roles in the cell.

METHODS

Flexor carpi radialis and biceps tendons were collected at surgery from discarded tissue (UNC Memorial Hospital). Specimens for nucleic acid extraction were placed in labeled plastic tubes and snap frozen in liquid nitrogen in the operating room then transferred to a -80 °C freezer until processed. Specimens for cell isolation were placed in DMEM-H medium with 20 mM HEPES pH 7.4, and antibiotics in preparation for cell isolation. Existence of different TNMD isoforms were determined with a quantitative real time PCR and western blot. TNMD knock-down was performed with a commercial siRNA targeting exon 5.

RESULTS

1. Data mining showed that three different transcripts exist in human tenocytes.
2. Three sets of primers were designed based on the sequences of TNMD isoforms so that measurement of different isoforms could be quantitated.
3. Differential expression of each isoform in human FCR and BT was identified.
4. Different sizes of TNMD proteins were detected in western blot assay (Figure 1). No secreted TNMDs were detected.
5. Overexpression of each isoform showed that isoform I and II were nuclear envelope-associated in COS-7 cells while isoform III was diffusely distributed in the cytoplasm. In porcine Achilles tendon cells, isoforms I and II showed nuclear envelope association, with isoform I less strongly associated (Figure 2).
6. Cells treated with TNMD siRNAs reduced cell proliferation and upregulated the expression of myostatin and Scx.

DISCUSSION

The existence of different TNMD isoforms with distinct predicted functions and localization suggests that TNMD may play multiple functions in the cell. Further functional studies on TNMD isoforms will further understanding of tendon development and tendon diseases.

ACKNOWLEDGEMENTS

This study was supported by Flexcell International Corporation. Dr. Banes is president of Flexcell and receives compensation as such.

REFERENCES

- 1.Brandau et al. 2001 2. Shukunami et al. 2001.

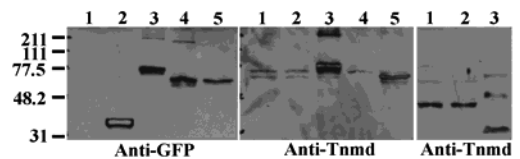


Figure 1. Western blot of human tenomodulin. Left and middle panels are from the same membrane, probed with anti-GFP and anti-hTNMD antibodies, respectively. 1-5 lanes are control, pEGFP-C1, GFP-fused hTNMD1, 2, 3 transfected COS-7 cell lysate. Right panel are human tenocyte lysate (1, 2) and tendon tissue.

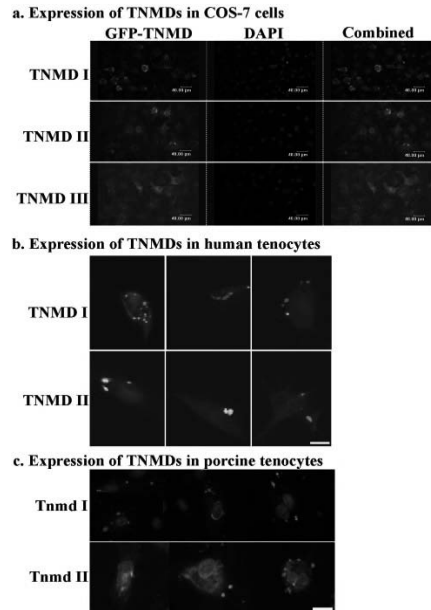


Figure 2. Expression of TNMD isoforms.

EFFECTS OF STRESS DEPRIVATION ON LUBRICIN SYNTHESIS AND GLIDING OF FLEXOR TENDON

¹Y.L. Sun, ¹C. Zhao, ²G.D. Jay, ³T. Schmid, ¹K.N. An, ¹P.C. Amadio

¹Biomechanics Laboratory, Department of Orthopedic Surgery, Mayo Clinic, Rochester, MN

²Department of Emergency Medicine, Rhode Island Hospital and Brown University, Providence, Rhode Island

³Department of Biochemistry, Rush University, Chicago, IL

INTRODUCTION

Lubricin facilitates boundary lubrication of cartilage¹. The synthesis of lubricin in cartilage could be regulated by mechanical stimuli, especially shear force^{2,3}. Lubricin was also found in flexor tendon⁴. However, little is known about the effect of mechanical loading on lubricin synthesis in tendons, or the function of lubricin in flexor tendon. In this study, the relationship of mechanical loading, lubricin expression and gliding resistance of flexor tendon was investigated.

METHODS

Animals and Tendons Twenty flexor digitorum profundus (FDP) tendons were harvested from the 4th digits of the forepaws of 10 adult mongrel dogs, which involved surgery on the 2nd and 5th digit tendons of one fore paw of each dog. The dogs were treated with a non-weightbearing protocol, in which the operated fore paw in each dog was splinted in wrist flexion, and a sling was used to maintain the paw underneath the chest with a custom-made canine jacket for 21 days. Another fore paw in each dog moved freely as a control in the whole process.

Friction Measurement After the dogs were sacrificed, the 4th digit was dissected from each fore paw. FDP tendon, proximal phalanx and its pulley were preserved. The friction between the FDP tendon and proximal pulley was measured⁵.

Lubricin Quantification After the friction measurement, 10-mm long segments of FDP were dissected and weighted. Lubricin in each segment was extracted with 2 M NaCl in PBS supplemented with 10 mM EDTA and a protease inhibitor cocktail at 4°C for 24 hours. A sandwich ELISA using peanut agglutinin and anti-lubricin MAb S6.79 was used to quantify lubricin.

Statistical Methods The comparisons of friction and lubricin content between control group and stress deprivation group were analyzed by Student's t-test. A p-value of less than 0.05 was considered to indicate statistical significance.

RESULTS

Lubricin in the tendon segments was extracted and quantified with ELISA. The flexor tendon in the suspended limb has significantly less lubricin than the flexor tendon in the contralateral limb with free motion ($P < 0.02$) (Fig. 1). Although the stress deprivation resulted the decrease of lubricin in flexor tendon, the gliding resistance of tendon did not change (Fig. 2).

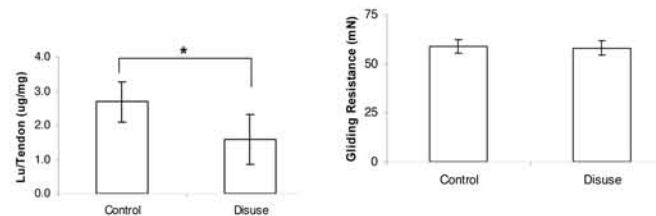


Fig. 1. Lubricin in flexor tendons in the normal and disused limbs.

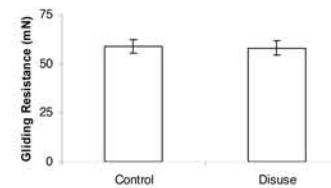


Fig. 2. Gliding resistance of flexor tendons in the normal and disused limbs.

DISCUSSION

Mechanical stress plays the important role in the development, degeneration and regeneration of tendon. The suspension of canine limb results in the decrease of compression and tensile forces applied on the flexor tendon. The expression of aggrecan, collagen I and II significantly reduced in the disused flexor tendon⁶. In addition to compressive and tensile forces, limb suspension results in the decrease of the extent of the gliding of flexor tendon. Surface motion regulates the biosynthesis of lubricin in articular cartilage^{3,7}. In this study, we found the synthesis of lubricin significantly reduced in the flexor tendon in the suspended limb comparing with those in the flexor tendon in the limb with free motion. It was demonstrated that mechanical loading affects lubricin expression in a similar manner in tenocytes as chondrocytes.

Lubricin is believed to serve as a boundary lubricant in physiological motion. It was found that the decrease of lubricin to half in FDP tendon did not result in the change of the friction of FDP tendon against its pulley. If lubricin plays the lubricating role in flexor tendon same as it does in joints, the result indicates lubricin normally presents excess in flexor tendon as it does in articular cartilage¹.

Lubricin biologically impairs the integration of separated tissues in addition to its physical function of lubrication^{8,9}. It indicates that the decrease in lubricin expression and content associated with immobilization and reduced loading, which was identified in this study, could be a factor predisposing to adhesion formation after tendon injury and repair.

ACKNOWLEDGEMENTS

This study was funded by a grant from Mayo Foundation.

REFERENCES: 1. Schmidt, T.A. et al. *Arthritis Rheum* 2007; 2. Grad, S. et al. *Tissue Engineering* 2005; 3. Nugent, G.E. et al. *Arthritis Rheum* 2006; 4. Sun, Y.L. et al. *J Orthop Res* 2006; 5. Sun, Y.L. et al. *J Orthop Res* 2004; 6. Sun, Y.L. et al. *J Appl Physiol* 2010; 7. Nugent-Derfus, G.E. et al. *Osteoarthritis Cartilage* 2007; 8. Schaefer, D.B. et al. 2004; 9. Englert, C. et al. *Arthritis Rheum*. 2005.

BMP12 AND BMP14 PROMOTE TENOGENESIS IN ADIPOSE-DERIVED STEM CELLS

H. Shen, R.H. Gelberman, M. J. Silva, S. Sakiyama-Elbert, and S. Thomopoulos
Department of Orthopaedic Surgery, Washington University, St. Louis, MO, USA

INTRODUCTION

Despite advances in the treatment of tendon injuries, clinical outcomes are often poor. BMP12 and BMP14 induce tendon-like tissue formation both *in vitro* and *in vivo* and hold promise as growth factors for tendon tissue engineering.¹⁻⁴ Bone marrow and adipose derived stem cells have the potential to differentiate into tendon fibroblasts.⁵ As the underlying mechanisms of BMP12/14-induced tenogenesis remain unclear, the purpose of this study was to study the effects of BMP12 and BMP14 on adipose-derived stem cell differentiation.

METHODS

Cell isolation and culture: Adipose-derived stem cells (ASCs) were isolated from murine and canine sub-cutaneous fat. Murine and canine tendon fibroblasts (TFs) were prepared from tail and flexor digitorum profundus tendons, respectively. All cells were cultured in alpha-MEM medium supplemented with FBS and antibiotics and various doses of BMP12 or BMP14. **Quantitative RT-PCR:** SYBR-green based real-time PCR was performed in triplicate. The expression levels of target genes were determined with $\Delta\Delta C_t$ method using GAPDH as the endogenous reference gene. **Scleraxis activity assay:** ASCs from *ScxGFP* transgenic reporter mice⁶ were treated with multiple doses of BMP12. Scleraxis activity was assessed by examining the expression of GFP. **Smad phosphorylation:** ASCs were treated with BMP12 (1000 ng/ml) for 0, 15, 30, and 60 min, BMP2 (200 ng/ml) for 30 min, or TGFbeta3 (10 ng/ml) for 30 min. Smad phosphorylation in cell lysates were examined by western blot using antibodies against phosphorylated Smad1/5/8 and phosphorylated Smad2. **Statistical analysis:** All data are shown as mean \pm standard deviation. A two-way ANOVA was performed to compare groups (* $p < 0.05$, ** $p < 0.001$).

RESULTS

BMP12 and BMP14 promoted tenogenesis in ASCs: Both BMP12 and BMP14 led to dose-dependent increases in gene expression of the tendon-specific transcription factor scleraxis in ASCs, reaching levels equal to or higher than those in the TFs (Fig. 1A). BMP12 but not BMP14 significantly increased the expression of the tendon marker tenomodulin in ASCs (Fig. 1B). BMPs enhanced the expression of the cartilage matrix gene aggrecan, however, the levels were less than 4% of those in corresponding TFs. BMP12 and BMP14 suppressed the expression of the osteogenic gene osteocalcin. **BMP12 induced scleraxis activity in ASCs:** Using a *ScxGFP* reporter⁶ GFP was expressed in the nucleus of TFs but not untreated ASCs. BMP12 induced dose- and time- dependent expression of GFP in ASCs (Fig. 2). **BMP12 signaling occurred through Smad1/5/8:** BMP12 led to the phosphorylation of Smad1/5/8 but not Smad2 in ASCs (Fig. 3).

DISCUSSION

- BMP12 and BMP14 promoted tenogenesis in adipose derived stem cells.
- Tenogenic differentiation in ASCs occurred via Smad1/5/8 signaling.
- These growth factors have significant utility for tendon tissue engineering.

ACKNOWLEDGEMENTS

This study was funded by the NIH (R01 AR033097).

REFERENCES

1. Berasi et al. Growth Factors 2011. 2. Lee et al. Plos One 2011. 3. Park et al. Tissue Eng Part A 2010. 4. James et al. Biomed Mater 2011. 5. Gimble et al. Front Biosci 2011. 6. Pryce et al. Dev Dyn 2007.

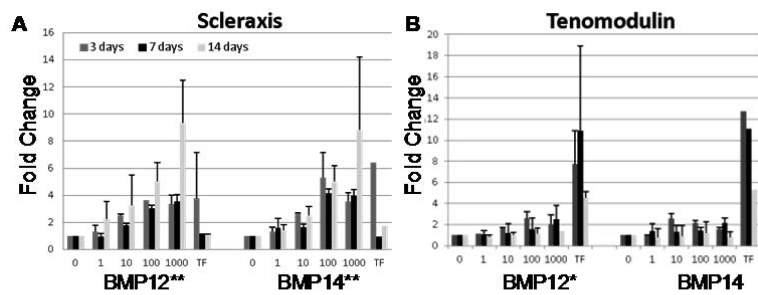


Figure 1: Gene expression.

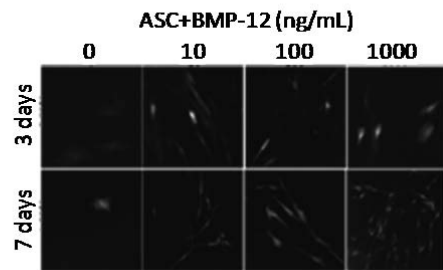


Figure 2: Scleraxis GFP expression.

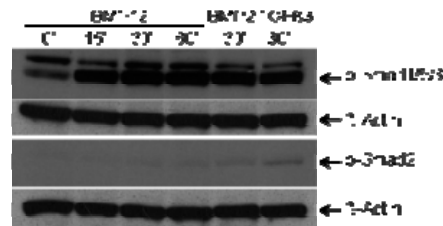


Figure 3: Smad phosphorylation.

CYCLIC AND STATIC STRESS-RELAXATION PROPERTIES OF BOVINE TENDON FASCICLES – THE EFFECT OF RECOVERY TIME

^{1,2}K. Legerlotz, ¹G.P. Riley and ²H.R.C. Screen

¹BIO, University of East Anglia, Norwich, UK; ²SEMS, Queen Mary University London, UK

INTRODUCTION

Stress relaxation tests are commonly used to characterize the stress relaxation behavior of tendons. Physiological loading conditions are generally cyclic in nature, and tendons have been reported to perceive cyclic stress relaxation conditions *in vivo*. With cyclic stress relaxation regimes also commonly used to characterize tenocyte metabolism and investigate mechanotransduction behavior, it is important to characterize the tissue response to these loading conditions, and establish how tendon may respond to, and recover from both static and cyclic stress relaxation tests. The aim of our study was to investigate if cyclical and static strains affect the mechanical properties of tendon fascicles differently and if this effect is reversible after a recovery period.

METHODS

Tendon fascicles were dissected from the extensor tendons of 8 bovine feet. Fascicle diameters were determined using a laser-micrometer and the cross sectional area calculated assuming a circular shape. Fascicles were secured in custom made loading chambers¹ and subjected to a stress-relaxation test for 30min, straining the fascicles statically to 16% strain (groups SR and SR-2h), or straining the fascicles cyclically at a frequency of 1Hz to 16% strain (groups SRC and SRC-2h). Fascicles were then either loaded to failure directly after the stress-relaxation test (SR and SRC), or after a recovery period of 2h (SR-2h and SRC-2h) and compared to an unloaded control. The reduction in stress during the 30 minute relaxation test was monitored, after which the stress-strain response during the quasi-static test to failure was recorded, to provide mean failure properties and moduli for each test group.

RESULTS

The percentage stress relaxation was significantly greater in the cyclically strained specimens compared to those held under static strain at all time points from the 5th cycle onwards. After 30 cycles, the difference between statically and cyclically loaded specimens remained constant, at a value of 13%. Concerning the failure tests, cyclic stress-relaxation led to a significant decrease of modulus, stress and strain, while static stress-relaxation resulted in a less pronounced but also significant decrease of stress and strain compared to an unloaded control. Comparing loading conditions, there were significantly lower failure strains in samples after cyclic than after static stress-relaxation. There was also a significant effect of recovery, with samples failing at higher stress and strain values after 2h recovery, compared to testing directly after stress-relaxation (Figure 1).

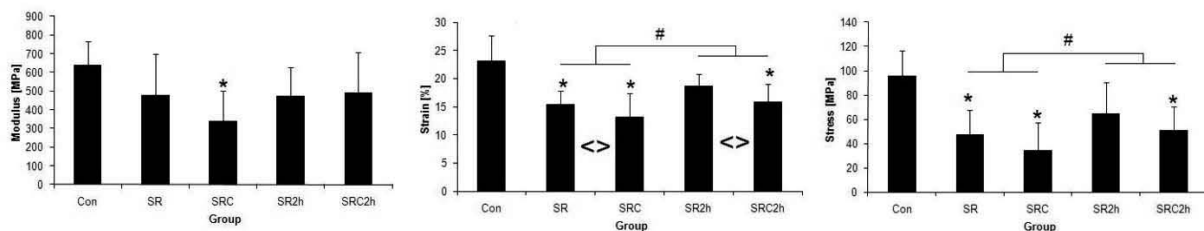


Figure 1: Mechanical properties after stress relaxation as determined by failure test: (A) modulus, (B) failure stress and (C) strain at failure. # = significant recovery effect (Two-way ANOVA). <=> = significant cyclic versus static straining effect (Two-way ANOVA). * = significantly different to control (One-way ANOVA). Mean \pm SD

DISCUSSION

We have shown that cyclic stress relaxation tests result in more pronounced stress relaxation than static tests. However, the reduction in mechanical properties was partly reversible in all samples, given a recovery period of 2h. This has implications for mechanical testing protocols, as a time delay between fatiguing specimens and characterization of mechanical properties will affect the results. The origins of relaxation behavior are poorly understood, but water movement and matrix reorganization have both been implicated. The current data supports these hypotheses, with cyclic loading facilitating a more pronounced contribution from these mechanisms, and evidence of sample recovery indicating that the fascicle structure is not damaged permanently, but may recover as the glycosaminoglycan content of the tissue encourages sample rehydration. We will test this hypothesis in future experiments.

REFERENCES

¹Legerlotz et al. (2011): Cyclic loading of tendon fascicles using a novel fatigue loading system increases interleukin-6 expression by tenocytes, *Scand J Med Sci*. accepted for publication 15 Sept. 2011

TENDON GLYCOSAMINOGLYCAN S - INTERFIBRIL GLUE OR LUBE? AFM OBSERVATIONS OF COLLAGEN ULTRASCALE MECHANICS

¹S. Rigozzi, ¹R. Müller, ²A. Stemmer and ^{1,3*}J. G. Snedeker

¹ Institute for Biomechanics, ETH Zurich, Zurich, Switzerland; ² Nanotechnology Group, ETH Zurich, Zurich, Switzerland; ³ Orthopedic Research Laboratory, University of Zurich, Zurich, Switzerland

INTRODUCTION

The extracellular matrix of tendon is mainly composed of discontinuous Type-I collagen fibrils and small leucine rich proteoglycans (PG). Macroscopic tendon behaviors like stiffness and strength are determined by the ultrastructural arrangement of these components. When a tendon is submitted to load, the collagen fibrils both elongate and slide relative to their neighboring fibrils. The role of PG glycosaminoglycan (GAG) side chains in mediating inter-fibril load sharing remains controversial, with competing structure-function theories suggesting that PGs may mechanically couple neighboring collagen fibrils (cross-linking them to facilitate fibril stretch) or alternatively isolating them (promoting fibril gliding). In this study we sought to clarify the functional role of GAGs in tensile tendon mechanics by directly investigating the mechanical response of individual collagen fibrils within their collagen network in both native and GAG depleted tendons.

METHODS

A control group of Achilles tendons (N=15) from adult mice (19 weeks of age) was compared with tendons (N=15) in which GAGs were enzymatically depleted using chondroitinase ABC. Tendons were loaded to specific target strains, chemically fixed under constant load, and later sectioned for morphological analysis by an atomic force microscope (AFM). Increases in periodic banding of the collagen fibrils (D-period) or decreases in fibril diameter were considered to be representative of collagen fibril elongation and the ultrascale mechanical contribution of GAGs was quantified.

RESULTS

Native D-period elongated in accordance with applied tendon strain, while collagen fibril diameter decreased at higher strains. The GAG depleted group showed similar trends, with longer D-periods and smaller collagen fibril diameters at 15% applied strain compared to 0% and 5% strain groups (p-value <0.005 with 0% strain and p-value <0.05 with 5% strain). In both native and GAG-depleted tendons, no D-period lengthening was observed until 5% applied strain, which at the macroscale corresponds to loss of collagen fiber crimping. However, a direct comparison between native and GAG-depleted samples at 15% applied strain showed higher levels of fibril strains in the GAG digested tendons (p-value <0.05). Simultaneously, the collagen fibrils diameter of the digested group was smaller than in native tendons, although not significantly. It thus appears that GAG content in native tendon is related to lower collagen strains (reduced collagen fibril stretching, with an implied corresponding increase in collagen fibril sliding).

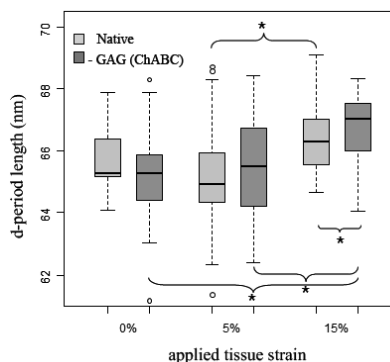


Figure 4. Increased collagen fibril strains in GAG depleted tendon under load.

DISCUSSION & CONCLUSIONS

We conclude that the hydrophilic GAGs do not act as mechanical crosslinks but rather act to promote collagen fibril sliding under tension. These findings thus complete our previous studies using mechanical testing on GAG-depleted tendons to demonstrate that tensile mechanics of native tendon is not heavily dependent on GAG content. The current study does however introduce a subtle, and perhaps important, mechanical role that GAGs play in promoting fibril sliding. This may play a key role in “slow” viscoelastic mechanical processes such as creep or relaxation, and GAGs could plausibly enable creep recovery under cellular tension of the matrix. In any case, GAGs play an essential role in collagen fibrillogenesis and are essential to the attainment of proper mechanical properties in tendon development and healing. Further, aberrant levels of PGs and their associated GAG chains are correlated to poor functional recovery after injury. So although we can now confidently conclude that tendon PGs do not play a “collagen cross-linker” role, the small leucine rich proteoglycans continue to lie at the center of tendon structure and function.

TRACKING OF MESENCHYMAL STEM CELLS IN TENDON INJURIES FOLLOWING IN VIVO ADMINISTRATION

¹J. Dudhia, ²P. Becerra, ²M.A. Valdés, ²F. Neves, ³N.G. Hartman, ¹A. Fiske-Jackson and ¹R.W.K. Smith

¹Veterinary Clinical Sciences, Royal Veterinary College, Hatfield, Herts. AL9 7TA. UK

²Hospital de Referencia La Equina, Apdo 110, Camino de Martagina Km 1 29692 – Manilva, Spain

³Department of Nuclear Medicine, Barts & The London NHS Trust, West Smithfield, London EC1A 7BE. UK

jdudhia@rvc.ac.uk

INTRODUCTION

There is increasing use of mesenchymal stem cells (MSCs) for the treatment of tendon and ligament injuries and both experimental^{1,2} and clinical studies³ suggests improved outcome measures. Labelled MSCs implanted intra-lesionally show persistence for up to 4 months after implantation into the tissue however the cells survive only in relatively small numbers^{4,5}. It is unclear when this loss occurs, how many survive the initial implantation process and whether alternative injection routes can utilise the ‘homing’ ability of MSCs. We hypothesised that MSCs are retained in tendon after intra-lesional injection and can home to the sites of injury when injected intravenously or by regional intravenous perfusion under a tourniquet.

METHODS

Aliquots of 10 million cells were each labelled using 200MBq of technetium-99m pertechnetate (Tc-99m) in hexamethylpropyleneamine oxime (HMPAO). 10, 20 and 30 minute incubation times and two different incubation media (Dulbeccos Modified Eagles Medium (DMEMs) or phosphate buffered saline (PBS)) were compared to optimise labelling efficiency.

Nine horses with naturally occurring tendinopathies (of the superficial digital flexor tendon; SDFT) and 3 horses with desmopathies (of the accessory ligament of the deep digital flexor tendon; ALDDFT) were used. After clinical and ultrasonographic examination, bone marrow was harvested from the sternum and MSCs were isolated and culture expanded using standard protocols^{3,6}. After approximately 3 weeks, three aliquots of 10 million MSCs in bone marrow aspirate were returned to the hospital and labelled with Tc-99m-HMPAO before administration. Labelling efficiency was calculated for each aliquot.

Cells were administered to each horse by each of three randomized routes on consecutive weeks: 1) Intralesional injection under ultrasonographic guidance (intralesional – IL); 2) Regional perfusion by injection into the palmar digital vein in the pastern region while a tourniquet was applied in the proximal metacarpal region (regional perfusion – RP); 3) Intravenous administration via the jugular vein (intravenous – IV). Labelled MSCs were traced by gamma scintigraphy study at 5 minutes and 1, 3, 6, 12, 24 and 36 hours after treatment. Gamma scintigrams were obtained from the lesion area, the same area of the contralateral limb, the left lung and the left thyroid (as a measure of unbound Tc-99m). In addition, values obtained from regions of interest (ROI) on the gamma scintigrams were analysed for the lesion area over time.

RESULTS

Maximum cell-labelling efficiency in validation experiments was 55% with 90% cell viability in DMEM or PBS. Labelling efficiencies of cells prepared for clinical implantation varied between 2.7% and 22.5 % with a mean of 9.2%. Cells were retained in lesions after IL administration but cell persistence within the tendon over the first 24 hours was only 15%. IV administration resulted in distribution of the cells largely to the lung fields, with no detectable cells in the tendon lesions. In contrast, significant labelling of the tendon lesions was observed in 11/12 horses following RP.

DISCUSSION

Cells used clinically labelled less efficiently most likely due to the protracted period between Tc-99m elution and delivery since decayed Tc-99m is inhibitory to HMPAO binding and should optimally be within 2 h of elution. The optimal number of cells for regenerative efficacy is not known but the highest cell numbers were retained after IL injection indicating this is still the most effective route for administering large numbers of cells, although there is considerable cell loss during the first few hours after implantation. RP appeared to be a viable alternative if no core lesion was present although it is not possible from this data to conclude if the cells were able to leave the vasculature. The absence of cells in lesions after IV administration may be a consequence of low labelling efficiencies, but cells appeared not ‘home’ to the lesion in large numbers by this route.

REFERENCES

1. Schnabel LV, Lynch ME, van der Meulen MC, Yeager AE, Kornatowski MA, Nixon AJ. *J Orthop Res*. 2009 27(10):1392; 2. Nixon AJ, Dahlgren LA, Haupt JL, Yeager AE, Ward DL. *Am J Vet Res*. 2008 69(7):928. 3. Godwin EE, Young NJ, Dudhia J, Beamish IC, Smith RK. (2011) *Equine Vet J*. 2011 [Epub ahead of print]. 4. Guest DJ, Smith MR, Allen WR. *Equine Vet J*. 2008 40(2):178. 5. Guest DJ, Smith MR, Allen WR. *Equine Vet J*. 2010 42(7):636. 6. Smith RK, Korda M, Blunn GW, Goodship AE. *Equine Vet J*. 2003 35(1):99.

ACKNOWLEDGEMENTS

Funded by Consejería de Innovación Ciencia y Empresa, Spain, and Quy Biosciences Ltd, U.K.

THE EFFECT OF INCREASING LOAD ON TENDON BIOMECHANICS DURING ECCENTRIC AND CONCENTRIC TRICEPS SURAE EXERCISES

^{1,2}S. Chaudhry, ¹H.R.C.Screen, ¹D.Bader, ²R.Woledge, and ²Morrissey.D.
School of Engineering and Material Science¹, Centre for Sports & Exercise Medicine²,
Queen Mary University of London, UK

INTRODUCTION

There is increasing evidence of the efficacy of eccentric loading EL of the triceps surae in the management of chronic Achilles tendinopathy (AT) ¹⁻⁴. EL has shown to be more effective than concentric loading (CL) in treating the condition². However, the mechanisms by which EL results in greater therapeutic benefits are unclear. Indeed, there are no clear definitions of the optimal loading protocols for treating AT, and it is notable that the additional load is often prescribed during the course of a training regime; a decision based on clinical experience, rather than derived from any evidence based study. Recent studies have suggested that it may not be the force on the tendon that varies during EL and CL, but the way in which the muscle-tendon complex perturbate,^{5,6} and this plays an important role in tendon healing. The purpose of this study was to measure load-dependent differences in biomechanical characteristics, during typical EL and CL training protocols. It was hypothesized that tendon stiffness and perturbations will both be higher during EL than CL and further increased with load.

METHODS

Seven healthy volunteers were recruited and consented to participate, with a mean age of 27.8 years (SD = 2.9). Subjects performed EL or CL with or without 18kg of weight in a backpack. To biomechanically characterize the triceps surae response to exercise we combined ultrasonography to track the musculo-tendinous junction, motion analysis to track the lower limbs and ultrasound probe movements, force plates to measure the ground reaction force and EMG recording to measure muscle activation. From these measures, tendon stress-strain and perturbations were determined. A four way ANOVA was performed inputting subjects, contraction type, movement load and frequency as factors, and summed power or EMG or AT force or Tendon stiffness from individual tests as the dependent variable. Statistical significance was accepted at $P < 0.05$.

RESULTS

Stress, strain and modulus all increased with load, stress increased from 13.2 ± 1.1 MPa during EL to 17.7 ± 1.95 MPa during HEL ($p < 0.05$) and increasing from 12.9 ± 0.9 MPa during CL to 18.1 ± 0.16 MPa during HCL ($p < 0.05$). While perturbations varied among individuals, there was a significant difference in the force perturbations between EL and CL. Significantly higher power vibrations were observed in the 5-6Hz and 8-13Hz range in EL compared to CL ($p < 0.05$) (Figure 5). Furthermore, in a narrow 9-11Hz range of power densities, heavy EL demonstrated significantly ($p < 0.05$) higher fluctuations compared to EL. For concentric loading no significant differences were observed between CL and heavy CL.

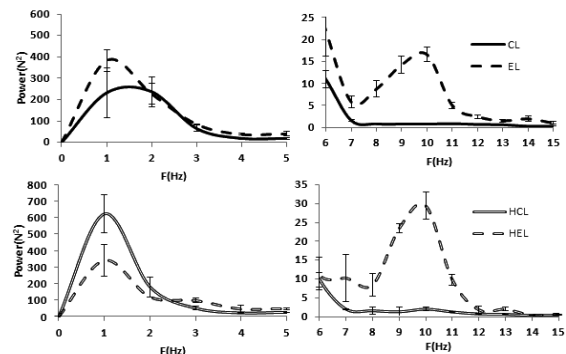


Figure 1: Mean \pm SE for the power spectrum during EL and CL (top) EL with load (HEL) and CL with load (HCL) (bottom).

DISCUSSION

Clinical practice has utilized additional load during exercise with the rationale that it will increase the tendon force³. The current data has demonstrated that additional load does significantly increase the forces passing through the tendon during both EL and CL. However, this study has additionally reported elevated vibration intensity during EL and even higher vibrations during heavy EL. Mechanical conditioning is well known as one of the drivers enhancing tendon healing, with cells converting mechanical stimuli into biochemical signals through mechanotransduction.⁷ If EL does promote optimal healing, our data suggests that the 9-11 Hz range may be key for stimulating healing, with heavy loading leading to even higher vibration. This may explain, in part, the clinical observation that heavy load training is more effective than bodyweight resistance alone.

REFERENCES: 1 Alfredson, H. et al. *Am J Sports Med* 1998. 2 Mafi, N. et al. *Knee Surg Sports Traumatol Arthrosc* 2001. 3 Stanish, W. D. et al. *Clin Orthop Relat Res* 1986. 4 Kingma, J. J. et al. *Br J Sports Med* 2007. 5 Rees, J. D. et al. *Rheumatology* 2008. 6 Henriksen, M. et al. *Journal of Biomechanics* 2009. 7 Bacabac, R. G. et al. *FASEB J* 2006.

A HIGH CALCIUM DIET IMPROVES THE ADAPTIVE RESPONSE OF TENDON TO EXERCISE

¹N. Andarawis-Puri, ¹S.J. Ros, ²K.J. Jepsen

¹Leni and Peter W. May Department of Orthopaedics, Mount Sinai School of Medicine, New York, NY and ²Department of Orthopaedic Surgery, University of Michigan, Ann Arbor, MI

INTRODUCTION

Tendinopathy is a common musculoskeletal injury associated with impaired tendon healing and rupture. Damaging loads that are disruptive to the extracellular matrix during adulthood may not be harmful when applied during growth.¹ We expect that loading during growth can improve the ability of the tendon to resist injury and heal during adulthood. Since calcium is one of the primary second messengers that is integral to cellular transduction of mechanical signals,² we tested the hypothesis that a high calcium diet will be integral to the adaptive response of a young tendon to voluntary exercise. We hypothesize that (H1): Under normal cage activity, mice fed a high calcium diet will exhibit greater mechanical properties of their Flexor Digitorum Longus tendon (FDL) than mice fed a regular diet; and (H2): Mice allowed free access to a cage wheel and fed a high calcium diet will show greater changes in FDL mechanical properties compared to mice allowed free access to a cage wheel but with a regular diet.

METHODS

Following IACUC approval, 4-week old, female C57BL/6J (B6) mice were randomly assigned into 1 of 4 groups (Table I). Since B6 mice exhibit seasonal variation in musculoskeletal tissue³, groups were matched by calendar period. Mice in exercise groups were individually housed in a cage with a monitored exercise wheel. Average revolutions/day and total revolutions were determined. Mice were sacrificed at 16 weeks of age. The FDL was harvested from the left limb, gripped between sandpaper grips (~7.5mm length), attached to an Instron testing machine, and tested in a 37°C PBS bath. A pre-load of 0.1N was applied, followed by preconditioning with 10 cycles to 1.5% strain at 0.5 Hz. Stress-relaxation was conducted by ramping to 5% strain at 5%/sec and holding this strain for 5 minutes. The tendon was then unloaded for 1 minute. The pre-load and pre-conditioning were re-applied, followed by monotonic load to failure (0.4%/sec). Percent relaxation after 2 minutes was calculated from stress-relaxation. Stiffness, ultimate load and failure displacement were calculated from monotonic load to failure.

H1 was assessed by comparing groups 1‡ and 3‡ with a t-test. H2 was assessed by normalizing FDL properties of groups 2† and 4‡ by those of groups 1† and 3‡ respectively, and then comparing the ratio with a t-test.

RESULTS

Mice ran 7.04 ± 1.39 km/day. There was no significant difference in average revolutions/day or total number of revolutions between the two exercise groups (data not shown). Contrary to H1, under normal cage activity, a high calcium diet did not improve the mechanical properties of the FDL over a regular diet (Table II). Surprisingly, exercise with a regular diet resulted in a small but significant decrease in FDL stiffness when compared to mice fed a regular diet with normal cage activity (Fig 1). Supporting H2, exercise combined with a high calcium diet resulted in increased FDL stiffness and ultimate load compared with a high calcium diet with cage activity or with exercise combined with a regular diet.

DISCUSSION

We found that the adaptive response of tendon to exercise during growth was impacted by diet. Calcium is essential for modulation of many cell functions, including gene transcription, cell growth and proliferation.² In tenocytes, a threshold of extracellular calcium concentration is necessary to allow cells to sense strain.⁴ It is likely that a diet that is high in calcium ensures availability of the needed amount of calcium to allow the cells to respond to loading. In addition, since calcium is expected to increase bone strength, greater loads may be transmitted through the tendon motivating further adaptation. Findings emphasize that adaptation to exercise can be modulated to improve function and result in stronger tendons that may be more resistant to injury in adulthood. Future studies will assess the underlying mechanisms by which ingested calcium improves the ability of the tendon to adapt to exercise.

ACKNOWLEDGEMENTS: This study was supported by NIAMS/NIH (AR44927, AR058123). The authors thank Dr. Evan L. Flatow for his input and Valerie Williams and Mohammad Khan for the daily care of the mice.

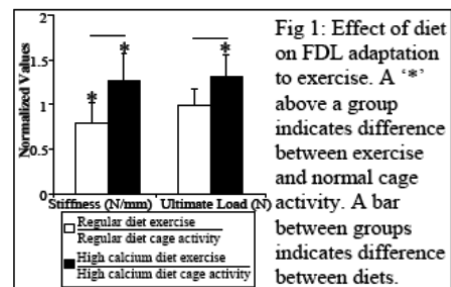
REFERENCES: 1. Kasashima et al. J Appl Physiol 2008. 2. Berridge et al. Nat Rev Mol Cell Biol 2003. 3. Delahunty et al. J Clin Densitom 2009. 4. Wall et al. J Musculoskelet Neuronal Interact 2005.

Table I: Groups that share a '†' or '‡' were collected in the same calendar period.

Group	Diet	Activity
1 †(n=8) ‡(n=10)	Regular	Cage
2 †(n=10)	Regular	Exercise
3 ‡(n=10)	High calcium	Cage
4 ‡(n=10)	High calcium	Exercise

Table II: Effect of diet with cage activity (averages \pm standard deviations).

	Percent Loss (%)	Stiffness (N/mm)	Ultimate Load (N)	Failure Displacement (mm)
Regular Diet	44.31 \pm 7.93	7.46 \pm 3.17	4.28 \pm 1.72	0.98 \pm 0.33
High Calcium Diet	46.37 \pm 4.42	7.24 \pm 1.62	4.22 \pm 1.15	0.92 \pm 0.25



MECHANICAL AND MOLECULAR EFFECTS OF AGING ON NORMAL LIGAMENTS

G.M. Thornton, C.R. Reno, D.A. Hart

McCaig Institute for Bone and Joint Health, University of Calgary, Calgary, Alberta, Canada

INTRODUCTION

Aging alters the mechanical properties of ligaments. In medial collateral ligaments (MCLs) from 1-year-old and 3-year-old rabbits, ultimate tensile strength (UTS) was not affected, but modulus was decreased with age [1]. Also, water content was not affected, but collagen concentration and synthesis were decreased with age [2]. Our purpose was to examine the effect of aging on MCLs from 1-year-old and 3-year-old rabbits comparing low-load (creep) and high-load (failure) mechanical properties, water content, and molecular expression of collagens and proteoglycans. Our hypothesis was that MCLs from 3-year-old rabbits would have greater total creep strain, greater failure strain, and decreased modulus compared to MCLs from 1-year-old rabbits. Also, 3-year-old rabbit MCLs would have decreased collagen expression but similar proteoglycan expression and water content to 1-year-old rabbit MCLs.

METHODS

Female rabbit MCLs were creep tested at 4.1MPa. After mounting the knee in an MTS system and measuring MCL geometry, an environment chamber was installed (37°C and 99%RH). For cyclic creep, the MCL underwent 30 cycles at 1Hz from +0.1N to a force corresponding to 4.1MPa. For static creep, the MCL was held at that force for 20 minutes. After recovery, the MCL was elongated to failure at 20mm/min. Total creep strain was the increase in strain from the peak of the first cycle in cyclic creep to the end of static creep. The UTS was the failure force divided by MCL cross-sectional area. Failure strain was the deformation at the failure force divided by MCL length. Modulus was the slope of the linear regression of the upper 50% of the failure stress-strain curve. On untested MCLs, RT-qPCR was performed using rabbit specific primers for collagens (COL-I, -III, -V) and proteoglycans (biglycan, decorin, lubricin/PRG4), and the housekeeping gene 18S. Water content was the difference in MCL wet weight and dry weight divided by wet weight to express as a percentage. Data were compared using Student's t-tests.

RESULTS

Comparing MCLs from 3-year-old to 1-year-old rabbits, total creep strain was not different but failure strain was increased with age ($p=0.02$; Figure 1). Modulus was decreased with age ($p=0.04$) with no change in UTS (Figure 1). Expression of lubricin/PRG4 in the MCL increased with age ($p=0.06$; Figure 1) with no changes detected for the other proteoglycans or the collagens investigated. Water content of the MCL was not affected by aging (Figure 1).

DISCUSSION

With age, modulus decreased with no change in UTS or water content comparing MCLs from 3-year-old to 1-year-old rabbits which is consistent with previous findings [1,2]. The low-load mechanical property of total creep strain was not affected by aging, but the high-load mechanical property of failure strain increased with age. These age-related mechanical changes may have implications for potential damage accumulation differences with age. Lubricin was affected by aging and its speculated role in ligament may be related to interfascicular lubrication [3,4].

ACKNOWLEDGEMENTS: NSERC, CIHR

REFERENCES: [1] Woo SLY et al. Mech Ageing Dev 56:129, 1990; [2] Amiel D et al. J Gerontol 46:B159, 1991; [3] Funakoshi T et al. J Bone Joint Surg Am 90:803, 2008; [4] Zhang D et al. J Orthop Res 29:1916, 2011.

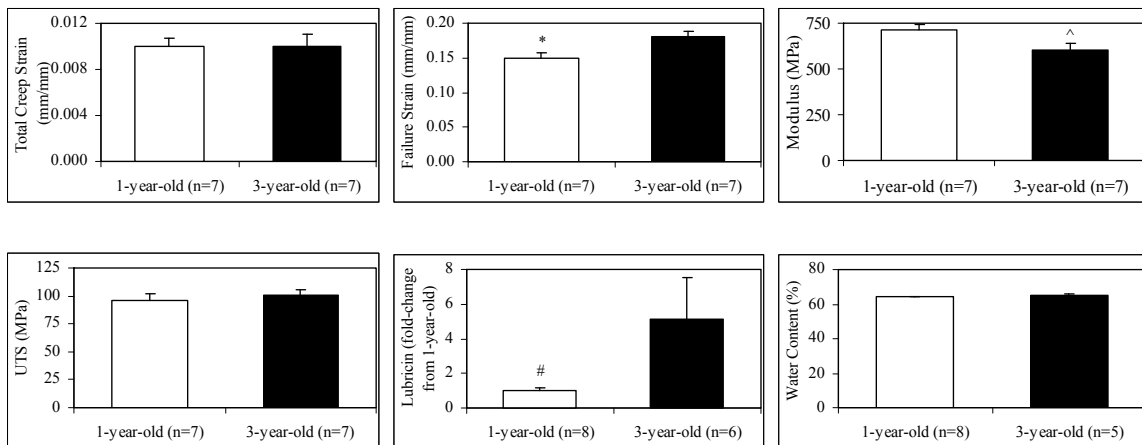


Figure 1: Total Creep Strain, Failure Strain, Modulus, UTS, Lubricin/PRG4 Expression and Water Content of MCLs from 1-year-old and 3-year-old rabbits. Data are shown as mean \pm sem. * $p=0.02$; ^ $p=0.04$; # $p=0.06$.

INVESTIGATING FIBRE MECHANICS IN FUNCTIONALLY DISTINCT TENDONS

C T Thorpe^{1,2}; H L Birch³; P D Clegg² and H R C Screen¹

¹Queen Mary, University of London, London, UK, ²University of Liverpool, Liverpool, UK, ³UCL, London, UK.
c.thorpe@qmul.ac.uk

INTRODUCTION

The function of most tendons is to position the limb correctly for locomotion. Specific tendons, including the equine superficial digital flexor (SDFT) also function as energy stores. To perform this function, they must be able to withstand high strains without damage. While it is well established that the tendon mechanical properties differ between energy storing and positional tendons (such as the equine common digital extensor (CDET))¹, it is not clear how differences in the organisation of the matrix throughout the levels of the tendon hierarchy contribute to the gross mechanical response. Previous work has established that fibre sliding contributes to tendon extension, resulting in a shear strain environment surrounding the cells². Characterising the cell strain environment allows understanding of mechanotransduction cues within the tissue. We hypothesise that the fibre level strain environment and resulting cell mechanotransduction cues vary in functionally distinct tendons. The objectives of this study were to investigate the microstructural strain response in two functionally distinct tendon types; the equine SDFT and CDET.

METHODS

Fascicles were dissected from the SDFT and CDET from 4 horses (n=8 from each tendon), incubated in 5-dicholorotriazinyl fluorescein, washed in PBS and secured in a tensile straining rig. Each fascicle was viewed under a confocal microscope using a x20 objective, and a grid was photobleached onto the fascicle (Fig. 1). Images of the fascicle were taken at 2% strain increments up to 8%. Deformation of the grid at each strain increment was measured (Fig. 1). Statistical significance was set at $p < 0.05$ and is indicated by *. Data is displayed as mean \pm SEM.

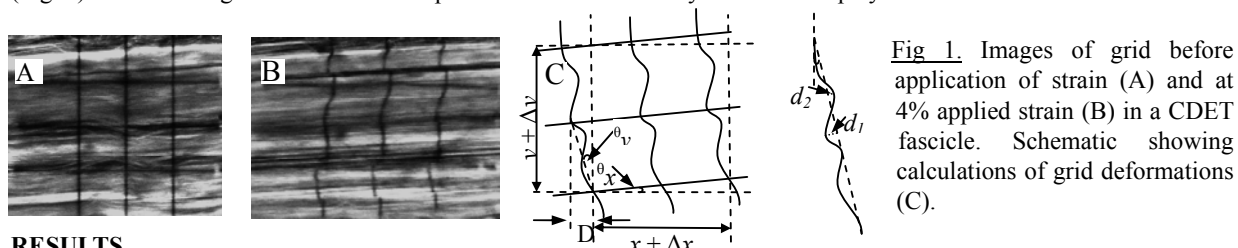


Fig 1. Images of grid before application of strain (A) and at 4% applied strain (B) in a CDET fascicle. Schematic showing calculations of grid deformations (C).

RESULTS

Local strains in the x plane ($x + \Delta x$) were heterogeneous but consistently smaller than applied strains (Fig. 2). However, large compressive strains were measured in the y direction ($y + \Delta y$), which were significantly greater in the CDET ($p < 0.016$, Fig. 3). The maximum displacement ($d_1 + d_2$) of the vertical gridline was significantly greater in samples from the CDET than those from the SDFT (Fig. 4, $p < 0.006$), indicating larger movements between adjacent fibres in the CDET than the SDFT. Both θ_x and θ_y increased with each strain increment, indicating fascicle rotation.

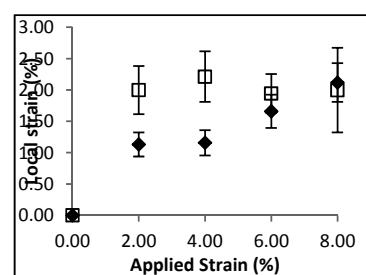


Fig. 2 Local strains in the x plane

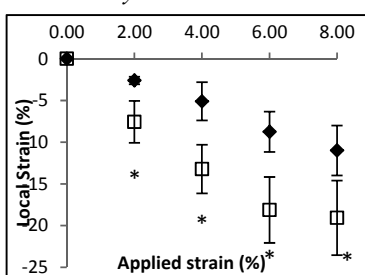


Fig. 3 Local strains in the y plane

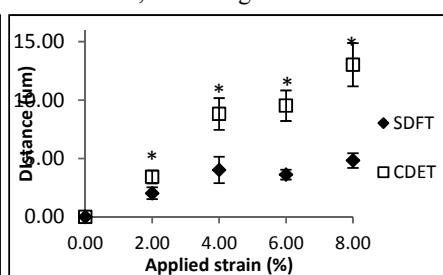


Fig. 4 Displacement of vertical gridline

DISCUSSION

In agreement with previous results², local strains were heterogeneous and much smaller than the applied strain, and fascicle rotation was observed. However, samples from the positional CDET demonstrated significantly larger compressive strains and levels of fibre sliding than those from the energy storing SDFT. These differences may reflect considerable variations in fibre packing and organisation between the tendon types. Taken in conjunction with our previous data³, these results indicate that there are large differences in tendon mechanics and strain distribution through all levels of the hierarchy. Furthermore, the large compressive strains perpendicular to the loading axis, and higher fibre sliding in the CDET indicate that the cells may be exposed to greater levels of shear and compressive strain, possibly leading to the distinct phenotypes previously observed in the two cell types⁴.

REFERENCES ¹Batson et al, EVJ 2003; ²Cheng & Screen, J Mater Sci 2007; ³Thorpe et al, ORS 2012; ⁴Birch et al, Matrix Biol 2008.

MEASURING TRANSVERSE CARPAL LIGAMENT THICKNESS BY ULTRASOUND

¹Zhilei Liu Shen, ¹Joshua L. Gordon, ¹John Cheng, ^{1,2,3}Zong-Ming Li

Departments of ¹Biomedical Engineering, ²Orthopaedic Surgery, and ³Physical Medicine and Rehabilitation, Cleveland Clinic, Cleveland, OH, USA

INTRODUCTION

The transverse carpal ligament (TCL) forms the palmar boundary of the carpal tunnel and prevents volar migration of the underlying median nerve and flexor tendons. TCL hypertrophy has been postulated as one of the etiological factors of carpal tunnel syndrome (CTS).¹⁻⁴ Confirmation of this hypothesis relies on a method that qualifies TCL morphology *in vivo*. Attempts have been made to examine the dimension of the TCL using caliper, micrometer, photograph, histology, silicon casting, computed tomography, and magnetic resonance imaging. However, ultrasound is particularly advantageous for TCL imaging because of its capability of detecting the interfaces between TCL and other tissues. Furthermore, ultrasound is inexpensive, quick, non-invasive, and suitable for routine clinical assessment. The purposes of this study were to develop an ultrasound-based method to measure the TCL thickness and to test its validity and reliability.

METHODS

Three operators conducted two sessions of ultrasound examination on 8 cadaveric specimens and 8 healthy volunteers using a Siemens Acuson S2000 ultrasound system. Each operator captured three images per specimen/volunteer during each session. A customized MATLAB script was used to calculate the thickness of the TCL (arrowheads in Fig. 1) at the thenar muscle attachment site (arrow in Fig. 1). The validity of ultrasound measured TCL thicknesses against those obtained directly on dissected cadaveric specimens were analyzed with the Pearson's correlation coefficient and intraclass correlation coefficient (ICC). The inter- and intra-operator reliability was examined with ICC and standard error of measurement (SEM) based on ultrasound images taken during different sessions and by different operators, respectively.

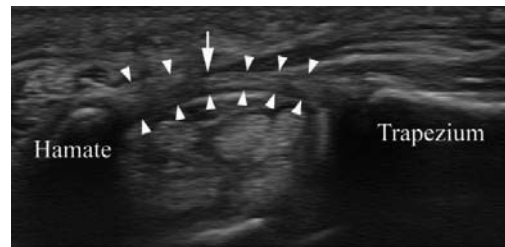


Fig. 1 An ultrasound image of the carpal tunnel

RESULTS

At the thenar muscle attachment site, the TCL thicknesses of 8 cadaveric specimens were in the range of 1.02-1.80 (1.38 ± 0.25) mm based on ultrasound measurements and 1.13-2.30 (1.69 ± 0.36) mm based on dissection measurements. Validity analysis (N = 8) showed that the Pearson's correlation coefficient was 0.904 and the ICC value was 0.726. Reliability analysis for ultrasound measurements was performed based on all 16 cadaveric specimens and healthy volunteers. The inter-operator reliability showed an ICC value of 0.859 and a SEM of 0.13 mm. The intra-operator reliability showed ICC values of 0.853-0.909 and SEMs of 0.10-0.14 mm (Table 1).

Table 1 Intra-operator reliability (N = 16)

	TCL thickness (mm)		ICC	SEM (mm)
	session 1	session 2		
operator 1	1.58 ± 0.41	1.67 ± 0.47	0.909	0.13
operator 2	1.44 ± 0.22	1.39 ± 0.30	0.853	0.10
operator 3	1.51 ± 0.43	1.63 ± 0.39	0.875	0.14

DISCUSSION

The ultrasound measured TCL thickness (1.02-1.80 mm) agreed well with the TCL thickness (1-3 mm) in the previous studies.⁵⁻⁸ The high correlation coefficients (Pearson's = 0.904, ICC = 0.726) obtained from the validity analysis indicate that ultrasound is a valid method to measure TCL thickness. However, the ultrasound based TCL thickness was consistently smaller (0.16-0.31 mm) than the dissection based measurements, suggesting that there was a systematic bias. This bias is likely due to the inclusion of non-ligament tissues of the dissected TCL.⁶ The excellent inter- and intra-operator reliability (ICC > 0.85) indicates that ultrasound is a reliable tool to measure TCL thickness. For ultrasound data, the SEM was relatively small (0.10-0.14 mm) compared with the TCL thickness (1.02-1.80 mm), suggesting that ultrasound is a valuable imaging modality to monitor subtle morphological changes of the TCL. For example, a clinical study showed that the TCL was as thick as 2-10 mm in 61 CTS patients.⁴ In the future, our ultrasound methodology can be potentially used to identify TCL related etiology of CTS.

ACKNOWLEDGEMENTS: NIH R03AR054510

REFERENCES: 1. Moore *Am J Ind Med* 2002. 2. John et al. *AJNR Am J Neuroradiol* 1983. 3. Ferrari et al. *Radiol Med (Torino)* 1997. 4. Yamagami et al. *No Shinkei Geka* 1994. 5. Merhar et al. *Skeletal Radiol* 1986. 6. Stecco et al. *J Hand Surg Am* 2010. 7. Cobb et al. *J Hand Surg [Am]* 1993. 8. Pacey et al. *Hand (N Y)* 2010.

DOES LOCKING CONFIGURATION AFFECT THE BIOMECHANICAL CHARACTERISTICS OF EXTENSOR TENDON REPAIR IN ZONE IV?

KC Chung, J Scott, BJ Jun, MH McGarry, TQ Lee

Orthopaedic Biomechanics Laboratory, VA Long Beach Healthcare System and University of California, Irvine, California USA

INTRODUCTION

The purpose of this study was to compare the complexity and biomechanical properties of modified locking configurations with modified Becker extensor repair in Zone IV.

METHODS

Nine cadaveric hands were used. Tendons of the index, middle and ring fingers were exposed over the proximal phalanx, sharply transected at midpoint and repaired in situ with one of three locking configurations: modified Becker with two cross-locks, combination of one cross- and circle-lock and combination of two cross- and circle-locks. The tendons within each hand were sequentially randomized for configuration. The numbers of needle passages to complete core suture were recorded. Biomechanical properties and gap formation were measured with an Instron material testing machine and video digitizing system. After a 5 N preload, each repair was cyclically loaded from 5 to 25 N for 30 cycles at a rate of 20 mm/min to simulate loads during postoperative rehabilitation. After cyclic loading, the specimen was loaded to failure. A repeated-measures ANOVA with a Tukey post hoc test was used to compare the effects of locking configurations.

RESULTS

The extensor repair with one cross- and circle-lock required 8 less needle passages and showed superior gap resistance and stiffness during cyclic loading compared to modified Becker with two cross-locks and two cross- and circle-locks ($p < 0.05$). For load to failure, one cross- and circle-lock also resulted in higher linear stiffness and yield load ($p < 0.05$). There was no significant difference in ultimate load and energy absorbed. All repairs failed by knot slippage.

CONCLUSION

Extensor tendon repair with one cross- and circle-lock may improve clinical outcome by providing superior biomechanical properties for load seen with postoperative rehabilitation. One cross- and circle-lock extensor repair also reduces operative time and tendon damage due to less needle passages. Extensor tendon repair with one cross- and circle-lock provides superior biomechanical properties and may reducing operative time and tendon damage due to less needle passages.

EFFECTS OF COLLAGEN CROSSLINK INHIBITION ON EMBRYONIC TENDON

Joseph E. Marturano, Zachary A. Schiller, and Catherine K. Kuo
Department of Biomedical Engineering, Tufts University, Medford, MA, USA

INTRODUCTION

The mechanical properties of adult tendon have been well described, however, the mechanisms responsible for their development remain unknown. Quantitative characterization of the mechanical contributions of tendon constituents during development would provide new insight into the functional development of tendon, and would establish guidelines for tissue engineering strategies using development as a template. In our previous work, we quantified tendon elastic modulus during embryonic development and correlated the changes in mechanical properties with changes to tendon dry mass, DNA and GAG content¹. The objective of the present study was to quantitatively characterize the contribution of collagen crosslinking to embryonic tendon elastic modulus by inhibiting lysyl oxidase activity and new crosslink formation during embryonic development using β -aminopropionitrile (BAPN) treatment *in ovo*. In addition, we investigated the effect of BAPN on embryonic tendon cell density, proliferation, and metabolism using histology and *in vitro* assays.

METHODS

Tissue preparation: Chick embryos were injected with BAPN or saline (controls) between Hamburger-Hamilton (HH)² stages 28-43 (ca. 5.5-18 days) and sacrificed after 24 h. Calcaneal tendons were then excised for analysis. **FV-AFM:** Indentation arrays (16 \times 16) were captured in PBS over 10 \times 10 μ m areas using a 20 nm probe on cryosectioned tendon (N=5 chicks, n=3 arrays). **Histology:** HH 43 tendons were embedded, stained with H&E, and midsubstance nuclei were counted. **BAPN *in vitro* assay:** HH 42 embryonic tendon cells were plated in DMEM, 10% FBS and 1% P/S with BAPN at concentrations known to inhibit lysyl oxidase activity *in vitro*³.

RESULTS

BAPN treatment significantly reduced average tendon elastic modulus during development, by up to 38% at HH 40 ($p < 0.05$) and by 68% at HH 43 (Fig. 1a; $p < 0.01$). At HH 40 and 43, BAPN reduced modulus to less than 15 kPa, whereas saline control tendons had moduli up to 40 kPa (Fig. 1b). BAPN treatment did not significantly affect cell densities of HH 43 tendon midsubstance (Fig. 2; $p > 0.05$). In addition, *in vitro* proliferation and metabolic activity of HH 42 embryonic tendon cells were not significantly affected by BAPN treatment over 72 hrs (Fig. 3; $p > 0.05$).

DISCUSSION

Previous studies have reported that collagen fibril length⁴ and diameter⁵ increase rapidly during the latest stages of embryonic chick tendon development (HH 40-43). These changes were coincident with our previously reported increases in late-stage elastic modulus¹, suggesting a potential link between elastic modulus and collagen structure in developing tendon. Here we show that inhibiting lysyl oxidase with BAPN significantly reduces late-stage (HH 40 & 43) embryonic tendon elastic modulus (Fig. 1). This effect did not seem to be due to changes in tendon cell density, as indicated by *in ovo* and *in vitro* assays (Fig. 2-3). In addition, we previously showed that BAPN treatment does not affect total collagen¹ or GAG⁶ content in embryonic tendon. Taken together, these findings suggest that late embryonic-stage increases in modulus are, in part, a function of collagen crosslinking via lysyl oxidase. Current work is aimed at characterizing these mechanisms and identifying potential contributors to developing tendon mechanical properties.

REFERENCES: 1. Marturano et al. ISL&T Transactions 2010. 2. Hamburger & Hamilton J Morphol 1951. 3. Tang et al. J Biol Chem 1983. 4. Birk et al. Dev Dyn 1995. 5. Eikenberry et al. Int J Biol Macro 1982. 6. Marturano et al. ORS Transactions 2012.

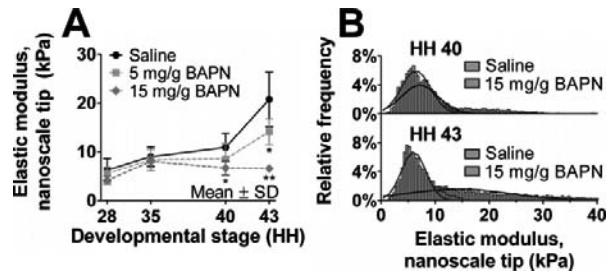


Fig 1: (A) Average tendon elastic modulus as a function of developmental stage and BAPN dose (* = $p < 0.05$; ** = $p < 0.01$). (B) Elastic modulus histograms of HH 40 and 43 tendon with saline and 15 mg/g BAPN treatment.

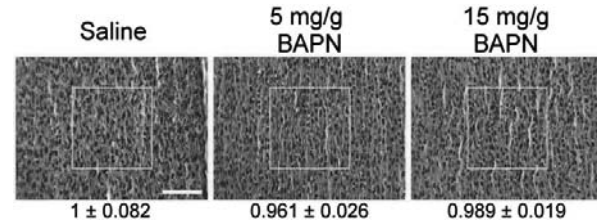


Fig 2: H&E stained sections of HH 43 tendon mid-substance as a function of BAPN dose (40x). Bar = 50 μ m. Numbers represent cell densities relative to saline control (mean \pm SD).

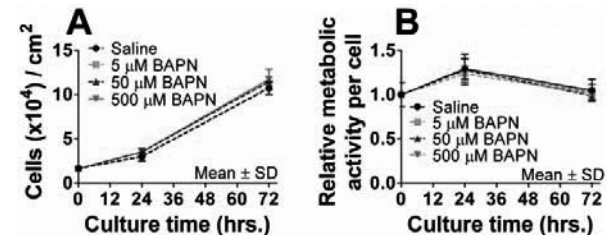


Fig 3: Effect of BAPN treatment on HH 42 cell proliferation (A) and metabolic activity (B) *in vitro*.

RAPAMYCIN ATTENUATES AGE-ASSOCIATED CHANGES IN TIBIALIS ANTERIOR TENDON VISCOELASTIC PROPERTIES

¹L.K. Wood, ²R.A. Miller, and ¹S.V. Brooks

Departments of ¹Biomedical Engineering and ²Pathology, University of Michigan, Ann Arbor, MI

INTRODUCTION

Rapamycin (Rapa) has been shown to increase life span in genetically heterogeneous mice¹, but the extent to which Rapa prevents age-associated changes in specific tissues remains unclear. In humans, old age is associated with increased rates of tendinopathy and risk of tendon rupture, which may be linked causally to alterations in the viscoelastic properties of tendons with aging. We previously showed that tendons stiffen and lose elasticity in a region-dependent manner with aging in mice². In the present study, we aimed to determine if Rapa slows the progression of age-associated changes in viscoelastic properties of tendon.

METHODS

Genetically heterogeneous UM-HET3 female weanlings were fed a diet of standard chow until 270 days of age, when a portion of the mice were switched to a diet that included 14ppm Rapa. Tibialis anterior (TA) muscle-tendon units (MTUs) were extracted from 4-month-old (Young Control, n=4) and 22-month-old (Old Control, n=9) mice fed standard chow, and 22-month-old mice fed the Rapa diet (Old RAPA, n=7). MTUs were mounted in our custom tensile tester, and polystyrene beads were brushed along the tendon to serve as optical strain markers. Tendons were subjected to a load-unload cycle of 10% grip-to-grip strain at 1% per second. Stresses and nominal strains were calculated for the end-to-end response and for the proximal (near the muscle), central, and distal (near the bone) regions of the tendons. Regional data were compared using ANOVA. All procedures were approved by UCUCA.

RESULTS

Maximum tangent modulus of the proximal region increased with age in the control groups (4mo: 232 ± 86 MPa, 22mo: 489 ± 86 MPa, $p < 0.05$), but was decreased in old RAPA mice as compared age-matched controls ($p < 0.05$) and was similar to the 4mo control modulus. Overall tendon modulus trended towards the same pattern ($p \approx 0.10$; Fig 1). Hysteresis area in the proximal tendon region decreased with age for control mice (4mo: $42.6 \pm 8.4\%$, 22mo: $27.8 \pm 7.5\%$, $p < 0.05$), but increased to the 4mo control level for RAPA mice ($49.9 \pm 10.1\%$). The same pattern was seen for the end-to-end tendon hysteresis response (Fig 2).

DISCUSSION

Our findings indicate that administration of Rapa slows age-associated changes in both elastic (tangent modulus) and viscous (hysteresis area) properties of TA tendons. Collagen has a slow turnover rate, allowing for the accumulation of post-translation modifications that can compromise the structural and mechanical integrity of collagen rich tissues, such as tendons. Collagen degradation by MMP-1 is critical for the maintenance of the extracellular matrix (ECM), and age-associated changes in collagen turnover may account for the increased risk of tendon injury in old age. MMP-1 expression by fibroblasts in culture has been shown to be increased by treatment with Rapa⁴. Thus, Rapa may contribute to the preservation with aging of the ECM by altering collagen turnover. Enhanced degradation of aged, damaged collagen would allow for the deposition of young, healthy collagen. Moreover, the observations that tendinopathy was associated with increased col III levels in human tendons³ and treatment with Rapa decreased col III production⁴ suggests that Rapa may delay age-associated tendinopathies by preventing the accumulation of col III. An effect of Rapa on collagen turnover has potential significance for preventing age-associated tendon dysfunction through the maintenance of structural and mechanical integrity of tendons from adulthood to old age. Future studies are warranted to establish the molecular mechanisms by which Rapa delays age-associated changes in tendon mechanics.

ACKNOWLEDGEMENTS

Financial support provided by NIH grants AR055624, AG022303, and AG000114.

REFERENCES

- [1] Harrison D, et al. *Nature*. 2009;560:392-396. [2] Wood L, et al. *J Appl Physiol*. 2011;111:999-1006. [3] Riley G, et al. *Ann Rheum Dis*. 1994;53: 359-366. [4] Poulalhon N, et al. *J Biol Chem* 2006;281:33045-33052.

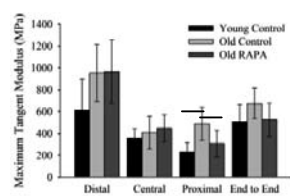


Fig 1. Maximum modulus increased with age in the proximal TA tendon region, but was reduced in age-matched RAPA mice ($p < 0.05$). Data are means \pm S.D.

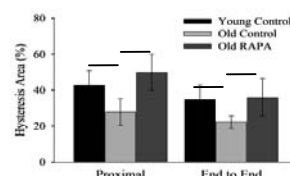


Fig 2. Proximal region and end-to-end hysteresis area decreased with age ($p < 0.05$). Hysteresis increased for RAPA mice compared to age-matched controls ($p < 0.05$). Data are means \pm S.D.

BMP-2 PROMOTED PROTEOGLYCAN DEPOSITION AND STIMULATED NON-TENOGENIC DIFFERENTIATION OF TENDON-DERIVED STEM CELLS (TDSCS) IN VITRO – POTENTIAL ROLES OF ECTOPIC BMP-2 IN THE PATHOGENESIS OF TENDINOPATHY

*^{1,2,3}Pauline Po Yee Lui, *^{1,2}Yun Feng Rui, ^{1,2}Q Tan, ^{1,2}YM Wong, ^{1,2}Kai Ming Chan

¹Department of Orthopaedics and Traumatology, The Chinese University of Hong Kong.

²The Hong Kong Jockey Club Sports Medicine and Health Sciences Centre, Faculty of Medicine, The Chinese University of Hong Kong.

³Program of Stem Cell and Regeneration, School of Biomedical Science, The Chinese University of Hong Kong

*Lui PPY and Rui YF have equal contribution in this study.

INTRODUCTION

Tendinopathy histopathologically shows a failed healing response with increase in proteoglycans (PG) and glycoaminoglycans (GAG) deposition, chondrometaplasia and occasional adipose and bony metaplasia, resulting in poor mechanical property of the affected tendon.^[1] Our previous studies showed that there was ectopic expression of BMP-2, BMP-4 and BMP-7 in clinical samples and animal model of tendinopathy.^[2-3] We hypothesized that BMP-2 might induce the non-tenocyte differentiation of tendon-derived stem cells (TDSCs), contributing to the increased production of proteoglycans *in vitro*, as seen in tendinopathy. This study therefore aimed to investigate the effects of BMP-2 on the non-tenocyte differentiation and production of proteoglycans in TDSCs *in vitro*.

METHODS

TDSCs isolated from rat patellar tendon were treated without or with BMP-2. At various times, the osteogenic, adipogenic, chondrogenic differentiation and tendon-related marker expression of TDSCs were assessed by (1) Alizarin red S staining assay; (2) Oil Red O staining assay; (3) haematoxylin-eosin staining, Safranin-O staining, immunohistochemical staining of Sox9 and collagen type II as well as (4) qRT-PCR analysis of lineage-specific markers. The production of GAG in the BMP-2-treated cells was assessed by alcian blue staining and quantification. The mRNA expression of decorin (*Dcn*), biglycan (*Bgn*), fibromodulin (*Fmod*) and aggrecan (*Acn*) in TDSCs after treatment with BMP-2 was also assessed by qRT-PCR.

RESULTS

Our results showed that BMP-2 promoted the osteogenic, adipogenic and chondrogenic differentiation but inhibited tendon-related marker expression of TDSCs. GAG production in TDSCs increased after BMP-2 stimulation. *Acan* increased while *Dcn*, *Bgn* and *Fmod* decreased after treatment of TDSCs with BMP-2.

DISCUSSION

In conclusion, BMP-2 promoted GAG deposition, aggrecan expression and enhanced non-tenocyte differentiation of TDSCs *in vitro*, consistent with the increased PG and GAG deposition as well as the presence of chondrocyte phenotype, adipose and bony metaplasia observed in tendinopathy.

REFERENCES

[1] Kannus P, Jozsa L. 1991. J Bone Joint Surg Am 73: 1507-1525. [2] Rui YF et al. KSSTA, DOI ; 10.1007/s00167-011-1685-8 [3] Yee Lui PP et al. J Orthop Res 2011 ; 29(6) :816-821.

ALTERED FATE OF TENDON-DERIVED STEM CELLS (TDSCS) IN OSSIFIED FAILED TENDON HEALING

*^{1,2,3} Pauline Po Yee Lui, *^{1,2} Yun Feng Rui, ^{1,2} Yin Mei Wong, ^{1,2} Qi Tan, ^{1,2} Kai Ming Chan

¹Department of Orthopaedics and Traumatology, The Chinese University of Hong Kong.

²The Hong Kong Jockey Club Sports Medicine and Health Sciences Centre, Faculty of Medicine, The Chinese University of Hong Kong.

³Program of Stem Cell and Regeneration, School of Biomedical Science, The Chinese University of Hong Kong

*Lui PPY and Rui YF have equal contribution in this study.

INTRODUCTION

Chondro-ossification and failed healing were observed in our collagenase-induced (CI) tendon injury model of tendinopathy. We hypothesized that altered fate of tendon-derived stem cells (TDSCs) might contribute to these histopathological changes. This study aimed to compare the yield, proliferative capacity, and differentiation potential of TDSCs isolated from healthy and CI tendons.

METHODS

TDSCs were isolated from healthy (HT group) and CI (CI group) tendons. The yield and proliferative capacity of TDSCs (CI) and TDSCs (HT) were compared by colony-forming unit assay and BrdU assay, respectively. Their osteogenic and chondrogenic differentiation potential were compared using standard assays. The mRNA expression of tendon-related markers was compared using qRT-PCR.

RESULTS

More TDSCs which showed lower proliferative potential and higher cellular senescence were present in the CI patellar tendons compared to HT tendons. There was higher ALP activity and mineralization in TDSCs (CI) compared to TDSCs (HT) in both basal and osteogenic media. More chondrocyte-like cells and higher proteoglycan deposition, Sox9 and collagen type II expression were observed in TDSCs (CI) pellets compared to TDSCs (HT) pellets upon chondrogenic induction. There was lower mRNA expression of *Colla1*, *Scx* and *Tnmd* in TDSCs (CI) compared to TDSCs (HT) in basal medium.

DISCUSSION

TDSCs (CI) showed altered fate, higher yield but lower proliferative capacity compared to TDSCs (HT), which might contribute to ossified failed tendon healing in this animal model.

ACKNOWLEDGEMENT

This project is supported by equipment / resources donated by the Hong Kong Jockey Club Charities Trust and the CUHK Direct Grant (2009.1.043).

FUTURE TREATMENT OF ACL ARTHROSIS: COMPLETE CARTILAGE REPLACEMENT

^{1,2}Stone, KR; ¹Pelsis, JR; ^{1,2}Walgenbach, AW; ¹Turek, TJ

¹Stone Research Foundation, San Francisco, CA; ²The Stone Clinic, San Francisco, CA

INTRODUCTION

Post-ACL injury arthrosis is an enormous problem, both in the civilian population and in the military population for patients with chronic, previously-untreated ACL tears. The arthrosis often progresses more rapidly in patients who have lost portions or all of their meniscus cartilage at the time of their ACL injury. At our clinic, we have treated these patients since 1991 with articular cartilage paste grafting and then subsequently with a meniscus allograft transplant in order to provide articular cartilage repair tissue and the shock absorber for these progressively arthritic knees. No other cartilage repair method has been indicated in the setting of generalized osteoarthritis. Isolated chondral defect techniques have had limited success in the progressively arthritic knee, most likely due to articular cartilage and bony deformity as well as a degradative environment into which these have been placed.

However the problem of total cartilage loss over a large area is not solvable by current regeneration techniques and needs, in our view, a complete cartilage replacement solution. Our goal is to replace the severely damaged or destroyed articular cartilage with intact repopulated articular cartilage and bone.

METHODS

We propose the following device and technique to meet this goal: articular cartilage harvested with a thin bone layer (shell graft) from a cadaveric donor, frozen and stored, vacuum infused with stem cells, platelets, and autologous growth factors at the time of implantation, and transplanted to the morselized recipient knee surface and fixed with resorbable nails.

We have developed and tested protocols for graft harvest, shaping, and processing to remove the donor cells as well as a graft/cell vacuum seeding protocol. In our initial *in vitro* work, grafts were vacuum seeded with culture-expanded human bone marrow derived mesenchymal stem cells (hBM-MSC) at a variety of seeding densities (0×10^6 to 80×10^6 cells/ml). The seeded grafts were subjected to both short-term (5 days) and long-term (up to 6 weeks) culture. Vital cell labeling and fluorescence microscopy were performed.

For clinical utility, point-of-service blood and bone marrow cell isolates (PoS-BBM) were investigated using a variety of graft volume to seeding volume ratios.

Our *in vivo* studies are in progress, comparing the PoS-BBM cell-seeded grafts, ELA cell-seeded grafts, and control grafts of fresh harvested thin shell grafts retaining viable cells. Twelve week assessments include CT imaging with postmortem gross pathology and ordinal histological scoring for cartilage integrity and repair. Our larger formal *in vivo* study will include comparison of optimal MSC-seeded grafts and control; graded MRI assessments at 0, 16, and 26 weeks; and postmortem assessments including gross pathology at necropsy, indentation biomechanics, biochemical assays of GAG content and collagen typing, and ordinal histological scoring.

RESULTS

After five days in cell culture, the cells were associated with the trabeculae and within the lacunae in the articular surface. There was low cellular retention in long-term culture compared with the short-term culture, which is predictable considering the static culture conditions.

The results of the PoS-BBM cell seeding *in vitro* trial demonstrated a high initial cell volume with staged vacuum loading demonstrating the highest cell penetration, and cell-loaded grafts exhibited most of the live cells distributed from the hyaline layer through the cartilage to the tidemark. The results paralleled the findings and densities found in the culture-expanded bone marrow mesenchymal stem cell short-term culture.

The *in vivo* results are pending.

DISCUSSION

In summary, the feasibility of seeding intact cartilage was tested *in vitro*, the viability of cells and the resulting construct was tested *in vitro*, and the pilot testing of *in vivo* viability and efficacy is in progress, the results of which will be reported to the ISL&T-XII meeting. Cartilage replacement holds the promise of full biologic knee reconstruction for people who have developed ACL arthrosis. The thin-shell grafts may provide a thicker, more durable cartilage repair option and may allow patients to delay knee arthroplasty and possibly a full return to sports. The treatment will be indicated in ACL arthrosis as an outpatient point-of-service treatment.

MRI DERIVED MORPHOLOGY AND SIGNAL INTENSITY TO DETERMINE STRUCTURAL PROPERTIES OF AN ACL RECONSTRUCTION GRAFT OR ACL PRIMARY REPAIR AT ONE YEAR IN A PORCINE MODEL

¹A.M. Biercevicz, ¹D.L. Miranda, ²M.M. Murray, ¹J.T. Machan, ¹B.C. Fleming

¹Department of Orthopaedics, Warren Alpert Medical School, Brown University, Providence, RI, ²Department of Orthopaedic Surgery, Children's Hospital Boston, Boston, MA

INTRODUCTION

MR imaging has the potential to quantify ACL graft and ACL primary repair structural properties during healing. Potential MR-based measures include morphologic and signal intensity parameters [1,2]. Previous *in vivo* research has established a link between signal intensity and structural properties [2]. Currently, no MRI based method considers both signal intensity (a surrogate for tissue quality) and volume (graft morphometry) as separate quantifiable parameters to predict graft or repaired ligament structural properties. If successful, a non-invasive MRI technique to accurately predict the graft or repaired ligament structural properties would be a valuable technique for clinical research and possibly a clinical reference tool to guide patient rehabilitation. The objective of this study was to evaluate MR derived signal intensity and volume measurements of the ACL graft and repaired ACLs in a multiple regression model to predict structural properties.

METHODS

Thirty-two adolescent Yucatan minipigs underwent unilateral ACL transection surgery. Eight of the animals received ACL reconstructions with a bone-patellar tendon-bone allograft (BTB), eight received ACL reconstructions with BTB and a collagen-platelet composite, 8 received ACL primary repair with a suture bridge and a collagen-platelet composite, and 10 were left untreated. After 1 year of healing, the animals were euthanized and the knees were harvested. A T2* weighted 3-D-CISS sequence (TR/TE/FA, 14.5/7.3/ 35°; FOV, 160 mm; matrix 512X512, slice length/gap, 1mm/0; avg, 1) of the injured knee was performed (Siemens 3T Trio; Erlangen, Germany) after harvest [3]. Signal intensities were evaluated as gray scale values normalized to the femoral cortical bone. The grafts and repaired ligaments were then segmented from the MR images in the coronal and sagittal planes (Mimics 9.11; Materialize, Ann Arbor, MI), and 3-D surface models and grayscale volumes were created. The median grayscale value (MGV) and the volume (VOL) of the graft or repaired ligament were recorded. Tensile failure testing was performed on the isolated bone-ligament-bone constructs at 20mm/min. The ligament structural properties (yield load, maximum load, linear stiffness) were determined as previously reported [4]. Linear regressions were performed to fit the linear combination of MGV and VOL to the graft structural properties.

RESULTS

The VOL of the ligament or graft significantly predicted maximum load, yield load, and linear stiffness ($R^2 = 0.68, 0.69,$ and 0.69 respectively; $p < 0.001$) (Fig 1a). The median signal intensity (MGV) was also a significant predictor of maximum load, yield load and stiffness ($R^2 = 0.70, 0.68,$ and 0.69 respectively; $p < 0.001$) (Fig 1b). Using MGV in conjunction with VOL, the multiple linear regression prediction for maximum load, yield load and linear stiffness was improved; $R^2 = 0.85, 0.85, 0.85,$ respectively ($p < 0.001$).

DISCUSSION

Both size and signal intensity independently predicted the structural properties of the graft or repaired ligament after 1 year of healing. By combining both factors, the prediction was further improved. While the results presented herein represent only a single time point they support findings presented by Weiler et al. [2], where ACL graft signal intensity was significantly correlated to structural properties over multiple time points. Building on their work, we also found that the prediction could be improved by considering the graft volume in the analysis. The combination of these two MRI parameters offers a more synergistic evaluation of graft integrity than either parameter alone, explaining 85% of the variability seen in structural properties. There are some study limitations that should be considered. The knees were imaged post-mortem at a single time point. The MRI-based predictions of the graft structural properties at 1 year may be different at other healing time points and future studies are needed to address the temporal changes. Nonetheless, this study demonstrates the feasibility of non-invasively evaluating the structural properties of an ACL graft.

ACKNOWLEDGEMENTS

This study was funded by grants from the National Institutes of Health (RO1-AR056834) and National Football League Charities.

REFERENCES: [1] Figueroa *et al.*: Arthroscopy 2010; [2] Weiler *et al.*: Am J Sports Med 2001; [3] Bowers *et al.*: Am J Sports Med 2010; [4] Fleming *et al.*: Am J Sports Med 2009.

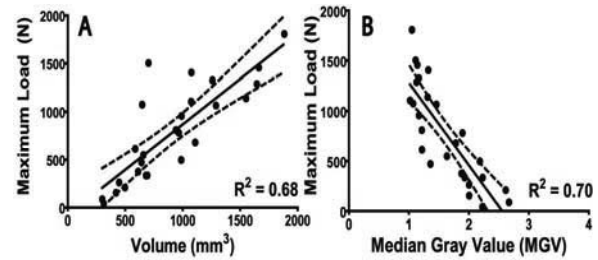


Figure 1: Maximum Load vs (A) Volume and (B) MGV

BIOMECHANICAL AND HISTOLOGICAL ANALYSIS AFTER TENOTOMY OF THE LONG HEAD OF THE BICEPS IN THE RABBIT SHOULDER MODEL

†Ji Wook Choi, *Sae Hoon Kim, *Joo Han Oh, *Goo Hyun Baek, *Seung Han Shin, *Seok Won Chung,
*Seoul National University College of Medicine, Korea, †Seoul Mirae Orthopaedic Clinic, Korea

INTRODUCTION

Many patients who undergo tenotomy of the long head of biceps tendon (LHBT) experience the “autotenodesis” phenomenon instead of distal migration of LHBT. However, this phenomenon has never been verified histologically or biomechanically. Especially given that the LHBT has a double-lined synovium at the bicipital groove, there arises a question that the adhesion of the LHBT after tenotomy is possible. Therefore, the purpose of this study was to verify the autotenodesis phenomenon by comparing biomechanical pullout strength of the 6 weeks post-tenotomy group with the immediate post-tenotomy group, and by observing the histological characteristics and the gross specimens of the LHBT at the bicipital groove in the rabbit model.

METHODS

The study was designed to compare biomechanical pullout strength and histological differences between the immediate post-tenotomy and 6 weeks post-tenotomy in the rabbit model (New Zealand white male rabbits, 24 weeks old, 3.2–3.7 kg). To accomplish this, sample size analysis based on pullout strength as the primary outcome variable was completed after pilot study. Finally, 10 experimental subjects and 10 control subjects were included. Three more rabbits were included for histological analysis of the 6 weeks post-tenotomy model. For the pullout-strength testing, 20 right shoulders (10 for each group) were tested using a custom fixture clamping system and an Instron materials testing machine. Length of the proximal part of the bicipital groove and tendon clamp was 2 cm. Finally, for tensile testing of the pullout strength of the LHBT, the tendon was loaded to failure at a rate of 10 mm/min with no preload applied. We measured ultimate load for the analysis. For histological analysis, 6 previously assigned rabbit left shoulders (3 for each group) were harvested after euthanasia. Specimens were fixed in neutral buffered 10% formalin (pH 7.4), and decalcification was done. Paraffin blocks were made in the bicipital groove region and 1 mm-wide serial sections perpendicular to the biceps tendon were cut and stained with Hematoxylin-Eosin and Masson’s Trichrome to measure connective tissue around the LHBT at the groove area. To minimize any bias on the part of the observer during the analyses, all examinations were performed in blinded fashion with respect to the group assignment. Assessment was done by a pathologist who was blind to the study.

RESULTS

Of the 13 specimens from the 6 weeks post-tenotomy model, there was no distal migration of the LHBT out of the bicipital groove. That is, there was some retraction of the proximal tenotomized tendon ends into the bicipital groove; however, all tendons were retained at the groove. On biomechanical testing, pullout strength of the immediate post-tenotomy model was measured to be 5.53 ± 2.22 N and that of the 6 weeks post-tenotomy model was 44.07 ± 7.75 N, and the difference was statistically significant ($p < 0.001$). On histological analysis, there was marked fibrosis around the LHBT at the bicipital groove in the 6 weeks post-tenotomy model. That is, loose areolar tissue between the LHBT and the bicipital groove was replaced and filled with dense connective tissue (Fig. 1).

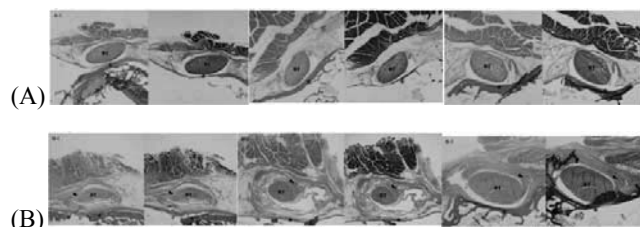


Fig. 1 Hematoxylin-Eosin and Masson’s Trichrome stain of the immediate post-tenotomy (A-1, 2, and 3) and 6 weeks post-tenotomy (B-1, 2, and 3) tendon (x200). (A) There is loose areolar tissue between the tendon and bicipital groove. (B) The LHBT is enclosed by dense fibrotic tissue and is shown adhering to the surrounding tissue (arrowhead). Biceps tendon (BT) and bicipital groove (asterisk)

DISCUSSION

This is the first study to evaluate biomechanical and histological changes after tenotomy of the LHBT in the rabbit model. The results show that autotenodesis at the bicipital groove is an actual phenomenon that occurs after tenotomy of the LHBT, even in situations where biceps pathology is not present. Pullout strength of the LHBT was statistically higher after 6 weeks post-tenotomy model compared with that of the immediate post-tenotomy model. Histologically, there was marked fibrosis between the LHBT and the bicipital groove area in the 6 weeks post-tenotomy model; therefore, we could conclude that this is the site of adhesion after tenotomy. This could support use of the tenotomy procedure over tenodesis in the diseased LHBT.

EXPRESSION OF IGF-1 RECEPTOR AND MYOSIN HEAVY CHAIN IN RABBIT'S ROTATOR CUFF AFTER ROTATOR CUFF REPAIR AND INJECTION OF ADIPOSE-DERIVED STEM CELL

Sae Hoon Kim, Joo Han Oh, Seok Won Chung, Jin Young Chung
Seoul National University College of Medicine, Korea,

INTRODUCTION

Fatty degeneration of rotator cuff muscle after tendon tear is a well-known phenomenon, and this is closely related with outcome after repair even in integrity. Considering that our principal goal of rotator cuff repair is restore the insertion point of muscle to work as a motor, even excellent integrity would be worthless when complete muscle degeneration has been taken place. In these respects, we intended to regenerate the muscle, by way of using adipose-derived stem cells (ADSCs). Therefore, the purpose of this study was to evaluate effect of ADSCs after repair of subacute rotator cuff tear model in the rabbit by way of comparing expression of insulin-like growth factor type 1 receptor (IGF-1R) and myosin heavy chain (MyHC) in ADSC injected side and contralateral control side.

METHODS

Adipose tissue was acquired from New Zealand male rabbits (weight, approximately 3.5kg) and treated to select the ADSCs. ADSCs from passage 3 were labeled with a fluorescent cell membrane marker (Vybrant DiI) with the manufacturer's protocol. To perform the transplantation, cells were suspended to a concentration of 1×10^7 labeled cells in 500 μ l of Hank's balance salt solution. Eight rabbits were included (5 for immunohistochemistry (IHC) and 3 for Western blot analysis) in this study. Bilateral tear model of rotator cuff tendon (supraspinatus) was created by surgical manner, then, 3 weeks later, the torn supraspinatus tendon was sutured to the greater tuberosity using trans-osseous technique with two 2-0 ethibond sutures. After completion of repair, either side of shoulder was randomly selected and injection of the ADSC (1×10^7) at the muscle belly (near the musculoskeletal junction) was performed. Same amount of the saline was injected to the contralateral supraspinatus muscle. On postoperative 3rd weeks, 5 rabbits were assigned for IHC. For the detection of IGF-1R and MyHC immunoreactivity, anti-IGF-1R and anti-MHC antibodies were used. Immunoperoxidase labeling was performed using a DAB kit, and evaluated using an Olympus BX51 microscope. In addition, another 3 rabbits were assigned for Western blot analysis. Proteins were probed with anti-IGF-1R and anti-MHC. Peroxidase anti-rat IgG was used as a secondary antibody, and actin as an internal control.

RESULTS

At postoperative 3rd weeks, ADSC injected and saline injected muscles were analyzed using Western blot for determination of IGF-1R and MyHC levels. The size of IGF-1R exists as 95 kD and MyHC as 200 kD. ADSC injection increased the IGF-1R protein level (Fig. 1A) and MyHC level (Fig. 1C). IHC showed that ADSCs injection increased IGF-1R and MyHC stainings, which is located overlapping with staining of ADSCs, but there are no staining in saline injected side (Fig. 1B and 1D).

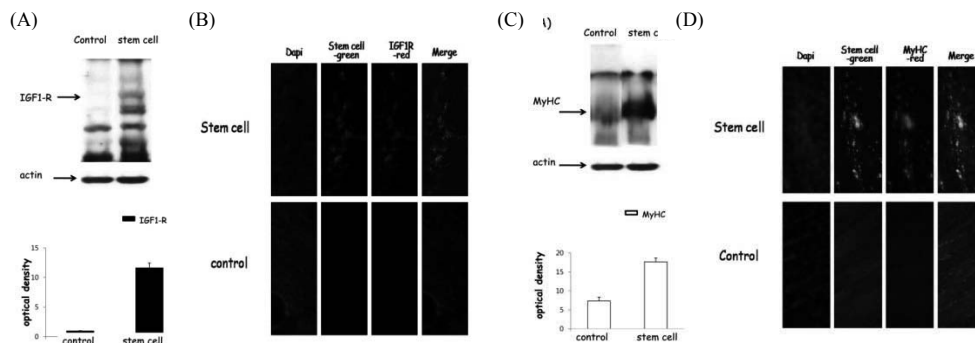


Fig.1 Expression profiles of IGF-1R and MyHC

DISCUSSION

Local injection of ADSC increased well-known muscle growth factors, that is, IGF-1R and MyHC, in rabbit's rotator cuff repair model after subacute tear. This was evident by IHC and Western blot analysis, however, did not reached statistical significance owing to small number of cases. From this study result, we could speculate muscle regeneration can be expected in rotator cuff tear model by local administration of ADSCs. Anabolic effect of stem cell in the muscle could help treating muscle disorders as well as muscle degeneration after rotator cuff tear. Future study should be needed to verify histologic and functional change of the muscle with stem cell.

EFFICIENCY OF ULTRASOUND THERAPY IN PREVENTION OF ADHESIONS AFTER ZONE- II FLEXOR TENDON REPAIR: A RANDOMIZED, CONTROLLED CLINICAL TRIAL

Liu Muqing, Ji Liu, Sheng Lin, Qin Yongping, Xu Minna
Department of Hand Surgery, Yuquan Hospital, Tsinghua University, Beijing, China

INTRODUCTION

Peritendinous adhesions are an important complication of flexor tendon injury, particularly in zone II. The application of pulsed, low intensity pulsed ultrasound (LIPU) is emerging as a potent therapy for sports-related tendinopathy. The purpose of the study was to investigate whether LIPU would reduce adhesion formation and improve digital function after Zone-II flexor tendon repair.

METHODS

Between August 2010 and August 2011, 67 patients (80 digits) with zone-II flexor tendon repairs were assigned randomly into control group and LIPU group. In control group, the operated hand was allowed to heal without ultrasound therapy. In LIPU group, pulsed ultrasound therapy was started on 15 days post operation at intensity of 1 W/cm² for 20 min daily for 14 consecutive days. All the patients received a modified rehabilitation technique with active flexion starting at four weeks postoperatively. All the patients were evaluated at 4, 8 and 12 weeks after surgery by blinded observers. The Strickland formula (total active motion) system, the Disabilities of the Arm, Shoulder, and Hand (DASH) outcome questionnaire, pinch and grip strength, pain score on a verbal scale and swelling and neurologic recovery was assessed. Ultrasonography was performed on week 4, 8 and 12 post-tenorrhaphy.

RESULTS

Resolution of inflammatory swelling, pain, weight bearing and tendon gliding movement was earlier in the LIPU group than control. Ultrasonography examination in the LIPU group revealed that there was a marked regression of peritendinous adhesion between the tendon and skin on week 4 post-tendon repaired and the tendon at the reconstructive site attained near normal thickness and density. Adhesions were present in the reconstructed site in all patients of the control group. At all time points, patients treated with LIPU had greater interphalangeal joint motion. We could identify no difference between the groups in terms of the DASH scores or dexterity tests. When the groups were stratified, those who had a concomitant nerve injury or multiple digit injuries had less range of motion, larger flexion contractures, and decreased satisfaction scores compared with patients without these comorbidities.

DISCUSSION

LIPU therapy provides greater active finger motion than control group after zone-II flexor tendon repair without increasing the risk of tendon rupture. Concomitant nerve injuries, multiple digit injuries, and a history of smoking negatively impact the final outcome of tendon repairs. Further experiments are needed to reveal the mechanism of LIPU on tendon healing.

FIBER-TYPE SWITCHING AND REDUCTION IN SPECIFIC FORCE PRODUCTION FOLLOWING ROTATOR CUFF TEAR

¹Gumucio JP, ¹Davis ME, ¹Stafford PL, ¹Bradley JR, ¹Schiffman CJ, ¹Lynch EB, ²Claflin DR, ¹Bedi A, ¹Mendias CL
¹Department of Orthopaedic Surgery and ²Section of Plastic Surgery, University of Michigan, Ann Arbor

INTRODUCTION Full-thickness tears to the rotator cuff tendons can cause severe pain and disability, leading to the development of glenohumeral arthropathy. Untreated tears progress in size and atrophy of the rotator cuff muscles, as well as an infiltration of fat to the area, a condition referred to as "fatty atrophy." Even after successful repair of the torn tendon, the muscles of the rotator cuff often fail to regenerate, resulting in persistent weakness and impaired functional outcomes. In order to improve the treatment of rotator cuff tears, a greater understanding of the changes in the contractile properties of muscle fibers, as well as the molecular regulation of muscle fiber atrophy, fat accumulation and fibrosis is essential. Using a rat model of rotator cuff injury, we measured the force generating capacity of individual muscle fibers and determined changes in muscle fiber type distribution after a full thickness rotator cuff tear. Additionally, we measured the expression of genes involved in muscle atrophy, lipid accumulation, and matrix synthesis. We hypothesized that there is a decrease in specific force of rotator cuff muscle fibers, an accumulation of type IIb fibers, and an upregulation in fibrogenic, adipogenic, and inflammatory gene expression in torn rotator cuff muscles.

METHODS This study was approved by the University of Michigan IACUC. Six male Sprague-Dawley rats (6 months of age) were subjected to a full tenectomy of the right supraspinatus and infraspinatus tendons and the left side was the sham-operated control. After one month, the rats were humanely euthanized and the supraspinatus and infraspinatus muscles of each side were processed for fiber contractility, histology, and RNA isolation. For muscle fiber contractility, bundles of the infraspinatus muscle were chemically skinned and the contractility of individual muscle fibers was assessed as previously described (Mendias 2011, Claflin 2011). To determine fiber type distribution, distal infraspinatus muscles were snap frozen in OCT, cryosectioned and incubated with primary antibodies against specific myosin heavy chain isoforms and AlexaFluor conjugated secondary antibodies. The extracellular matrix was labeled using WGA-lectin-AF488. For gene expression analysis, RNA was isolated from supraspinatus muscles, reverse transcribed into cDNA, and real-time qPCR was used to measure the expression of several target genes which were normalized to β -actin.

Table 1

	Control	Tear
Supra mass (mg)	740±30	349±22*
Infra mass (mg)	726±32	396±24*
Fiber CSA (μm^2)	8120±250	5540±260*
Fiber F_0 (mN)	1.03±0.03	0.61±0.03*
Fiber sF_0 (kPa)	130±3	109±3*

Figure 1

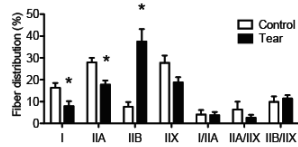


Figure 2

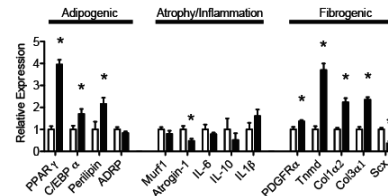


Table 1. Rotator cuff tear reduces the mass, and muscle fiber CSA and force production.

Figure 1. Rotator cuff tear decreases the number of type I and IIA muscle fibers, and increases type IIB muscle fibers.

Figure 2. Rotator cuff tear changes the expression of various adipogenic, atrophy/inflammatory and fibrogenic genes.

* indicates significantly different from control using Student's t-test ($p < 0.05$)

DISCUSSION To our knowledge, this is the first study to investigate force production at the single fiber level after a rotator cuff tear, and also provide a detailed analysis of changes in specific myosin isoform distribution. Fiber contractile force was decreased after a tear, as was force normalized to cross sectional area (sF_0). The reduction in sF_0 suggests that rotator cuff tears cause dysfunction at the level of the myofibril. Additionally, rotator cuff tear caused a shift from type I and IIA fibers to type IIB fibers.

We also sought to determine changes in the expression of genes that regulate muscle atrophy, lipid accumulation, and matrix synthesis. Despite a dramatic accumulation in fat visible from Oil Red-O staining (data not shown), there was only a modest increase in the adipocyte-specific lipid droplet protein perilipin-1, and no change in the expression of the intramuscular lipid droplet protein ADRP. Additionally, while there was an increase in perilipin-1, the overall expression was quite low, reaching threshold cycle near the end of the qPCR run. While the increase in the fat content of rotator cuff muscles following tear has been postulated to occur due to an accumulation of adipocytes, these results suggest that the "fat" in "fatty atrophy" may not arise from true adipogenesis and may arise due to another pathological process such as autophagy.

ACKNOWLEDGEMENTS

This study was funded by grant AR058920 from NIAMS.

INDUCTION IN SCLERAXIS EXPRESSION AND NEOTENDON FORMATION IN THE PLANTARIS TENDON FOLLOWING ACHILLES TENDON ABLATION

Gumucio JP, Flood MD, Phan AC, Mendias CL

Department of Orthopaedic Surgery, University of Michigan, Ann Arbor

INTRODUCTION Tendons are organized into functional cable-like units of matrix and cells called fibrils, and surrounded by a basement membrane layer of tissue known as the epitenon. In response to mechanical loading, tendons grow by increasing their cross-sectional area (CSA). It is not known whether tendons grow by adding additional fibrils (hyperplasia) or by increasing the size of existing fibrils (hypertrophy). Previous studies from our lab have shown that the bHLH transcription factor scleraxis plays an important role in the growth of tendons in response to physiological loading. Following a progressive and gradual 6-week treadmill training program, there was an increase in scleraxis expression, tendon CSA, collagen content and fibroblast density, with particularly high expression of scleraxis in fibroblasts migrating from the epitenon into tendon fibrils. To gain a greater understanding of the cellular mechanisms of adult tendon growth, we used a synergist ablation model whereby a tenectomy of the Achilles tendon was performed to induce growth of the synergist plantaris (Pln) tendon. In contrast to the progressive treadmill loading regime which causes slow, physiological loading, the synergist ablation model causes rapid and dramatic tendon growth. We hypothesized that following synergist ablation, cells in the epitenon would migrate toward the interior of the tendon and increase the size of existing tendon fibrils.

METHODS This study was performed with IACUC approval using eight six-month old male mice that express GFP under the control of the scleraxis promoter (ScxGFP). Four mice were subjected to a bilateral Achilles tenectomy, and four mice served as controls. Pln tendons were isolated from mice 14 days after surgery. For histology, tendons were sectioned and stained with either safranin O and fast green, or hematoxylin and eosin, or prepared for fluorescent microscopy using β -tubulin antibodies and DAPI. For gene expression analysis, RNA was isolated from plantaris tendons, reverse transcribed and real time qPCR was used to measure the expression of scleraxis and type I collagen which were normalized to β 2-microglobulin. Differences between control and overloaded groups were tested using Student's t-test ($\alpha=0.05$). Data are presented as mean \pm SEM.

RESULTS

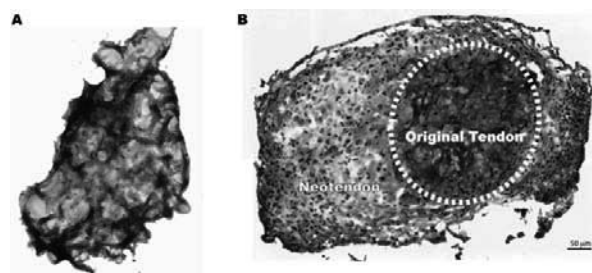


Figure 1. (A) Control Pln tendon and (B) Pln tendon 14 days after surgery demonstrating new matrix (neotendon) formation.

	Control	Overloaded
Original Tendon		
CSA (mm ²)	0.107 \pm 0.01	0.132 \pm 0.03
Cell density (cells/mm ²)	1954 \pm 304	1704 \pm 195
Neotendon		
CSA (mm ²)		0.256 \pm 0.06
Cell Density (cells/mm ²)		3236 \pm 1031
Total Tendon		
CSA (mm ²)	0.107 \pm 0.01	0.363 \pm 0.04*
Cell Density (cells/mm ²)	1954 \pm 304	2637 \pm 649

Table 1. Morphological changes of Pln tendons after synergist ablation. * Different from control ($p<0.05$)

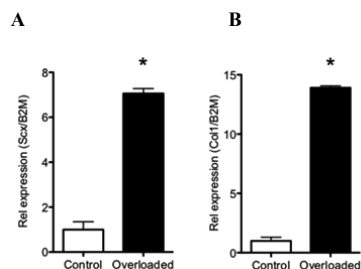


Figure 2. Synergist ablation induces (A) scleraxis and (B) type I collagen expression in Pln tendons. *Different from control ($p<0.05$).

DISCUSSION The results of this study provide novel insight into the cellular mechanisms of tendon growth. We were surprised to see that, following synergist ablation, Pln tendons form an immature neotendon matrix with scleraxis expressing fibroblasts between the epitenon layer and the original tendon, causing an increase in cross sectional area. While there was an overall increase in CSA in overloaded tendons

the increase came about due to an expansion of new tendon matrix outside of the original tendon, as opposed to growth of existing tendon fibrils. This growth was coupled with an increase in the expression of scleraxis and type I collagen. While further studies are necessary, these data support the notion that tendon growth in response to mechanical loading occurs by hyperplasia.

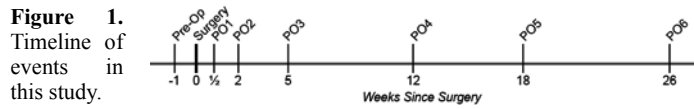
ACKNOWLEDGEMENTS This study was supported by grant AR058920 from NIAMS. The ScxGFP mice were kindly provided by Dr. Ronen Schweitzer.

CHANGES IN SERUM CARTILAGE OLIGOMERIC MATRIX PROTEIN AND C-REACTIVE PROTEIN LEVELS IN PATIENTS UNDERGOING ANTERIOR CRUCIATE LIGAMENT RECONSTRUCTION AND REHABILITATION

Lynch EB, Sibilsky Enselman ER, Davis ME, Harning JA, DeWolf PD, Makki TA, Bedi A, Mendias CL
Department of Orthopaedic Surgery, University of Michigan, Ann Arbor

INTRODUCTION Anterior cruciate ligament (ACL) tears are among the most common knee injuries sustained in athletes, with an estimated 100,000 new ACL tears per year. After rupture and subsequent reconstruction of the ACL, patients often experience substantial, refractory quadriceps muscle atrophy and weakness, and are at increased risk of developing osteoarthritis (OA). There is limited information on the biology of regeneration, including the role of relevant biomarkers of inflammation and regeneration. Cartilage oligomeric matrix protein (COMP) plays an important role in extracellular matrix stabilization and is an established marker of cartilage catabolism, with previous studies demonstrating elevated circulating levels of COMP in OA patients. C-reactive protein (CRP) is an acute phase protein that plays an important role in initiating inflammatory processes, and is commonly used as a biomarker of inflammation. To gain a greater understanding of the biology of tissue regeneration following ACL reconstruction, we measured circulating levels of COMP and CRP at several time points in patients undergoing ACL reconstruction and rehabilitation, from 1 week prior to surgery through clearance to return to full activities. Additionally, we measured COMP and CRP levels in healthy control subjects with no previous history of knee injuries. We hypothesized that patients with ACL tears would have higher levels of COMP and CRP, and that following surgical reconstruction, these values would return to normal levels.

METHODS The study was approved by the University of Michigan Medical School IRB. Subjects who suffered a non-contact complete ACL tear (N=18, mean age 28±2 years) and elected to undergo surgical reconstruction of their torn ACL were enrolled in the study. Blood was drawn from an antecubital vein at a pre-operative visit (Pre-Op) and at several post-operative (PO) visits throughout the course of treatment and rehabilitation (Figure 1), and also drawn from an additional set of subjects (N=27, mean age 23±1 years), with no previous history of knee injuries who served as controls. Circulating levels of COMP (R&D Systems) and CRP (Calbiotech) were measured from subjects' plasma using ELISAs. Differences between control and ACL subjects were tested using Student's t-test ($\alpha=0.05$), and within ACL subjects differences were tested with a repeated measures one-way ANOVA ($\alpha=0.05$) followed by Dunnett's post-hoc sorting to identify differences from the Pre-Op visit.



RESULTS

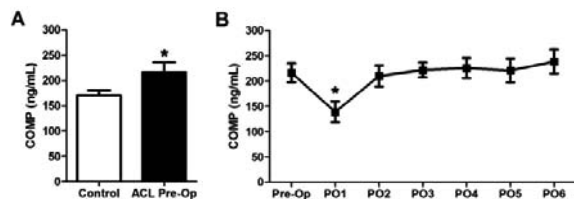


Figure 2. (A) Compared with healthy controls, patients with ACL tears had higher baseline levels of COMP. (B) Following surgical reconstruction, compared with the Pre-Op visit there was a decrease in COMP at the first post-operative visit (PO1), but no difference at other time points. *, $P<0.05$.

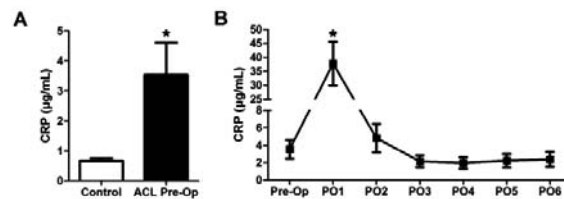


Figure 3. (A) Compared with healthy controls, patients with ACL tears had higher baseline levels of CRP. (B) Following surgical reconstruction, compared with the Pre-Op visit there was a dramatic increase in CRP at the first post-operative visit (PO1), but no difference at other time points. *, $P<0.05$.

DISCUSSION Patients who suffered an ACL tear had higher levels of COMP and CRP than healthy control subjects. Since the patients underwent a pre-operative rehabilitation program lasting 6-8 weeks prior to surgery, these results support the notions that the initial injury to the joint that occurs at the time of the tear increases cartilage catabolism and inflammation, and that these elevations in baseline biomarkers do not resolve by the time the patient is discharged to return to full activities. Future directions include examining the role of other biomarkers and pro- and anti-inflammatory cytokines throughout the course of ACL reconstruction and rehabilitation.

ACKNOWLEDGEMENTS We thank Christopher Walsh for his assistance with this study. Funding was provided by grant AR058920 from NIAMS.

INTRA-OPERATIVE VITAMIN-C SUPPLEMENTATION PROMOTED TENDON HEALING IN RATS

Mok TY, Fu SC, Cheng WH, Cheuk YC, Yung SH, Hung LK, Chan KM

Department of Orthopaedics and Traumatology, Faculty of Medicine, CUHK, Hong Kong SAR, China

INTRODUCTION

Tendon injuries are frequently disabling and associated with compromised tensile strength. Our previous study on tendon adhesion demonstrated that application of antioxidant immediately after surgical operation can reduce tendon adhesion¹. We therefore aim to further investigate the effect of Vitamin C supplementation on restoring the tensile strength of the healing tendon.

METHODS

Seventy-two Sprague-Dawley rats were recruited in this study. A well established central-third donor site injury was induced in the rats. The rats were divided into low, middle, or high-dose (3, 10, or 30 mg/ml) of Vitamin C groups and a saline group. 5ml of surgical irrigation solution with Vitamin C or saline was applied to the injured site intra-operatively. Ten animals from each group were euthanized and harvested at day 42 post-injury for biomechanical testing. Ultimate tensile stress and elastic modulus were calculated. The remaining eight animals from each group were euthanized at day 1 or day 42 post-injury for histological analysis (n=4). Immunohistochemical staining of tenomodulin was also performed to detect the presence of tendon specific healing cells.

RESULTS

Elastic modulus and ultimate tensile stress of the healing tendon in the low and middle-dose groups were significantly higher than the saline group (Fig 1). No difference was observed between the high-dose and saline groups. In the low and middle-dose groups, histological examination of day 42 healing tendons under polarized illumination revealed better collagen fibre alignment in the healing tendons (Fig 2B), as compared to the high-dose and saline groups (Fig 2A). Increased cellularity was observed in the perivascular regions near the tendon wound at day 1 post injury in low and middle-dose groups. Only these cells were found to be tenomodulin-positive.

Figure 1

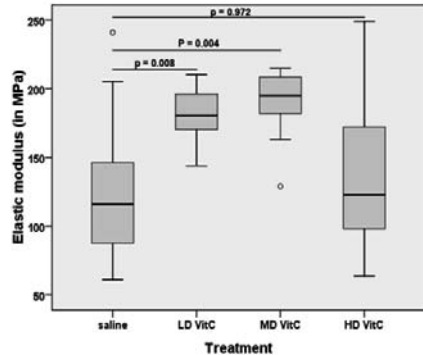
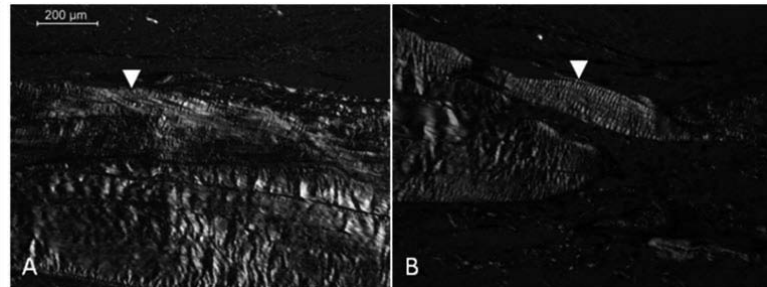


Figure 2



DISCUSSION

Previous study showed that post-operative intra-peritoneal injection of 150mg Vitamin C once every 2 days exerted positive effects on tendon healing by histological examination². We found that intra-operative administration of Vitamin C can also improve restoration of mechanical strength of the healing tendon. Improvement in the tensile strength may attribute to the better collagen fibre alignment, which may be associated with activation of tendon-specific healing cells (tenomodulin-positive) at early healing stages. It suggests that modulation of oxidative stress at early healing stage may affect healing outcomes by altering cell recruitment. The failure of high-dose group to improve healing outcome indicate that minimal levels of reactive oxygen species were still necessary for a better healing outcome.

REFERENCE

(1) Fu et al., ISL&T 2009 poster presentation. Las Vegas, NV. (2) Ömeroglu et al. Arch Orthop Trauma Surg. 2009.

DISCLOSURE

Results in this study have been used in patent applications in China and US.

THE FEMORAL INSERTION OF THE ANTERIOR CRUCIATE LIGAMENT: RELATIONSHIP BETWEEN THE DIRECT INSERTION AND THE DEPTH OF THE CALCIFIED FIBROCARILAGE AND BONE LAYER

Norihiro Sasaki, Yasuyuki Ishibashi, Eiichi Tsuda, Yuji Yamamoto, Shugo Maeda, Satoshi Toh
Department of Orthopaedic Surgery Hirosaki University Graduate School of Medicine, Hirosaki, JAPAN.

INTRODUCTION

In the anatomical ACL reconstruction, femoral tunnel position is one of the most important factors influencing knee kinematics and clinical results^{1, 2)}. To accurately identify the anatomical ACL insertion, the lateral intercondylar ridge has been used as the osseous landmark in anatomical ACL reconstruction³⁾. Although it is widely accepted that the ACL attaches posteriorly to the lateral intercondylar ridge, the optimal functional bone tunnel position remains a matter of debate. The purpose of this study was to investigate the femoral ACL insertion histologically.

METHODS

Twenty embalmed cadaver knees were used. The average age of the subjects was 69.8 years (range, 56–78 years). ACL-deficient knees and severe osteoarthritic knees were excluded from this study. The specimens were cut at the levels as shown in Fig.1. Adjacent sections were then stained with hematoxylin and eosin (H&E), azan, and alcian blue. ACL insertions were observed using a light microscope (BX41; Olympus Corp., Tokyo, Japan). The distance between the posterior cartilage border and the posterior edge of the direct insertion (a) (Fig. 2), and between the posterior cartilage border and the lateral intercondylar ridge (b) (Fig. 2-b) were measured. And the depth of the calcified fibrocartilage and bone layer (CFB) in the direct insertion (Fig. 3-A) and the depth of the bone layer at anterior and posterior segment of the direct insertion (Fig. 3-B) were measured.

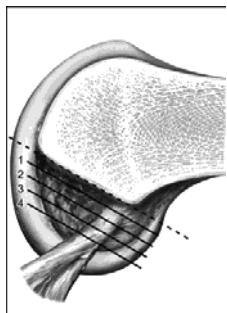


Fig. 1

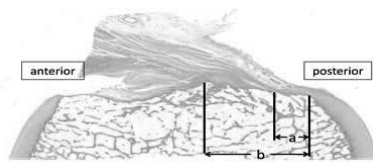


Fig. 2

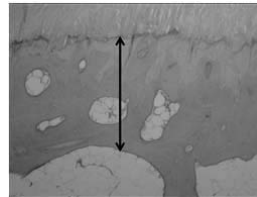


Fig. 3-A



Fig. 3-B

RESULTS

The average distance between the direct insertion and the posterior cartilage border was 4.4 ± 0.5 mm. The average distance between the posterior cartilage border and the lateral intercondylar ridge was 10.1 ± 1.3 mm. The depth of the CFB of the direct insertion was 0.8 ± 0.3 mm, which was deeper than that of the bone layer at anterior and posterior segment of the direct insertion (0.2 ± 0.1 mm and 0.2 ± 0.0 mm, respectively).

DISCUSSION

The direct insertion plays a major role in mechanically linking the ligament and bone in contrast to the indirect insertion⁴⁾. The CFB interface exhibited a complex interlocking pattern⁵⁾ and became deeper and more complex with greater stress^{6, 7)}. From this study, the direct insertion receives greater stress and plays a major role in mechanical links. In clinical situation, it is ideal to making the femoral bone tunnel at the direct insertion during ACL reconstruction.

REFERENCES: 1) Musahl V, et al. AJSM 2005. 2) Tashman S, et al. AJSM 2004. 3) Shino K, et al. KSSTA 2010. 4) Schneider H. Z Anat Entwicklungsgesch 1956. 5) Evans EJ, et al. J Anat. 1991. 6) Milz S, et al. J Anat. 2002. 7) Kumai T, et al. J Anat. 2002.

INCREASED METABOLITE LEVELS IN HUMAN ACHILLES TENDON REPAIR CAN BE ENHANCED BY INTERMITTENT PNEUMATIC COMPRESSION TREATMENT

Arverud E., Nilsson G., Labruto F., Bring D.K.I., Renström P., Ackermann P.W.

Karolinska Institutet, Stockholm, Sweden

INTRODUCTION

Achilles tendon healing after rupture is often protracted and associated with a high degree of complications such as deep venous thrombosis. We hypothesized that this may be due to an impaired blood circulation and a low metabolic activity in the tendon, which are even more restricted during limb immobilization. Metabolites including glutamate, glucose, lactate, pyruvate and glycerol, are known to meet biosynthetic and proliferative healing demands¹. This study assessed whether these metabolites are present and up-regulated in the healing Achilles tendon. We moreover hypothesized that adjuvant intermittent pneumatic compression (IPC), known to increase local blood flow, can up-regulate metabolite concentration at the tendon repair site.

METHODS

As part of a larger prospective randomized trial on acute Achilles tendon rupture eleven patients were recruited, operated on and subsequently randomized. The control group, five patients, received conventional treatment with two weeks of plaster cast immobilization, while 6 patients received adjuvant foot IPC system (Covidien, New Haven, Conn., USA) beneath the plaster cast. The settings used were 130 mm Hg pressure, 1 s pressure duration, 20 s compression frequency, 6 hours daily. At 2 weeks post-operatively microdialysis (CMA 71; CMA Microdialysis AB, Solna, Sweden; 100 kDa: 1.0 µL/min) of the healing and contralateral intact Achilles tendons was performed followed by quantification of metabolites using ISCUS Analyzer (CMA Microdialysis AB, Solna, Sweden). Significance p less than 0.05.

RESULTS

The control group exhibited in the healing Achilles tendons increased levels (mM) of glutamate (60±12 vs. 20±12), lactate (1.3±0.4 vs. 0.8±0.3), and pyruvate (81±24 vs. 43±33) compared to the contralateral intact tendons (p=0.028), whereas the levels of glucose, glycerol and the lactate/pyruvate ratio were not significantly changed. The injured tendons of the IPC vs control group displayed higher levels of glutamate (84±15 vs. 60±12) and glucose (3.4±0.6 vs. 2.5±1.1); (p=0.043) and produced a trend toward higher concentrations of pyruvate (113±33 vs. 81±24; p=0.068). The lactate/pyruvate ratio and the levels of lactate and glycerol were however not significantly changed after IPC. No significant differences were detected in the metabolite levels of the intact tendons that were IPC-treated during microdialysis compared to the intact tendons of the control group.

CONCLUSIONS

This study demonstrates that early human Achilles tendon repair entails and up-regulates local essential metabolites glutamate, lactate and pyruvate. This reparative metabolic response can be promoted by adjuvant IPC during plaster cast immobilization. The up-regulation of glutamate levels in the healing tendons are in agreement with experimental studies showing nerve ingrowth and subsequent release of several neuronal transmitters including glutamate, considered to be involved in the repair process by enhancing cellular proliferation². It may prove that compression therapies can promote healing, allow earlier rehabilitation and reduce the time to return to sports after tendon injury.

REFERENCES

1. Langberg, H., et al., Metabolism and inflammatory mediators in the peritendinous space measured by microdialysis during intermittent isometric exercise in humans. *J Physiol*, 1999. 515 (Pt 3): p. 919-27
2. Ackermann, P.W., P.T. Salo, and D.A. Hart, Neuronal pathways in tendon healing. *Front Biosci*, 2009. 14:p. 5165-87.

RELATIONSHIP BETWEEN STIFFNESS AND FAILURE: EXPERIMENT AND META-ANALYSIS

A.S. LaCroix, S.E. Duenwald-Kuehl, R. Lakes, and R. Vanderby, Jr.
University of Wisconsin-Madison

INTRODUCTION

Tendon is a complex tissue that has adapted in composition and organization to accommodate a wide range of forces that scale with size. Mechanical compromise and risk of failure can be measured *ex vivo* during pull-to-failure protocols, but such tests cannot be performed *in vivo*. If, however, failure levels depended on material properties that could be measured during subfailure testing, risk of failure can be inferred *in vivo*. The goal of this study was to determine whether a fundamental link exists between elastic modulus and ultimate stress in tendon, and whether such a relationship could allow for prediction of failure properties from non-destructive testing.

METHODS

Six rat tail tendons were excised and preconditioned using a sinusoidal wave to 2% strain in a mechanical test system (MTS Bionix, Minneapolis, MN). Tendons were then pulled to failure at 15mm/min. Elastic modulus and ultimate stress were calculated and plotted. To compare with trends in previously reported studies, a search of the published literature was performed. Keywords tendon, healing, mechanical properties, ultimate stress, and elastic modulus were used to identify relevant articles. Studies were selected if there was sufficient information to calculate relevant mechanical properties. Extracted data included elastic modulus and ultimate stress. In some cases, structural data (i.e. load, stiffness, cross-sectional area, deformation) were collected in order to calculate the mechanical properties of interest (ultimate stress, elastic modulus).

RESULTS

Elastic modulus (221.1 +/- 63.4 MPa) and ultimate stress (18.4 +/- 5.7 MPa), when plotted together (Fig 1), were found to be linearly correlated ($R^2 = 0.9893$). The literature search, which yielded 39 relevant articles (with data from mouse, rabbit, sheep, goat, wallaby, kangaroo, horse, and human specimens) also demonstrated a fundamental relationship between ultimate stress and elastic modulus (Fig 2), which correlated linearly ($R^2 = 0.807$).

While age, genetics, mechanical environment, and injury have important effects on tendon behavior, the fundamental relationship between modulus and ultimate stress remains consistent (for example, an injured tendon which undergoes a modulus decrease also undergoes a decrease in ultimate stress). This linear relationship, using the control (healthy) tendon mechanical behavior as a reference point, was then able to predict the failure stress (and failure load) for a treatment-group with a different elastic modulus. In both experimental and meta-analysis results, the ultimate strain of each tendon is insignificantly different.

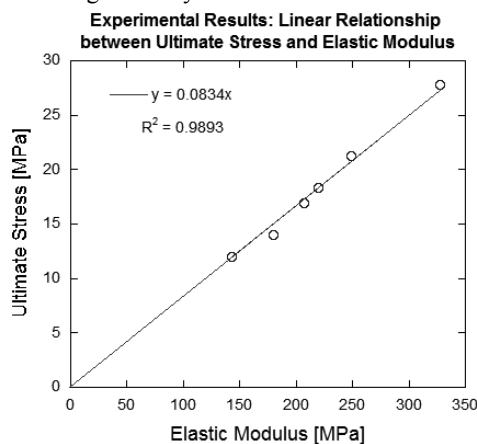


Figure 5. Experimental Rat Tail Tendon Results.

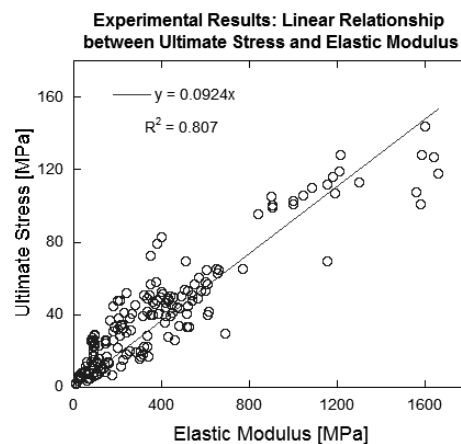


Figure 2. Literature Reported Results.

DISCUSSION

Tendon is a unique, hierarchical, highly specialized material that has been characterized by mechanical testing, histology, and microscopy. We show here a fundamental link between elastic modulus and ultimate stress. The inherent link between failure strength and modulus suggests that a constant value of strain could be used as a failure criterion for all tendons, even for different species, pathologies, or types of damage. The consistent relationship shown in this study suggests that sub-failure *in vivo* measurements of elastic modulus could be predictive of failure properties, thereby quantifying compromise in pathologic or partially torn tendons.

ACKNOWLEDGEMENTS

This work was funded in part by NSF 0553016 and NIH R21-EB 008548.

ALTERATIONS IN TRANSVERSE AND LONGITUDINAL MECHANICAL PROPERTIES OF ARTIFICIALLY AGED TENDON

G. Fessel^{1,2}, D. Brütsch¹, Y. Li^{1,2}, S. Wunderli¹, J.G. Snedeker^{1,2}

1. Dept. of Orthopedics, University of Zurich, Switzerland; 2. Institute for Biomechanics, ETH Zurich, Switzerland

INTRODUCTION

Ageing and diabetes are both associated with increased levels of advanced glycation end products (AGEs). AGEs affect cell-matrix interactions leading to inhibited wound repair and exacerbated inflammation¹. Some AGEs act as collagen cross-links and cause higher failure loads and stiffness^{1,2}. However, AGE cross-linked tendons are also associated with increased tendon fragility^{3,4} and a reduced remodeling capacity. Further, it remains unknown on which hierarchical level glycation induced cross-links affect tendon mechanics, thereby making it difficult to understand their functional repercussions on mechanotransduction and subsequent tissue remodeling. The goal of the present study was to test whether it is possible to quantify effects of cross-linking on collagen fibril-matrix or fibril-fibril interactions by use of standard macro-scale mechanical testing. To eliminate potentially confounding effects of age or disease (e.g. loss of collagen) we investigate the effects of cross-linking on the longitudinal and transverse mechanical properties of equine superficial digital flexor tendons (SDFT) after incubation in methylglyoxal solution, a metabolite known to induce the formation of AGEs¹.

METHODS

First, eight SDFT were dissected and cut along their collagen fiber direction with three parallel, equally spaced microtome blades to yield pairs of 60x3x1 mm (longitudinal) strips. Second, tendons were cut transverse to the collagen fiber direction yielding pairs of 30x2x1 mm (transversal) strips. One half of each pair was incubated for 42 hours in 0.02 M methylglyoxal in buffer at 36°C to induce cross-linking (aging/diabetes group). The other half was designated as a matched control and refrozen (-18°C) until the day of testing. After applying a stochastic surface pattern (graphite markers) to facilitate image registration for optical strain measurements, samples were clamped, pre-loaded, and tested in uniaxial tension until failure (Zwick 1456, Germany). Elastic image registration was used to calculate displacement/strain-fields that were then averaged over the mid-substance. Stress-strain plots were parameterized according to tangential modulus (1% strain increment in the linear part), failure stress (peak stress) and failure strain (strain at peak stress). Paired T-test and exact Wilcoxon Signed Rank test were used to assess the effects of cross-linking. Results are reported as means with standard deviations and p-values (p).

RESULTS

Incubation in methylglyoxal resulted in 100% increased tangential modulus (control: 1.09±0.82MPa vs. cross-linked: 2.08±1.07MPa, p =0.016) and maximal stress (control: 0.15±0.08MPa vs. cross-linked: 0.29±0.06MPa, p =0.008) in transverse strips. While cross-linking did not affect average normal strains, shear strains were strongly altered. Elastic moduli were reduced by cross-linking in longitudinal strips (control: 338.4±84.5 vs. cross-linked: 224.6 ± 82.0, p=0.06) while maximal stress (p=0.74) and strain (p=0.64) remained unaffected. Qualitative analysis of the stress-strain curve indicated partial removal of the toe-region and a shift of the linear region to higher strains by cross-linking. A first analysis of the surface strain indicated a trend to reduced shear-strains (p-value: 0.16).

DISCUSSION

To the best of our knowledge this is the first study to investigate AGE cross-linking related to functional alterations in tendon in both the transverse and longitudinal directions. Preliminary results indicate that methylglyoxal cross-linking increased fiber-fiber or fiber-matrix coupling as measured in transverse samples. This might explain the diminished toe-region and the trend to reduced shear strains observed in longitudinally tested strips. We conclude from these preliminary data that methylglyoxal cross-linking as a model for tendon aging or disease (e.g. diabetes) demonstrate complex changes in mechanical properties that are potentially dependent on the type of tendon, animal model or the hierarchical level tested. Further testing and analysis is required and ongoing.

ACKNOWLEDGEMENTS

We thank Mr. Hansrudolf Sommer for his expertise and contribution to the mechanical testing.

REFERENCES: 1. Avery and Bailey, Scand J Med Sci Sports 2005 2. Reddy, Exp Diabesity Res 2004 3. Fox et al. J Orthop Res 2011 4. Fessel et al. J Orthop Res *in press*.

THREE-DIMENSIONAL GEOMETRICAL CHANGES OF KNEE SOFT TISSUES DURING FLEXION BY ANATOMICAL-BASED FIBRE MAPPING. AN IN-VITRO STUDY.

¹C. Belvedere, ²A. Ensini, ²A. Feliciangeli, ¹F. Cenni, ¹A. Leardini

¹ Movement Analysis Laboratory & ² II Division of Orthopaedic Surgery, Istituto Ortopedico Rizzoli, Bologna, Italy

INTRODUCTION

In the human knee joint, the anterior (ACL) and posterior (PCL) cruciate ligaments, the medial (MCL) and lateral (LCL) collateral ligaments guide and stabilize the joint throughout the knee flexion arc (1); the patellar tendon (PT) is an essential part of the extensor apparatus. The literature reporting reliable anatomical-based fibre mapping and relevant patterns of fibre shortening/lengthening during knee flexion is still limited. This is essential for the identification of ligament sub-bundles and relevant specific functions, but not always analysed with the necessary care. Among possible measuring devices, current knee navigation systems, used in computer aided total knee arthroplasty, enable accurate anatomical-based bone tracking and direct digitization of landmarks and surfaces.

The aim of this study was to assess in-vitro, on whole lower limbs specimens, three-dimensional (3D) deformation of a number of fibres for these knee soft tissues, with the final scope of a thorough description of the relevant patterns of length and orientation change via a careful anatomical-based fibre mapping.

METHODS

Ten fresh frozen amputated lower limbs with the knee free from anatomical defects, and intact joint capsule, ligaments and quadriceps tendon were analyzed using a knee surgical navigation system (Stryker®-Leibinger, Freiburg, Germany) with 0.5°/0.5mm accuracy. Clusters with active markers were pinned onto the femur, tibia and patella. A handy pointer was used for system control and landmark digitations. Mechanical and anatomical conventions were according to standard recommendations (2,3). Series of 5 trials of manually driven knee flexions in a 0°-140° arc were recorded, under a 100 N load applied at the quadriceps femoris central tendon.

For ligament fibre recruitment analysis, the following bone-to-fibre attachments of sub-bundles were accurately identified and digitized: the antero-medial (AM) and postero-lateral (PL) in ACL, the antero-lateral (AL) and postero-medial (PM) in PCL, the anterior (AB) and posterior (PB) in MCL. Point strips were collected along fibres in known anatomical positions in PT, AB and LCL. Proximal and distal attachment centroids and the extremities of point strips were assumed as fibre origins and insertions, whose orientation and length were calculated during knee flexion, the former reported in the tibial reference frame and the latter in % of the corresponding maximum fibre length (L_{max}). The location of the most isometric ligament fibre (ISO) was also investigated.

RESULTS

Repeatable deformation patterns versus flexion were observed within each specimen, with standard deviation over trials being less than 1.7 mm and 4.0°. Over specimens, this becomes less than 18% L_{max} and 14°.

In ACL, AM and PL are tight in full extension; an average of 19.2 and 30.1 %L_{max} shortening occurred, respectively, during flexion. The difference between AM and PL orientation range in the frontal (34.0° and 23.1°) and sagittal (37.0° and 11.0°) tibial planes revealed that the two sub-bundles intertwine with each other. ACL ISO was found within AM and similarly oriented to AM. In PCL, AL and PM are slackened in full extension; a 25.7 and 9.0 %L_{max} lengthening occurred up to full flexion. The difference between AL and PM orientation range (26.0° and 10.3°, and 42.5° and 48° on tibial frontal and sagittal planes, respectively) revealed that they intertwine with each other, but less markedly than in ACL. PCL ISO was found within PM and similarly oriented to PM.

In MCL, a 10.1 and 26.0 %L_{max} shortening occurred in AB and PB during flexion. ISO was found very close to the most anterior fibre of AB. On average, the orientation range is 5.0° and 12.5° on tibial frontal and sagittal planes. In LCL, all fibres shorten of about 20.2 %L_{max} during flexion and with average orientation ranges of 15.0° and 20.3° on tibial frontal and sagittal planes. The calculated ISO has no anatomical significance.

In PT, a 3.5 %L_{max} fibre lengthening occurred in the initial 40°-50° of flexion. Fibre orientation range was 24.5° and 33.2° on tibial frontal and sagittal planes, respectively. ISO was found in PT central-medial portion.

DISCUSSION

The technique enabled reliable tracking of soft tissue attachment areas through careful fibre mapping for a best possible 3D representation of fibre sub-bundles throughout the passive flexion arc and the identification of isometric fibres. Thorough information about fibre deformation was provided in consistent anatomical-based reference frames as supported by the availability of whole lower limbs.

This study was aimed at contributing to the much controversial knowledge on soft tissue behaviour in the normal knee over the flexion range. The data here reported offer a useful reference for novel knee joint models and also in computer-aided total knee replacement or ligament reconstruction for the re-establishment of the natural ligament biomechanics.

REFERENCES: 1. Zavras et al. KSSSTA 2001. 2. Cappozzo et al. Clin Biom. 1995. 3. Grood and Suntay J.Biom.Eng 1983.

ANATOMICAL AND BIOMECHANICAL CONCEPTS IN ACHILLES TENDON PATHOGENESIS

T. Arndt

Institution CLINTEC, Karolinska Institute, Stockholm, Sweden
 Swedish School of Sport and Health Sciences, Stockholm, Sweden

INTRODUCTION

Orthopedic treatment and biomechanical modeling of the Achilles tendon is often based upon simplified notions concerning its morphological structure and biomechanics. The tendon is often assumed to be a uniform, simple proximal to distal structure, which transfers force in a direct line from the triceps surae muscle group to the calcaneus. Many of the more differentiated descriptions of the tendon refer solely to the twisting described by Cummins et al. [1]. A long series of studies has been conducted investigating the complexity of the macroscopic tendon fibre construction and asymmetric force transfer in different portions of the tendon.

METHODS

A number of methodological approaches have been taken in an attempt to better understand the tendon's anatomy and biomechanics and consequences for pathology and injury etiology. A cadaver series of 20 tendons was investigated using a newly developed preparation technique [2]. The possibility of asymmetrical stress distribution across the tendon's cross-section were analyzed with further cadaver specimens in a material testing machine and *in vivo* experiments using an optic fiber technique [2,3]. More recent studies have applied an ultrasound based technique utilizing speckle tracking algorithms for non-invasive, *in vivo* description of different tendon sections during controlled ankle joint motions on an isokinetic dynamometer [4] and during walking [5].

RESULTS

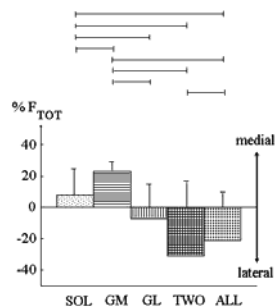


Figure 1. Percent of force in medial and lateral portions of the Achilles tendon depending upon which triceps surae muscles were loaded. Horizontal lines indicate sig. differences [2].

Morphological study confirmed the rotation of the Achilles tendon described by Cummins [1]. A previously not described diagonal line of fiber connection from proximal-lateral to distal-medial was described between the aponeuroses of the gastrocnemius and soleus [2]. Cadaver and optic fibre studies illustrated complexity in the transfer of muscle forces through the tendon (Fig 1, table 1).

	M_{GAST} [Nm]	M_{SOL} [Nm]	M_{PFF} [Nm]
$\alpha = 90^\circ$	0	60.3	84.3
$\alpha = 10^\circ$	53.2	60.3	40.0

Table 1. Contributions of gastrocnemius, soleus and other plantarflexors to the Achilles tendon force calculated at 0° and 90° knee angle [3].

Recent research [4] describing tendon displacement in superficial (posterior), central and deep portions of the tendon using a speckle tracking method revealed greater displacement in the deep portion (10.4 ± 2.1 mm) compared to the superficial (8.4 ± 1.9 mm) in 9 subjects performing passive ankle dorsi- plantarflexion cycles. Application of the same method in walking indicated a peak in tendon lengthening not necessarily corresponding to maximum triceps surae activation [5].

DISCUSSION

Complex 3D morphology and asymmetric force transfer depending upon ankle kinematics and muscle activation were quantified and should be taken into account in the description of injury mechanics, surgery, rehabilitation protocols and also modeling of the human Achilles tendon. Further research is presently underway on the quantification of the differentiated tendon dynamics during complex, controlled motions (eg. concentric/ eccentric triceps surae contractions in an isokinetic dynamometer) to further illuminate the presented phenomena.

REFERENCES: 1. Cummins et al., Surg Gynaecol Obst 1946. 2. Arndt, PhD Thesis, 1997. 3. Arndt et al., Clin Biomech 1998. 4. Arndt et al. submitted Knee Surg Sports Traum Arthroscopy. 5. Fröberg et al., submitted J Biomech.

TRIGGER FINGER, TENDINOSIS AND GENE EXPRESSION

¹A-C Lundin, ^{2*}P Eliasson, and ²P Aspenberg

¹Department of Hand and Plastic surgery, ²Department of Orthopaedics, IKE, Linköping University, Linköping, Sweden. * Presenting Author

INTRODUCTION

It is widely considered that the major pathology for trigger finger lies in the A1-pulley¹, but the tendons often appear swollen, with loss of natural colour and lustre. We have previously found histopathological changes suggestive of tendinosis². To get further support for our theory that trigger finger is a form of tendinosis, we now used gene expression analysis.

At other locations in the body, gene expression in biopsies from tendinosis lesions is different from normal tendons³. A couple of genes have been addressed in repeated studies and have shown up-regulation of collagen type I and III, matrix metalloproteinase-2 (MMP-2), cyclooxygenase-2 (COX-2) and interleukin-6 (IL-6), and down-regulation of matrix metalloproteinase-3 (MMP-3). We hypothesized that trigger fingers would be different from normal tendons, with an expression patterns similar to tendinosis at other locations.

METHODS

We obtained snap-frozen biopsies from 14 trigger finger tendons (TF) and from 15 apparently normal tendons (N) from patients operated for carpal tunnel syndrome. Six genes were chosen for real-time PCR: collagen type I and III, MMP-2 and -3, COX-2 and IL-6 (and three house keeping genes, 18S rRNA, cyclophilin A and ubiquitin-C). These genes are often differentially expressed tendinosis lesions. Mann-Whitney U test was used for the statistical analyses.

RESULTS

The housekeeping genes were stably expressed with no differences between the groups. Collagen type I was roughly 4 times more expressed in the trigger finger samples compared to the controls ($p=0.001$, figure 1) and collagen type III was 8 times more expressed in the trigger fingers ($p<0.001$). MMP-3 expression was less than half of the expression in normal tendons ($p=0.04$). The expression of MMP-2 was not different between the two groups. COX-2 and IL-6 were generally too weakly expressed for analysis.

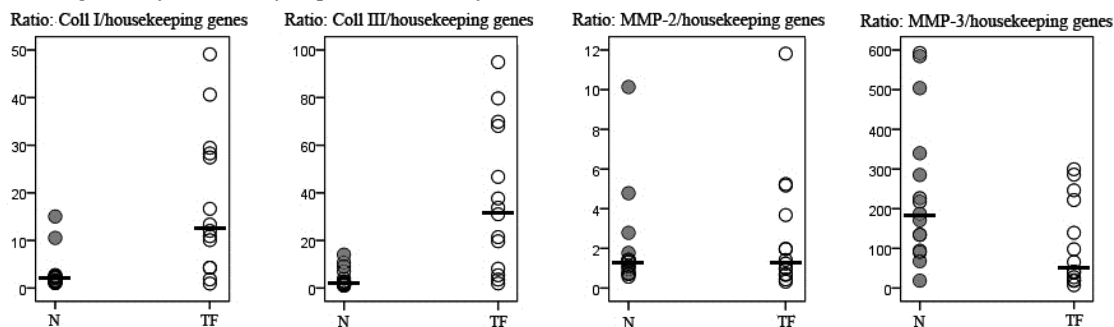


Figure 1. Gene expression for collagen type I, collagen type III, MMP-2 and MMP-3 in normal tendons (N) and tendons from trigger finger patients (TF). The vertical axis shows the relative ratio of the gene to the housekeeping genes (18S rRNA, cyclophilin A and ubiquitin C). Each circle represents one patient and the line represents the median.

DISCUSSION

The increased expression of collagen type I and III together with a decreased expression of MMP-3 all agree with previous studies on biopsies from tendinosis patients, and warrant analyses of a larger set of genes from these biopsies. These changes suggest that the normal function in the tendon is disturbed in the trigger finger tendons. MMP-2 has previously been shown to be up-regulated in tendinosis tendons, but this was not seen in our samples.

Weaknesses with this study are that we lack information about the trigger finger stages and that the control biopsies were obtained from patients with carpal tunnel disease, amongst which the incidence of trigger finger is known to be high. However, the control tendons appeared macroscopically normal and the patients had no previous history of trigger finger in that hand.

Altogether, the macroscopic appearance, the histological appearance and now the similarities in gene expression support the suggestion that trigger finger could be a form of tendinosis.

REFERENCES

- 1 Moore JS. et al. (2000). J Occup Environ Med 42(5): 526-45.
- 2 Lundin A.-C. (2011). J Hand Surg Eur Vol 1753193411421853, first published on October 10.
- 3 G.P.Riley. (2008). Nat Clin Pract Rheu. 4(2): 82-89.

“FAILURE WITH CONTINUITY”— A COMMON MECHANISM OF ROTATOR CUFF REPAIR “HEALING”

^{1,4}Kathleen A. Derwin, ²Jesse A. McCarron, ³Michael J. Bey, ^{1,4}Joseph P. Iannotti
¹Dept. of Biomedical Engineering Cleveland Clinic, Cleveland, OH
²Dept. of Orthopaedic Surgery, Oregon Health and Sciences University, Portland OR
³Henry Ford Hospital, Dept. of Orthopaedic Surgery, Bone and Joint Center, Detroit, MI
⁴Dept. of Orthopaedic Surgery, Cleveland Clinic, Cleveland, OH

INTRODUCTION

Despite reliable improvements in pain and function following rotator cuff repair surgery, tendon architecture, muscle atrophy, fatty infiltration and shoulder strength are rarely restored to normal post-operatively (1,2,3). We hypothesize that these persistent deficits are the result of gradual repair failure by displacement of the tendon away from the site of initial fixation, at a rate that is slow enough to allow for the formation of tissue and preclude the identification of a gap in the tendon using traditional MRI or ultrasound imaging.

METHODS

Thirteen patients with repairable tears of the supraspinatus and/or infraspinatus tendons underwent arthroscopic repair using a suture-bridge technique. In order to assess repair integrity after surgery, we monitored the 3D position of tantalum beads implanted within the repaired rotator cuff tendons using a low-radiation dose CT scanning protocol. CT scans were obtained on the day of surgery and at 6, 12, 26 and 52 weeks post-operatively, from which the scalar distance between the repair site anchors and the tendon beads was measured using custom imaging software. MR and ultrasound imaging of the shoulder was also obtained pre-operatively and at 6, 12, 26 and 52 weeks post-operatively to assess for the presence of a recurrent rotator cuff defect. VAS, PENN, and Constant and Murley scores were obtained pre-operatively and 52 weeks.

RESULTS

Four of thirteen patients were considered to have a recurrent tendon defect at 52 weeks by MRI assessment. Ultrasound identified two of the four defects seen on MRI. Over the 52 week study period, every patient demonstrated tendon retraction following repair (range 5.7 to 23 mm; mean 16 ± 5 mm). Between the day of surgery and 6 weeks, anchor-bead distance tended to increase significantly more in patients that formed a recurrent defect than in patients that did not ($p=0.08$, Fig. 1), yet the total amount of tendon retraction was not different between groups at 52 weeks. The anchor-bead distances in the intact subscapularis tendons varied ± 3 mm over the 52 week study period, which represents the uncertainty of our measurement technique.

DISCUSSION

Although our sample size is small and this is to a large extent a pilot study, the results have the following implications for rotator cuff repair and healing: Rapid tendon retraction may lead to a recurrent tendon defect, whereas, slow retraction may be a common and unrecognized phenomenon, so-called “failure with continuity”. Tendon retraction in all patients may explain, at least in part, why reversal of muscle fatty atrophy is not observed clinically. Since about 80% of the tendon retraction occurs in the first 12 weeks after surgery, these data also suggest that repairs should be protected in early post-op period and repair strategies should endeavor to mechanically augment the repair in this critical early period. Future work will utilize a second generation tendon marker to explore the relationships between tendon healing/retraction and muscle function. We also intend to use this technique for monitoring outcomes in tendon repair with and without a scaffold.

REFERENCES: (1) Boileau P et al, J Bone Joint Surg Am 2005 Jun;87(6):1229-40; (2) Fuchs B et al, J Bone Joint Surg Am 2006 Feb;88(2):309-16. (3) Gladstone JN et al, Am J Sports Med 2007 May;35(5):719-28.

Funding: This work was supported by Pfizer Pharmaceuticals and the Dept of Orthopedic Surgery, Cleveland Clinic.

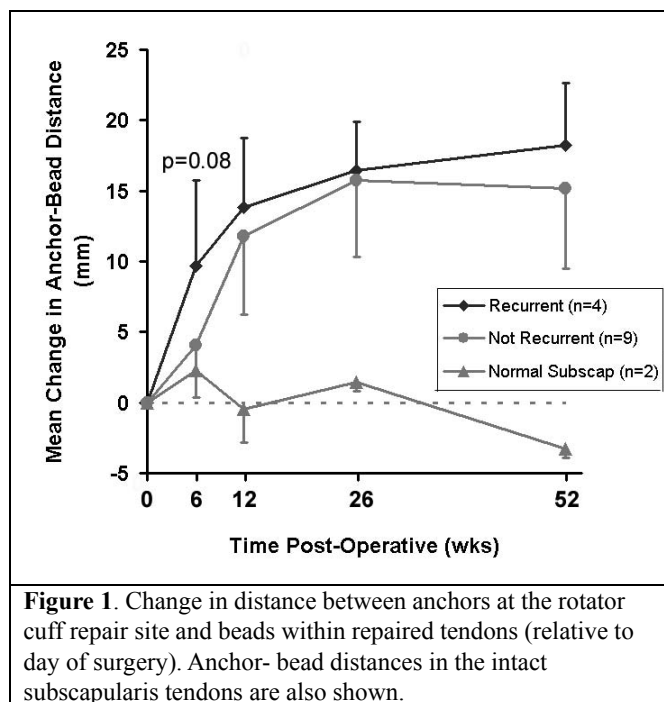


Figure 1. Change in distance between anchors at the rotator cuff repair site and beads within repaired tendons (relative to day of surgery). Anchor-bead distances in the intact subscapularis tendons are also shown.

SYSTEMIC ADMINISTRATION OF OXYTETRACYCLINE INDUCES AN AGE-DEPENDENT DECREASE IN THE VISCOELASTIC PROPERTIES OF RAT TAIL TENDONS

Gardner, K., Wintz, L., Lavagnino, M., +Arnoczky, S. P.
 Laboratory for Comparative Orthopaedic Research, Michigan State University, East Lansing, MI

INTRODUCTION

Contracted tendons are a common flexural deformity in neonatal foals. These foals have a mismatch in length of distal limb bone and tendon and are unable to extend their digits appropriately. Recent clinical studies have shown that the systemic administration of oxytetracycline (OTT) has been successful in correcting tendon contracture in very young, but not older, foals (1,2). However, the mechanism(s) by which this tendon lengthening occurs is unknown. Previous studies from our laboratory have demonstrated that OTT inhibits myofibroblast expression of interstitial collagenase which is required for the remodeling and reorganization of collagen by fibroblasts in growing tendons (3,4). Therefore, it is possible that OTT may inhibit this reorganization, thereby decreasing the mechanical properties of the tendon allowing them to elongate. *We hypothesize that short term (4 day) systemic administration of OTT in young rats will cause a decrease in the viscoelastic properties of tendons when compared to untreated animals and will have no significant effect on these properties in older rats.*

MATERIALS AND METHODS

Ten one month old (1 m) and 10 six month old (6 m) Sprague-Dawley rats were used in this study. From each study group, five treated rats received intra-peritoneal (IP) injections of OTT at a dose of 50mg/kg/day for 4 days. Tendon fascicles were harvested from the rat tails immediately after euthanasia and frozen at -80°C in phosphate buffered saline (PBS) or fixed in formalin.

For testing, a 60 mm segment of each rat tail tendon was mounted onto a custom-made material testing system in PBS at room temperature. The testing system was equipped with a 5-lb load cell, a motion controller and a linear variable differential transformer to measure grip-to-grip displacement. Tendons were calibrated to 0% strain before loading to 3% strain. Values were recorded every 0.02 seconds for 10 minutes. Using tendon diameter and load/displacement values maximum modulus and equilibrium modulus were computed. Variables were compared using a Student's T test with significance set at P< 0.05.

Superficial digital flexor tendons donated from a deceased foal (1d) and an adult horse, as well as, rat tail tendons from 1 m and 6 m animals, were stained for interstitial collagenase and cellularity

RESULTS

No changes were noted in the weights of treated vs. untreated rats (p=0.3) over the treatment period. OTT-treated 1 m rat tail tendons demonstrated a lower maximum modulus (p = 0.03) and equilibrium modulus (p = 0.005) than untreated tendons. In the 6 m tendons, there was no difference in maximum modulus (p=0.218) or equilibrium modulus (p=0.392) between treated and untreated rats (Table 1). A qualitative increase in interstitial collagenase production and a statistical increase (p<0.001) in cellularity was observed between young and mature animals in both species.

DISCUSSION

Results of the current study demonstrate that systemic administration of OTT to 1 m rats produces a statistically significant decrease in the viscoelastic properties of tail tendons when compared to untreated animals. However, this change in mechanical properties was not observed in mature (6 m) rats.

Collagenase staining and cellularity analysis illustrates abundant interstitial collagenase production and increased cellularity in both young rat tail tendons and foal tendons when compared to adult tissues. Interstitial collagenase is a major regulator of collagen degradation during tissue remodeling (4), and OTT has been shown to inhibit collagenase expression in equine myofibroblasts (3). Therefore, it is possible that young animals undergoing rapid tendon growth and remodeling may be more responsive to OTT treatment than older animals.

REFERENCES

[1] Auer *et al*; *Clin Tech Equine Prac* 2006; [2] Trumble; *Vet Clinic Equine* 2005; [3] Arnoczky *et al*; *Am J Vet Research* 2004; [4] Parks *et al*; *Matrix Metalloproteinases* 1998

1 month	Untreated	OTT	P-value
Maximum Modulus (MPa)	164.6 ± 15.9	133.9 ± 21.6	0.034
Equilibrium Modulus (MPa)	46.4 ± 5.2	35.6 ± 3.6	0.005
6 month	Untreated	OTT	P-value
Maximum Modulus (MPa)	284.1 ± 44.9	254.7 ± 20.1	0.218
Equilibrium Modulus (MPa)	195.5 ± 32.9	180.7 ± 15.9	0.392

SUBSTANCE P ENHANCES COLLAGEN GEL REMODELING AND MMP-3 EXPRESSION BY HUMAN TENOCYTES

^{1,2,3}G. Fong, ²L. Backman, ⁴D. Hart, ²P. Danielson, and ^{1,3}A. Scott

¹Dept. of Physical Therapy, University of British Columbia, Vancouver, BC, Canada, ²Dept. of Integrative Medical Biology, Anatomy, Umeå University, Umeå, Sweden, ³Centre for Hip Health and Mobility, Vancouver Coastal Health Research Institute, Vancouver, BC, Canada, ⁴McCaig Institute for Bone and Joint Health, University of Calgary, Calgary, AB, Canada

INTRODUCTION

The loss of collagen organization is considered a hallmark histopathologic feature of tendinopathy. While the precise mechanisms that trigger the loss of collagen integrity have not been identified, it is postulated that the expression and activation of matrix metalloproteinases (MMPs) by tenocytes contribute to the development of tendinosis. Tenocytes produce several signal substances that were once thought to be restricted to neurons, including substance P (SP). Recent *in vivo* studies have shown that SP can influence collagen fibre reorganization [1]. *In vitro* studies have also established that tenocytes respond to SP primarily via activation of the Neurokinin-1 receptor (NK-1 R). In medial collateral ligament primary cell cultures, SP can alter the mRNA expression levels of tissue-remodeling genes including MMPs [1]. Thus, the focus of the present study was to examine the influence of SP on tissue remodeling by human primary tendon cells *in vitro*.

METHODS

Human Achilles and hamstring tenocytes were grown as primary cultures in a variety of substrates including 3D collagen matrixes for the collagen gel contraction assay, collagen I treated Bioflex culture plates for mechanical loading in the FlexCell system, and regular tissue culture plates for biochemical tests. Tenocytes from passages 3-5 were treated with SP or control (carrier). The collagen gel contraction assay was used to assess collagen remodeling as indicated by the decrease in gel area over time. The mRNA expression level of MMP-3 was determined by qPCR in all three culture methods. MMP-3 was selected for qPCR analysis after examination by Northern Blot of a larger panel of genes potentially involved in collagen gel remodeling and based on its known involvement in tendinosis.

RESULTS

The collagen gel contraction assay demonstrated the ability of tenocytes to contract collagen gels in a time dependent manner. Tenocytes cast in collagen gels treated with SP showed a greater rate and extent of contraction compared to control (carrier) with changes typically occurring within 6 hours post-release of the gel (control vs. SP $p < 0.001$, Figure 1). When tenocytes were exposed to SP in culture, increased MMP-3 mRNA expression was observed, compared to control ($p < 0.01$). Additionally, tenocytes exposed to cyclic loading also showed increased MMP-3 mRNA expression compared to the control ($p < 0.01$). When cells were treated with both SP and cyclic loading, they showed an even greater increase in MMP-3 mRNA expression (control vs. SP $p < 0.0001$, unloaded vs. loaded $p < 0.01$).

DISCUSSION

The administration of SP enhanced the intrinsic collagen remodeling activity of cultured tenocytes. In addition, the present study showed that exogenous SP led to increased MMP-3 expression in normal tenocytes. The simultaneous application of SP and cyclic loading resulted in further enhancement of MMP-3 expression, demonstrating a potential interplay between biochemical and mechanical factors that could contribute to the development of tendinosis.

Interestingly, within the MMP family, studies have shown MMP-3 (stromelysin) to be involved in tendinosis, with tendinopathic tendons displaying increased MMP-3 activity despite reduction in MMP-3 mRNA levels compared to normal tendons, suggesting MMP-3 activity to be regulated at both transcriptional and post-transcriptional levels [3]. A promising direction to pursue would be to determine whether there is a potential link between SP and MMP-3 via TGF-beta, a potent factor well known to promote collagen remodeling. Studies involving human osteoblasts have shown TGF-beta to influence MMP3 expression. Furthermore, substance P and mechanical loading are both known to upregulate TGF-beta expression in epithelial and fibroblast cell cultures respectively [4, 5].

REFERENCES

[1] Carlsson et al., 2011 [2] Hart et al., 1998 [3] Marieke de Mos et al., 2007 [4] Robbins et al., 1997 [5] Hu et al., 2002

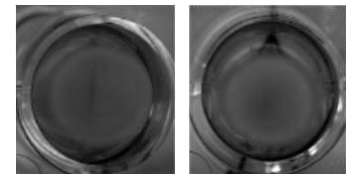


Figure 6. Contraction of tenocyte-seeded collagen gel 6h post-release. Tenocyte (left), Tenocyte + SP (right)

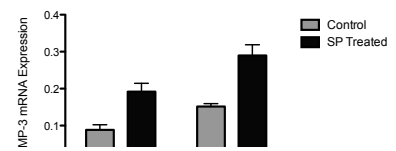


Figure 2. MMP3 mRNA expression affected by SP and mechanical loading.

BONE TUNNEL HEALING OF TISSUE ENGINEERED SCAFFOLD-LESS BONE-LIGAMENT-BONE CONSTRUCTS AND PATELLAR TENDON AUTOGRAFTS USED FOR ANTERIOR CRUCIATE LIGAMENT REPLACEMENT IN SHEEP

M.J. Smietana, J. Ma, E. Wojtys, E.M. Arruda and L.M. Larkin
Skeletal Tissue Engineering Lab (STEL), University of Michigan, Ann Arbor, Michigan

INTRODUCTION

Each year, over 100,000 anterior cruciate ligament (ACL) reconstructive surgeries are performed in the US¹. It is estimated that 10-15% of those cases experience graft failure or recurrent instability requiring revision ACL surgery². Tunnel enlargement from the initial reconstruction often complicates revision ACL surgery due to excessive bone loss and compromised graft fixation surfaces². Additional surgeries requiring staged bone grafting are then often required before reconstruction can begin. While the exact cause of tunnel widening is unknown, current theories include mechanical factors (graft position, fixation method, and motion of graft in tunnel) and biological factors (increased cytokine levels, synovial fluid infiltration) that can have significant effects on final ACL outcomes³. Our laboratory has developed a scaffold-less method to engineer a multi-phasic ligament with engineered bone at each end, or bone-ligament-bone (BLB) construct, with structural and functional interface characteristics similar to young native tissue, an initially extensible intra-articular region that accommodates knee motion and rapidly remodels *in vivo*, without requiring interference screws for tunnel fixation^{4,5}. Implantation of our BLBs into an adult sheep demonstrated that our *in vitro* engineered tissues grow and remodel quickly to a more advanced phenotype, promote bone ingrowth within the tunnel, and develop a biologically and mechanically relevant enthesis with the native tissue as early as 8 weeks without the use of interference screws. By 9-mo. the BLBs increase tangent modulus to 53% of the native ACL value. By comparison, patellar tendon autograft (PTG) reconstructions decreased in mechanics to 32% of the tangent modulus (Ma *et al*, Submitted for Publication, AOSSM 2011).

METHODS

Tissue engineered scaffold-less BLB constructs fabricated using previously described methods and PTG were arthroscopically implanted into a 6mm diameter bone tunnel to reconstruct the ACL in adult sheep. Tunnel healing was evaluated following 9-mo. recovery by performing Micro-computed Tomography (MicroCT, GE Healthcare) on both BLB and PTG reconstructed knees at a 138x138x138 μ m voxel size. Using MicroView2.2 analysis software, three-dimensional reconstructions of the bone tissue (HU 600) were created and cross sections perpendicular to the tunnel axis were imaged. Using a software tool, the unfilled area of the tunnel was selected and subtracted from the initially created tunnel diameter of 6mm yielding the volume of new bone ingrowth (Figure 1&2).

RESULTS

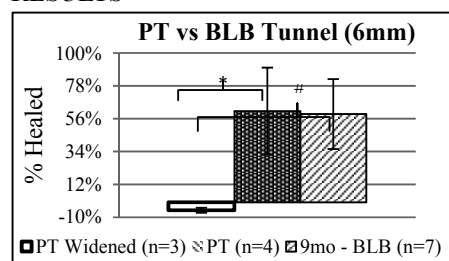


Figure 1. Percentage of tunnel healing 9-mo. following ACL reconstruction using BLB and PTG. PTG data was separated by bone tunnels that widened and tunnels that healed. All BLBs (n=7) filled in the tunnel, while only some PTG (n=4) showed bone ingrowth. Additionally, there were (n=3) PTG that showed tunnel widening, healing significantly less than both the PTG and BLBs. (P<0.019 and P<0.0003 respectively).

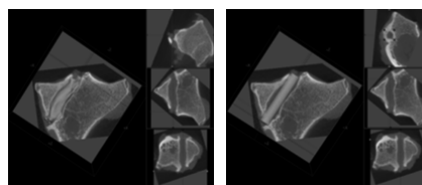


Figure 2. MicroCT of PT healing and bone ingrowth within the bone tunnel. Empty space within the tunnel was highlighted (Left) and subtracted from original 6mm tunnel (Right)

DISCUSSION

While the clinical implications of tunnel widening leading to graft failure are still unknown, it can pose a significant challenge to surgeons during revision surgery. While 57% of the PTG displayed similar bone ingrowth compared to our BLB constructs at 9-mo., tunnel widening was observed in 43% of the PTG possibly indicating issues with graft fixation or motion within the tunnel during normal knee motion potentially complicating revision surgery if necessary. Our BLBs possess an extensible ligament region that is able to respond to the mechanical strains of the knee while maintaining adequate fixation within the bone tunnel to establish a mechanically viable connection by 8wks and promote bone ingrowth at 9-mo. These evaluations, along with current data, (Ma *et al*, Submitted for Publication, AOSSM 2011) demonstrate that BLBs performed better than PTGs structurally and functionally after 9-mo., and do not experience tunnel widening, indicating that the BLB may be considered as an option for future ACL repair.

ACKNOWLEDGEMENTS

The authors would like to acknowledge our funding sources: Coulter Foundation and MICH

REFERENCES: 1. Wilson *et al*. Am J Sports Med. 2004. 2. Maak *et al*. J Am Acad. Orthop. Surg. 2010. 3. Nedderman *et al*. Am J Sports Med. 2009. 4. Ma *et al*. J. Biomech Eng. 2009. 5. Ma *et al*. Tissue Eng Part A. 2011.

TENDON MECHANICAL COMPROMISE AFTER PARTIAL TEAR SIMULATION

J.R. Kondratko, S.E. Duenwald-Kuehl, R. Lakes, and R. Vanderby
University of Wisconsin-Madison

INTRODUCTION

Tendons function to efficiently move and stabilize joints and to absorb impacts. Their mechanical properties are essential to complete these tasks. Tendons function well in the normal physiological range but can be torn as a result of abnormal movement or repetitive loading. Mechanical properties of partially torn tendons are diminished and result in a compromised ability to perform necessary functions. Traditionally, tendons are treated conservatively until tear sizes reach 50% of the cross sectional area, at which point a surgical treatment option is considered. However, robust mechanical studies showing the effects of different tear sizes on the mechanical properties of the tissue have not been performed to validate or falsify this criterion. This study examines the relationship between tear size and the elastic and viscoelastic properties of partially torn porcine flexor tendons.

METHODS

Porcine flexor tendons were preloaded to 1N and preconditioned with a sinusoidal wave at 0.5Hz to 2% strain (grip-to-grip) for 20s *in vitro* in a mechanical test system (MTS Bionix). Each tendon was cyclically loaded at 0.5Hz to 4% strain for 20s, allowed to recover for 1000s, and followed by a relaxation test for 100s at 4% strain. The tendons were then cut transversely with a 1mm, 2mm, and 2.75mm blade (n=8 each group). The 1mm, 2mm, and 2.75mm cut depths corresponded to about 20, 50, and 65% of the total cross sectional area. The cut was made 30mm from the distal insertion site to mimic a mid-substance partial tendon tear. Following the cut and a 1000s rest period, the cyclic and relaxation tests were repeated in the same manner as stated above. Parameters collected during cyclic testing were σ_{peak} (peak stress reached during 10 cycles) and $\sigma_{decrease}$ (decrease in peak stress from cycle 1 to cycle 10). Parameters collected during relaxation testing were σ_{max} (maximum stress reached during test) and σ_{decay} (decrease in stress from initial load application to the end of the relaxation test).

RESULTS

Regardless of cut size, mechanical properties of all tendons tested showed some degree of compromise after the simulated partial tear (Fig. 1, 2). Compromise was manifested as a decrease in all parameters after the cut, demonstrating both an elastic (σ_{peak} , σ_{max}) and viscoelastic ($\sigma_{decrease}$, σ_{decay}) effect. Cyclic testing parameters (σ_{peak} , $\sigma_{decrease}$) decreased following the cut, but did not show a significant difference between the cut sizes. Relaxation testing parameters (σ_{max} , σ_{decay}) showed a significant difference between the 3 cut sizes ($p=0.0013$, $p=0.0002$) (Fig. 3).

DISCUSSION

Mechanical properties of tendon are compromised after all cut sizes, but the effect is not linearly correlated to cut size. Interestingly, cyclic parameters show greater compromise than relaxation parameters. With compromised mechanical properties, tendons cannot perform their necessary functions as efficiently and are at a higher risk of further damage. Such compromise is seen with cuts as small as 20%, suggesting that further inquiry into the risk of failure in partial tears would be valuable.

ACKNOWLEDGEMENTS

This work was funded by NIH R21 EB08548.

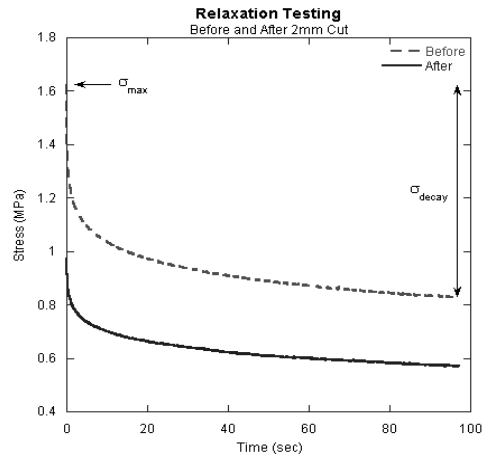


Figure 7. Relaxation testing (before & after cut)

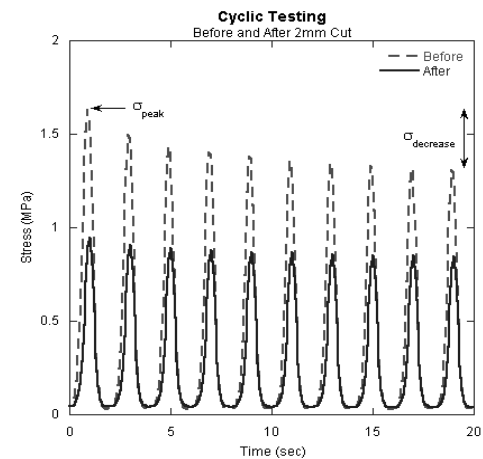


Figure 8. Cyclic testing (before & after cut)

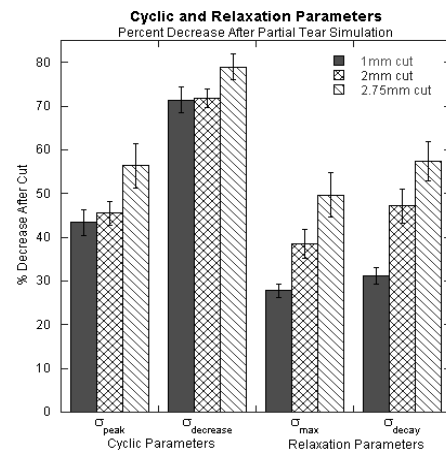


Figure 9. Mechanical compromise following cut

PROTECTIVE EFFECTS OF ADIPOSE-DERIVED MESENCHYMAL STEM CELLS ON TENDON FIBROBLASTS

C.N. Manning, R.H. Gelberman, S. Sakiyama-Elbert, M.J. Silva, S. Thomopoulos
Washington University in St Louis, St Louis, MO

INTRODUCTION

The inflammatory response that occurs during the early stages of tendon healing has been shown to contribute to poor outcomes. Mesenchymal stem cells have been identified as potential immunosuppressive-antiinflammatory agents [1, 2]. The purpose of this study was to investigate the ability of mesenchymal stem cells to protect tendon fibroblasts from an inflammatory environment.

METHODS

Cell Isolation: Adipose-derived mesenchymal stem cells (ASCs) and tendon fibroblasts (TFs) were isolated from canines (n=3) and rats (n=4). The following assays were performed at 1, 2, and 3 days. **Dose Response Study:** To determine an appropriate dosage of IL-1 β , rat-derived tendon fibroblasts were treated with varying amounts of IL-1 β (0 - 100 ng/ml) and quantitative real-time PCR (qPCR) was performed. **Co-culture Study:** ASCs and TFs were co-cultured at a 1:1 cell density ratio using transwell plates. The cells were treated with 10 ng/ml IL-1 β . The experimental groups examined were: 1) TFs alone (TF), 2) TFs treated with IL-1 β (TF+IL-1 β), 3) TFs co-cultured with ASCs (TF+ASC), and 4) TFs co-cultured with ASCs and treated with IL-1 β (TF+ASC+IL-1 β). **Live/Dead Assay:** TFs were stained with a Live/Dead kit and the percentage of live cells was determined. **ELISA:** Cell supernatants were collected and ELISAs for 27 inflammation-related factors and 2 MMPs were performed. **qPCR:** RNA from TFs was isolated and qPCR was performed for pro-inflammatory (IL-1 β , TNF α) and matrix metalloproteinase (MMP-1, 3, 13) genes. The expression levels were normalized to GAPDH.

RESULTS

Dose Response Study: Treatment with at least 10ng/ml of IL-1 β led to significantly higher gene expression levels of IL-1 β , TNF α , MMP1, 3, and 13 at all timepoints compared to control (i.e. 0 ng/ml). **Live/Dead Assay:** Cells were vulnerable to IL-1 β , leading to a survival rate of 14-22% after 1-3 days in culture. Co-culture with ASCs rescued TFs from cell death, with survival rates of 93% and 64% on days 1 and 3, respectively (Fig. 1). **ELISA:** Tendon fibroblasts cultured alone did not produce detectable levels of pro-inflammatory factors (i.e. IL-1 β , TNF α , IFN γ) and matrix metalloproteinases (i.e. MMP-1, 3). Treatment with 10 ng/ml IL-1 β , significantly increased inflammatory factors and matrix metalloproteinases in the supernatant. These levels were significantly reduced by co-culture with ASCs (i.e. TF+ASC+IL-1 β group) (Fig. 2). Similar results were observed for inflammation-related chemokines (i.e., CINC-1, -2, -3, Fractalkine, GM-CSF, MCP-1; data not shown). **qPCR:** The expression of genes related to inflammation (TNF, IL1 β) and matrix degradation (MMP1, 3, 13) were significantly observed when TFs were exposed to IL1 β . Co-culture with ASCs reduced the expression of those genes. Reductions were most dramatic on day 2 (Table 1).

DISCUSSION

- As shown here and in prior studies [3,4], tendon fibroblasts upregulate their expression of IL1 β and MMPs 1 and 3 in response to IL-1 β .
- The current study demonstrated that ASCs protect tendon fibroblasts from the harmful effects of IL-1 β (i.e., cell death, increased inflammation, and matrix degradation).
- The immunoprotective effects of ASCs on TFs provides support for the use of ASCs as adjunctive treatment in tendon repair and tendinopathy where inflammation is a critical factor, including flexor tendon lacerations, Achilles tendinitis, and rotator cuff degeneration.

REFERENCES: 1. Singer N, et al: Ann Rev Path Mech Dis 6:457-478, 2011. 2. Caplan A: J Pathol 217:318-324, 2009. 3. Tszuzaki MG, et al: J Orthop Res 21:256-264, 2003. 4. John TD, et al: J Orthop Res 28:1071-1077, 2010.

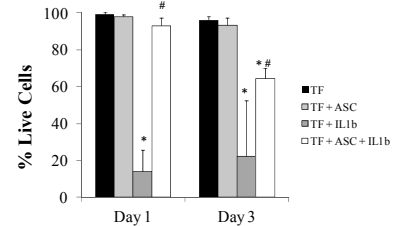


Fig. 1: Percentage of live cells at days 1 and 3. * Statistically different from day 0, # statistically different from TF+IL1 β group (p<0.05, paired ANOVA). N=3, canine-derived cells.

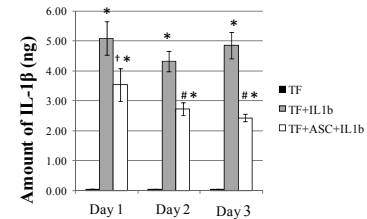


Fig. 2: Total amount of IL-1 β detected in the cell supernatants. * Statistically different from control (TF) (p< 0.01, paired t-test), #/† statistically different from TF+IL1 β group (# < 0.10, † p < 0.01, paired t-test). N=4, rat-derived cells.

DAY 2	Gene Expression			
	TF+IL-1 β vs. TF		TF+ASC+IL-1 β vs. TF+IL-1 β	
	Fold Change	P Value	Fold Change	P Value
TNF	240	0.01	-1.59	0.11
IL-1B	infinite	-	-4.52	0.02
MMP1	infinite	-	-1.95	0.12
MMP3	55,000	0.00	-1.65	0.02
MMP13	2,500	0.01	-1.56	0.18

Table 1: Fold changes in gene expression. Left: expression of genes increases in the TF+IL1 β group compared to the TF group. Right: expression of most genes decrease (although not significantly) in the TF+ASC+IL1 β group compared to the TF+IL1 β group. Fold change of 1.0 equals no change. Note: IL-1 β was not detected in the TF group. N=6, canine-derived cells.

DO MAST CELLS PLAY A ROLE IN LIGAMENT HEALING?

Brannagan, K M; Leonard, C; Zhang, M; Hildebrand, K; Bray, RC; Salo, P T
Faculty of Medicine, The University of Calgary, Calgary, Alberta

INTRODUCTION

Knee sprains and strains account for approximately 75% of all injuries in sports [1] and are responsible for substantial loss of productivity of active members of society. The study of joint connective tissues and their corresponding injuries has traditionally focused on structure and mechanics. Only more recently has research begun to address the cellular elements involved in the biological and biomechanical homeostasis of ligaments and tendons. Mast cells are immune cells that release numerous proteases and signalling molecules through degranulation and have been shown to be involved in wound healing and fibrotic pathologies [2]. As yet, mast cells have never been identified in articular ligament tissue and we sought to explore the presence, or lack thereof, of mast cells in both normal and injured ligament tissue.

METHODS

All experimental protocols were approved by the institutional animal care committee. Six female, one-year-old New Zealand White Rabbits were used in this study. Three animals were used as controls and received no surgical intervention (Normal) while the remaining three animals underwent a bilateral transection of the medial collateral ligament (MCL-X). The injured rabbits were allowed to heal for two weeks with unrestricted movement.

Two weeks following the surgeries, animals were euthanized and the left and right MCLs placed in phosphate-buffered 4% paraformaldehyde for 72 hours. Ligaments were then dehydrated using a series of ethanols and xylenes and embedded in paraffin wax blocks. The paraffin-embedded ligaments were cut into 10 μm sections, rehydrated and put through a heat-mediated antigen retrieval process in a Tris-EDTA buffer solution. Sections were blocked and stained with Anti-Mast Cell Tryptase antibody (Abcam) and the corresponding Cy3-conjugated secondary antibody (Jackson Immunoresearch) for immunofluorescence imaging.

RESULTS

We examined the images from a randomly selected number of sections to assess the presence of mast cells throughout the ligament tissue, including the epi-ligament tissue. Mast cells were detected in the epi-ligament of both normal and injured tissue, although the stained cells were extremely scarce in the control ligaments. No staining was present in the true ligament tissue of the control animals; however stained cells were present throughout the tissue at 2 weeks post transection [Figure 1]. In the tissue immediately surrounding the scar area, the mast cells appeared to be arranged in clusters as opposed to the more random distribution throughout the rest of the tissue [Figure 2].

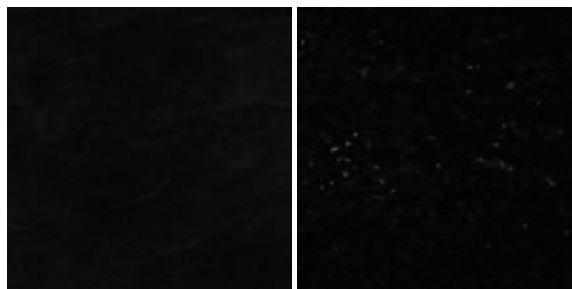


Figure 1. Rabbit MCL tissue stained with Anti-tryptase antibody, a marker for mast cells, in uninjured tissue [A] and tissue at 2 weeks post transection [B] at 20x objective.

DISCUSSION

It is evident that mast cells play a role in the healing of ligament tissue. These preliminary findings are the first reported evidence that mast cells are present in injured ligament tissue; however, further investigation is necessary to determine the full scope of these cells' involvement in the healing process. Mast cells release a whole host of cytokines, proteases and inflammatory mediators through degranulation and this multitude of factors undoubtedly affects the inflammatory and healing process in injured ligament tissue. It has been suggested that mast cells are involved at different levels throughout all three phases of healing [3] and the potential to modulate mast cell activity following ligament injury may lead to novel treatment options.

REFERENCES

1. Kujala et al. *Brit Med J*, 1995.
2. Artuc et al. *Exp Dermatol*, 1999.
3. Noli and Miolo. *Vet Dermatol*, 2001.

ACKNOWLEDGEMENTS

Funding provided by Alberta Innovates – Health Solutions.

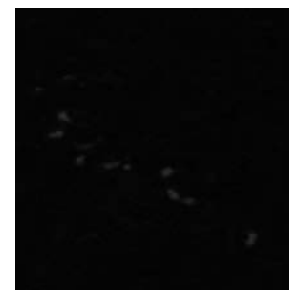


Figure 2. Example of a cluster of mast cells observed in tissue surrounding the scar at 2 weeks post transection.

A 6 MONTHS FOLLOW-UP STUDY OF T2 VALUE OF SUBSTITUTED ACL

¹Katsumata S., ¹Hung C C, ²Kuramochi R., ³Kudo M., ⁴Itakura H. and ⁵Fukubayashi T.

¹Graduated School of Sport Sciences, Waseda University,
2579-15, Mikajima, Tokorozawa, Saitama, Japan 359-1192

²Faculty of school of health and sport sciences, Chukyo University, Toyota, Nagoya, Japan

³The University of Tokyo Graduate School of Arts and Science, Meguro, Tokyo, Japan

⁴Women's College of Physical Education, Setagaya, Tokyo, Japan

⁵Faculty of Sport Sciences, Waseda University, Tokorozawa, Saitama, Japan

INTRODUCTION

This study aimed at early functional recovery in post-operative rehabilitation following anatomical double-bundle reconstruction of the knee anterior cruciate ligament (ACL) with the semitendinosus (ST) tendon. It has been known that the T2 values of regenerated ST tendon decreased in post-operative 6 months. Nevertheless, little is known about the level of reconstructed graft maturity as the ligamentization occurs after reconstruction. Therefore, the purpose of this study was to describe the level of ACL maturity using MR image.

METHOD

13 young female athletes volunteered to participate in this study. All subjects were following anatomic double-bundle anterior cruciate ligament (ACL) reconstruction using semitendinosus (ST) tendon autograft. Before participation, the procedures were explained to all subjects who enrolled in the same rehabilitation program instructed by physician assistants. Magnetic resonance imaging (MRI) were used to evaluate the morphological changes of the reconstructed graft for 6 months postoperatively. T2 transaxial sequences were measured as follows: 5mm slice thickness, 1mm gap space, repetition time 3000 ms, echo time 10, 20, 30 ms, field of view 160×160 mm, and matrix size 256×192 pixels. The signal intensity was also measured at the joint line. The T2 values measured on AM band.

RESULTS

Figure 1 and figure 2 show the time-course change in the site of AM band and the mean time-course change in the T2 value across post-operative 6 months. The T2 value of reconstructed graft increased between 1 month and 2 month, and had been gradually decreased after two month (fig.2).

There was a significant difference between post operative 2M and 6M.

CONCLUSION

The T2 relaxation time of the reconstructed graft after reconstruction is essential data for determining appropriate loading controls in rehabilitation. As our observation, T2 value of reconstructed graft reached its peak in post-operative 2 month. However, the mechanism of ligamentization cannot be explained by only the T2 value, although it can be one of the determinants to create rehabilitation program at this point.

Further

CELL INTERACTION DISTANCE MODULATE

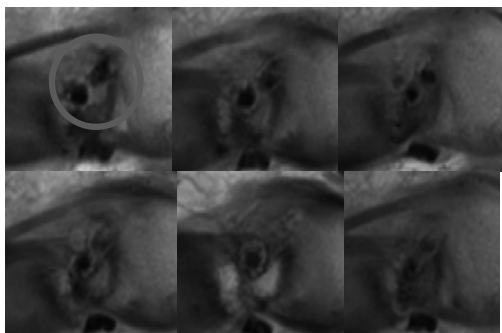


Fig.1 Typical MRI scans of the substituted ACL.

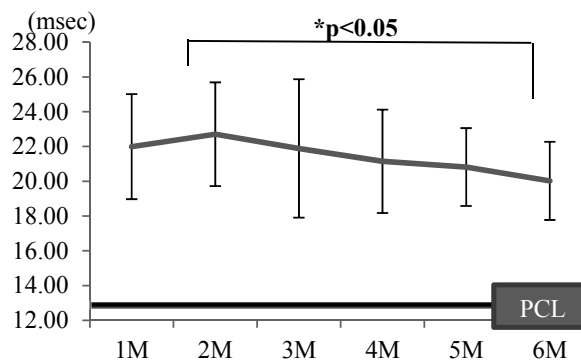


Fig.2 T2 relaxation time of the substituted ACL.

CHONDROCYTE RESPONSE ON STRATIFIED SCAFFOLDS

¹Zhang, X; ¹Moffat, K L; ¹Gorodon, S E; ¹Goldhaber, N H; and ¹Lu, H H;
⁺¹ Columbia University, Department of Biomedical Engineering

INTRODUCTION

Rotator cuff tears often result from avulsion of the tendon from bone at the insertion site [1], which consists of a fibrocartilaginous transition that subdivides into non-mineralized and mineralized regions. Regeneration of this multi-region interface is essential for functional load transfer from tendon to bone and integrative rotator cuff repair. To this end, biphasic scaffolds (Fig 1A) mimicking the native interface have been found to support chondrocyte-mediated deposition of contiguous non-calcified and calcified fibrocartilage-like matrices [2]. Given the compositional difference between scaffold phases, it is not known how cells seeded on one phase of the stratified scaffold can influence the response of cell cultured on the adjacent phase, and what are the ramifications of these interactions in multi-tissue formation and homeostasis. **It is hypothesized** that cell interaction distance between phases will play a role in directing cell response on the biphasic scaffolds. To test this hypothesis, the **objective of this study** is to compare cell response on single-phased vs. biphasic scaffolds, and evaluating chondrocyte growth and biosynthesis as a function of distance between scaffold phases.

METHODS

Scaffold fabrication: Single phased of aligned poly(lactide-co-glycolide) (PLGA 85:15, Lakeshore Biomaterials, AL) nanofibers with HA (15% w/w, PLGA-HA) or without HA (PLGA) were fabricated by electrospinning[3]. The biphasic scaffold was produced by direct electrospinning of PLGA-HA on top of PLGA. **Study Design:** Groups include single culture of PLGA or PLGA-HA, segregated co-culture of PLGA and PLGA-HA, & biphasic scaffold. Thus for distance between phases: single phase (infinite) > segregated co-culture (1mm) > biphasic scaffold (0mm). Bovine chondrocytes obtained by enzymatic digestion were seeded on the scaffolds (6×10^4 cell/cm², starting cell number same for all groups at day 0), and cultured for 1, 14 and 28 days. Cell viability (n=2, Live/Dead), cell number (n=5, Picogreen), ALP activity (n=5), collagen and glycosaminoglycan (GAG, n=5) were determined over time. **Statistical analysis:** Two-way ANOVA and the Tukey-Kramer *post-hoc* test (*p<0.05).

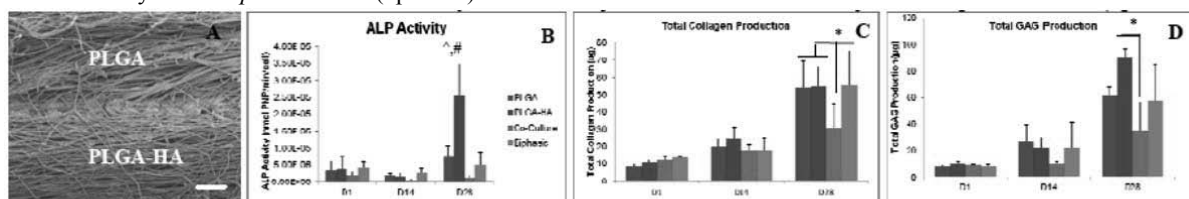


Figure 1: A: SEM image of biphasic scaffold (scale bar=20µm). B: ALP activity, C: Total collagen, D: GAG production on different scaffold over time (^: significant different over time, #: significant different between groups, *: significant different from each other)

RESULTS

Cells attached and proliferated on all scaffolds over time, with no significant difference observed between groups. In contrast, ALP activity peaked in the PLGA-HA single-cultured group at day 28, while remaining at basal levels for all other groups over time. By day 28, both collagen and GAG were significantly lower in the co-cultured group, with GAG deposition being the highest in the PLGA-HA single-cultured group. No significant difference in either collagen or GAG deposition was found for cells cultured on the single-phased and biphasic scaffolds.

DISCUSSION

In this study, the separation distance between scaffold phases decreased from infinity (single-phased PLGA or PLGA-HA) to a well-defined distance (1 mm in co-culture), and to none (biphasic). The results described above suggest that by increasing the distance between scaffold phases, or in other words, the interaction distance between cells cultured on PLGA or PLGA-HA, both cell mineralization potential and matrix deposition can be modulated. It was found that chondrocytes cultured on PLGA suppressed the ALP activity of chondrocytes cultured on PLGA-HA, as seen in both co-cultured and biphasic groups. Moreover, compared to single-cultured controls, both GAG and collagen syntheses were suppressed in co-culture, while this effect was absent in the biphasic group. It is possible that the paracrine suppression of biosynthesis experienced in segregated co-culture is rescued by enhanced cell-cell contact on the biphasic scaffold. These findings yield new insights into the mechanism of cellular interaction on complex scaffolds and future studies will explore the effects of these interactions for interface regeneration and integrative rotator cuff repair.

ACKNOWLEDGEMENTS: NIH/NIAMS (AR056459-02, AR055280-02), NYSTEM, NSERC (XZ)

REFERENCES: 1. Iannotti, J.Am.Acad.Orthop.Surg., 1994; 2. Moffat et al. 57th ORS Annual Meeting, 2011; 3. Moffat et al., Tissue Eng. 2009.

DOSE-DEPENDENT EFFECT OF 2-PHOSPHOASCORBATE ON MATERIAL PROPERTIES OF 3D PORCINE TENOCYTE-POPULATED BIOARTIFICIAL TENDON

^{1,2}A Cederlund, ³J Qi and ^{1,3}A J Banes

¹University of North Carolina, ²Lund University and ³Flexcell International, Hillsborough, NC

INTRODUCTION

Ascorbic acid has previously been shown to be an essential part of collagen synthesis for proline and lysine hydroxylation (1). However, it is not clear whether or not the increased accumulation of extracellular matrix in vitro will strengthen, significantly, tissue engineered constructs. Control of matrix expression, matrix maturation and cell proliferation are essential to build robust bioartificial tissues for tissue engineering. The aim of this study was to investigate the effects of an economical nutrient, ascorbic acid, on cell proliferation and bioartificial tissue-strength.

METHODS

Porcine tenocytes were isolated by collagenase digestion from Achilles tendons of mature hogs obtained from a local abattoir (Neece Sausage Co, Burlington, NC). Cells were cultured in DMEM-H with 20 mM HEPES pH 7.2, 15 mM glutamine, 20 mM sodium pyruvate and 2-phospho-ascorbate concentrations 0, 50 100 and 300 μ M. Cells were used between passages 0 and 5. Cells were plated at 100k cells/100 μ L PurCol collagen in linear BATs (bioartificial tendons) in TissueTrain culture plates (Flexcell Intl Corp (2), and tensile strength tests performed using a materials testing machine (n=6/time point; Enduratec ELF 3200). Linear BAT images were captured using a scanner in the CO₂ incubator (ScanFlexTM, Flexcell Intl.) and data reduced to yield matrix compaction indices (XYFlexTM, Flexcell Intl.; Figure 2).

RESULTS

Bioartificial tendons grown in 3D collagen gels treated with increasing concentrations of 2-phospho ascorbate showed a dose-dependent increase in ultimate tensile strength, (UTS 3.5 fold increased (3.2 ± 1 KPa and 11.4 ± 2.7 KPa) between control and 300 μ M $p < 0.05$) (Figure 1) Young's Modulus also showed an increase but was not statistically significant. The compaction rate was slightly but not significantly increased in 50 μ M ascorbate compared to the control (NS).

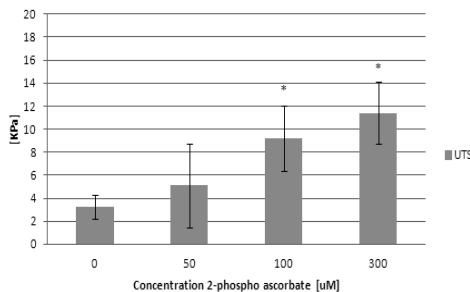


Figure 10 Ultimate Tensile Strength (UTS) strength (UTS) from bio artificial tissue, grown in three different concentrations of 2-phosphate ascorbate.

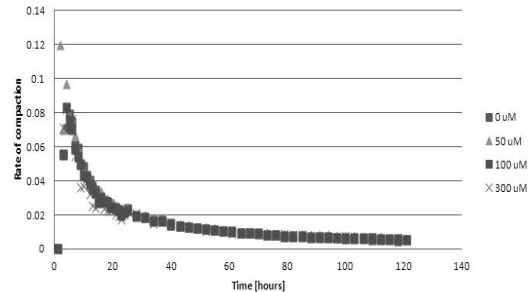


Figure 11 Compaction Rates for bio artificial tissue grown in three different concentrations of 2-phospho ascorbate.

DISCUSSION

Porcine Achilles tendon cells treated with 2-phospho ascorbate demonstrated a dose-dependent increase in UTS by day 7 in vitro. Preliminary data indicate that type I collagen expression was increased as well as expression of Col3a. The increased strength and expression of collagen genes is comparable to that shown for cells treated with TGF β 1 (3). Ascorbate may act via increased expression of CTGF and TGF β to increase collagen expression and strength. Modulating tenocytes with ascorbate is an economical method for accelerating the strength of tissue engineered connective tissue constructs in vitro.

REFERENCES

1. Kivirikko et al, JHEP 1991.
2. Banes et al, Tissue Eng 2003.
3. Grouf et al, Tissue Eng 2007.

A MAGNESIUM-BASED RING FOR MECHANICAL AUGMENTATION OF A TORN ANTERIOR CRUCIATE LIGAMENT – A NEW EXPERIMENTAL ANIMAL MODEL

K.F. Farraro, H. S. Eason, M.M. Tei, K.E. Kim, S. L-Y. Woo
Musculoskeletal Research Center, Department of Bioengineering
Swanson School of Engineering, University of Pittsburgh, Pittsburgh, PA

INTRODUCTION: In our research center, we have shown that an ECM bioscaffold with suture repair could promote healing of a fully transected anterior cruciate ligament (ACL) in the goat model at 12 weeks¹. The neo-tissue as well as the structural properties of the healing femur-ACL-tibia complex (FATC) were significantly better than suture repair alone. Still, the process of healing of the ACL is slow and mechanical augmentation to allow immediate loading of the ACL would be beneficial in limiting degradation of the insertion sites due to lack of stress²⁻³. Thus, the objective of this study was to use a biodegradable magnesium (Mg)-based ring to bridge the two ends of a transected ACL so that the repaired ligament and the entire FATC would be loaded at time zero to reduce disuse atrophy. The hypothesis under study was that the ring, when used in conjunction with suture augmentation, would provide additional mechanical support for joint stability to facilitate ACL healing. To test this, we obtained the tensile properties of the FATC with the Mg-based ring with suture augmentation and assessed the improvement over suture augmentation alone.

METHODS: In four pairs of cadaveric goat stifle joints, the ACL was transected at its mid-substance. One side of each pair was randomly assigned to have suture augmentation with an Mg-based ring (group 1) or suture augmentation alone (group 2). For group 1, a custom-made, cylindrical Mg-based ring designed based on the geometry of the goat ACL was sutured to both stumps of the transected ligament through holes around the ring's circumference. Suture augmentation was then added by passing two sutures through tibial and femoral bone tunnels drilled adjacent to the insertion sites and fixing them under manual tension with a titanium button. For group 2, only suture augmentation was performed. Each FATC was then subjected to uniaxial tensile testing and its stiffness and ultimate load were obtained. The results for the two groups were compared statistically using paired t-tests, with significance set at $p < 0.05$.

RESULTS: The load-elongation curve of the FATC with the Mg-based ring and suture augmentation (group 1) showed a toe region that is characteristic of the behavior of soft tissues, followed by a linear region until the yield point prior to failure. The failure mode was typically breakage of the holes of the ring or its attachment sutures at the ring's femoral attachment to the ACL, followed by snapping of the augmentation sutures. In contrast, the load-elongation curve for suture augmentation alone (group 2) was linear in appearance, with solely the sutures taking the load. Stiffness of the FATC was found to be significantly higher with the addition of the Mg-based ring compared to suture augmentation alone (22.5 ± 4.5 and 16.0 ± 1.5 N/mm, respectively; $p < 0.05$, see Fig.1) while values of ultimate load were not statistically different between groups (180.0 ± 44.6 N and 160.8 ± 14.3 N, respectively; $p > 0.05$).

DISCUSSION: This study showed that an Mg-based ring used to bridge a transected ACL could aid in the improvement of the stiffness of the FATC over suture augmentation alone, in support of our hypothesis. This increased stiffness demonstrates that the ring, working in parallel with the augmentation sutures, could help the repaired FATC to take on load to stabilize the knee as well as to help to prevent insertion site atrophy during its slow healing process. In contrast, the ultimate load did not differ between groups because the augmentation sutures had higher strength than the ring. Based on the results obtained, it is feasible to proceed with this model to in-vivo animal studies both in the short and longer terms to improve ACL healing.

ACKNOWLEDGEMENTS: Financial support from Commonwealth of Pennsylvania and NSF Engineering Research Center Grant (#0812348).

REFERENCES: 1. Fisher, et al. 2011, KSSTA (in press). 2. Fisher, et al. JOR 2010, 28(10):1373-9. 3. Fisher, et al., J Biomech 2011, 44(8):1530-5.

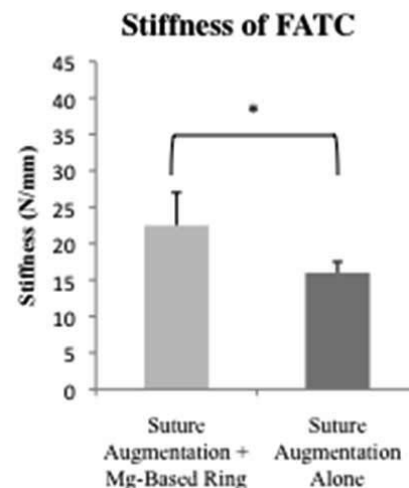


Figure 12: Stiffness of the FATC with the Mg-based ring and suture augmentation and suture augmentation alone ($*p < 0.05$)

TENOMODULIN PROMOTED TENDON-DERIVED STEM CELL PROLIFERATION AND INHIBITED ANGIOGENESIS – A POSSIBLE MOLECULAR MECHANISM OF TENDINOPATHY?

¹Qi Tan, ^{1,2}Pauline Po Yee Lui

¹Department of Orthopaedics and Traumatology;

²Program of Stem Cell and Regeneration, School of Biomedical Science, The Chinese University of Hong Kong

INTRODUCTION

Tendon has a low cell density and has a poor blood supply. However, hypercellularity and hypervascularity, accompanied by matrix degeneration and failed tendon healing, are common histopathological findings in tendinopathy. The weakening of normal tendon structure by these events leads to spontaneous tendon rupture. Tendonmodulin (Tnmd) is a type II transmembrane protein that is predominantly expressed in tendons, ligaments and eyes. Hence it is often used as a marker for tendons and ligaments. However, the roles of Tnmd in tendon physiology and pathology remain unclear. We hypothesized that Tnmd regulates tendon-derived stem cell (TDSC) proliferation, angiogenesis and matrix metalloproteinase (MMP) activation in tendons. We further hypothesized that there would be down-regulation of Tnmd expression in tissues and TDSCs of tendinopathy, which might be associated with failed healing, hypervascularity and matrix degeneration in tendinopathy. The expression of Tnmd in TDSCs may be down-regulated by BMP-2, a factor reported to be produced in tendinopathic tissue and expressed in TDSCs upon repeated cyclic tensile loading.¹⁻³ This study therefore aimed to investigate the effect of Tnmd on the proliferation of healthy TDSCs and tube formation of endothelial cells in vitro. The expressions of Tnmd in tendinopathic tissues and TDSCs isolated from tendinopathic tendons were also investigated. The effect of BMP-2 on the expression of Tnmd in healthy TDSCs was also studied in vitro.

METHODS

Human TDSCs (hTDSCs) were isolated from healthy and tendinopathic tendons (both n=3). The proliferation of healthy hTDSCs +/- *Tnmd* gene silencing was studied by BrdU assay in vitro. The effect of Tnmd on tube formation was examined by treating HUVEC with conditioned medium of healthy hTDSCs +/- *Tnmd* gene silencing. The mRNA expression of *Tnmd* in hTDSCs isolated from healthy and tendinopathic tendons were compared by qRT-PCR. Tnmd protein expression was also examined in healthy and tendinopathic tendons by immunohistochemistry (n=5). The effect of BMP-2 on the mRNA expression of *Tnmd* in healthy hTDSCs was examined by qRT-PCR after treatment of cells with rhBMP-2 (300ng/ml) for 1 week.

RESULTS

Tnmd gene silencing in hTDSCs significantly reduced hTDSC proliferation ($p<0.001$). hTDSC-conditioned medium inhibited tube formation by HUVEC compared while conditioned medium of hTDSCs with *Tnmd* knock-down reversed the inhibition. There was higher expression of Tnmd in the paratendon compared to the tendon proper, consistent with higher vascularity in the paratendon. There was reduced Tnmd protein expression in tendinopathic tendons compared to healthy controls ($p=0.004$), consistent with higher cellularity ($p<0.001$), vascularity, VEGF ($p=0.004$) and MMP (MMP1, MMP9, MMP13) expression in tendinopathic tendons. There was significant lower *Tnmd* expression in hTDSCs isolated from tendinopathic tendons compared to healthy tendons ($p=0.02$). rhBMP-2 down-regulated *Tnmd* expression in healthy hTDSCs ($p=0.004$).

DISCUSSION

Tnmd promoted TDSC proliferation and Tnmd secreted by TDSCs has an anti-angiogenic effect. The anti-angiogenic effect of Tnmd is also evident by the higher expression of Tnmd in the paratendon, protecting the tendon proper from invasion by blood vessels. There was reduced expression of Tnmd in TDSCs and tissues of tendinopathy, which was associated with hypervascularity, MMP expression and failed healing in tendinopathy. BMP-2 reduced the expression of Tnmd in TDSCs, providing a possible mechanism for the reduced expression of Tnmd in tendinopathy.

REFERENCES

- (1) Rui et al. J Orthop Res 2011; 29(3): 390-396;
- (2) Rui et al. Knee Surg Sports traumtol Arthrosc 2011; doi: doi: 10.1007/s00167-011-1685-8;
- (3) Po Yee Lui et al. J Orthop Res 2011;29(6):816-821.

ISL&T-XII Supporters

We gratefully acknowledge the support of the following individuals, whose generosity helped make ISL&T-XII possible:

Professor Chih-Hwa Chen, Chang Gung Memorial Hospital at Keelung

Dr. Savio L-Y. Woo, Musculoskeletal Research Center,
University of Pittsburgh

Dr. Steven Arnoczky, The Laboratory for Comparative
Orthopaedic Research, Michigan State University

Professor Kai-Ming Chan, The Chinese University of Hong Kong

Dr. David Butler, University of Cincinnati

Dr. Ranjan Gupta, University of California, Irvine

Dr. Evan Flatow, Mount Sinai School of Medicine

Dr. Braden Fleming, Brown University

Dr. Lou Soslowky, University of Pennsylvania

Dr. Ray Vanderby, University of Wisconsin

Dr. Guoan Li, Massachusetts General Hospital

Dr. Martha Murray, Children's Hospital, Boston

Dr. Per Renstrom, Karolinska Institutet

Professor Toru Fukubayashi, University of Waseda

International Symposium on Ligaments and Tendons (ISL&T-XII)
Hilton San Francisco Financial District
February 3, 2012
San Francisco, CA

7:00-7:45	Registration and Light Breakfast
7:45-8:10	Opening Remarks Savio L-Y. Woo, PhD, DSc, DEng & K.M. Chan, MD, PhD
8:10-8:25	Clinical Talk Chair: Ranjan Gupta, MD
8:25-10:26	Session 1: ACL Session Chairs: Mitsuo Ochi, MD, Guoan Li, PhD
10:26-10:56	Break and Poster Session 1 Session Chairs: Louis Soslowky, PhD, Stavros Thomopoulos, PhD
10:56-12:35	Session 2: Tendon and Ligament Tissue Engineering Session Chairs: Helen Lu, PhD, Paul Ackermann, MD, PhD
12:35-13:35	Group Photo & Lunch
13:35-14:33	Session 3: Rotator Cuff Session Chairs: Zong-Ming Li, PhD, Chih-Hwa Chen, MD, PhD
14:33-15:33	Session 4: Tendinopathy Session Chairs: Braden Fleming, PhD, Nicola Maffulli, MD
15:33-16:03	Break and Poster Session 2 Session Chairs: Catherine K. Kuo, PhD, Wei-Hsiu Hsu, MD
16:03-18:15	Session 5: Biology and Biomechanics of Tendons and Ligaments Session Chairs: PPY Lui, PhD, Christer Rolf, MD, PhD
18:15-18:30	Closing Remarks K.M. Chan, MD, PhD, Giuliano Cerulli, MD, Chih-Hwa Chen, MD, PhD
18:30	Proceed to Dinner Venue
19:00	Reception/Dinner and Award Ceremony